SLOPE HYDROCLIMATOLOGY AND HYDROLOGIC RESPONSES TO GLOBAL CHANGE IN A SMALL HIGH ARCTIC BASIN

BY

KATHY L. YOUNG, B.Sc., M.Sc.

A Thesis

Submitted to the School of Graduate Studies

in Partial Fulfilment of the Requirements

for the Degree

Doctor of Philosophy

DOCTOR OF PHILOSOPHY (1995)
(Geography)

McMASTER UNIVERSITY
Hamilton, Ontario

TITLE: Slope Hydroclimatology and Hydrologic Responses to Global Change in a Small High Arctic Basin

AUTHOR: Kathy L. Young, B.Sc. (University of Toronto)
M.Sc. (University of Toronto)

SUPERVISOR: Dr. M.-K. Woo

NUMBER OF PAGES: 167 (cvxvii)

BROAD SIGNIFICANCE OF STUDY

Thesis Title: Slope Hydroclimatology and Hydrologic Responses to Global Change in a Small High Arctic Basin.

This study evaluated the present-day interactions between the atmosphere, soils, water flow and vegetation patterns of a remote area of Northern Canada. This study showed that microclimatic processes (temperature, radiation) are often the driving force behind snowmelt and ground thaw. This study also showed that it was possible to use limited field camp data (e.g. 2x daily cloud, temperature, wind) to simulate radiation and energy fluxes for a variety of surfaces. This suggests the model's utility by ecologists and earth scientists working in other areas of the Arctic. This thesis also showed that it was possible to use point data to simulate melt and evaporation for a small High Arctic basin and to investigate some possible implications of climate change to water movement. This last stage of the study will be particularly relevant to climatologists, ecologists and geomorphologists working in the north.

SLOPE HYDROCLIMATOLOGY AND HYROLOGIC RESPONSES TO GLOBAL CHANGE IN A SMALL HIGH ARCTIC BASIN

ABSTRACT

An understanding of the linkages between atmospheric-terrestrial and hydrologic processes is required before ramifications of future global changes to arctic environments can be assessed. Part of this study focussed on understanding the present-day spatial and temporal variability of topography, pedology and botany in relation to the local microclimatology and hydrology of a High Arctic site. Fieldwork (1989–1993) at Hot Weather Creek, Ellesmere Island, N.W.T. revealed the direct (i.e., radiation, temperature), recurrent i.e., (ground thaw, snow cover) and long-term patterns (e.g. soils, vegetation) arising within a small area (1km^2).

This study also indicted the importance of radiation as the driving force behind snowmelt patterns, ground thaw and soil moisture. Subsequently, much emphases was placed on the development and testing of a solar radiation model which employs summer field camp data (twice-daily air temperature and cloud information). The successful performance of this model especially when averaged over a four-day period suggests its utility in other areas of the Arctic where similar input data are available. The radiation model was employed within a surface energy balance model which similarly uses limited field camp data (twice-daily temperature, wind and cloud data) obtained at a point. The testing of this model with measured net radiation from both level and sloping surfaces with varying surface conditions, suggest that it is possible to use limited input data from a point to calculate surface energy fluxes (Q^*, Q_e, Q_h, Q_s) for a range of sites.

The surface energy balance model was used to simulate melt and evaporation for a small, continuous permafrost basin (Heather Creek, N.W.T.) during two contrasting summer seasons (1989—cool/wet and 1990—warm/dry). Model performance at the basin scale was

assessed in a simple water balance framework with both years showing simulated long-term storage of less than 20% of total precipitation input. Hypothetical alterations in atmospheric and terrestial impacts of +/- 10% revealed that slight changes in aerosols, cloud amount and temperature have more affect on basin hydrological processes (melt, evaporation and storage) than slight changes in surface conditions (e.g. resistance, albedo).

This study will be of interest to northern scientists wishing to better understand both the present-day linkages between atmospheric-terrestrial and hydrological processes and future global impacts.

ACKNOWLEDGEMENTS

I am very grateful to my supervisor Dr. M.-K. Woo for his wise supervision, caring friendship and contagious enthusiasm throughout this study. Without his great and unending support this study would not have been possible. I wish to thank other members of my supervisory committee, Dr. S.B. McCann and Dr. S.A. Edlund, for their friendship, useful discussions and lively comments. I would especially like to thank Dr. McCann for editing the final draft of this thesis and for making the arrangements for my defense. Many thanks go to Dr. J.A. Davies for reviewing the solar radiation paper and for also providing useful advice. Funding for this study was provided by a research agreement with the Department of Energy, Mines and Resources and a grant from Natural Sciences and Engineering Research Council to M.-K. Woo and a northern training grant from the Department of Indian and Northern Affairs. Generous logistical support was provided by the Polar Continental Shelf project, Department of Energy, Mines and Resources and S.A. Edlund. Support from McMaster University in the form of a Departmental Fellowship in 1989-1990 and teaching assistantships in subsequent years is gratefully acknowledged. I wish to acknowledge the Ontario Government with support from an Ontario Graduate Scholarship in 1993-1994. Special thanks must go to my field assistants over the course of this study: Tessa Fauquier, Shannon Glenn, Sharon Reedyk, Tim Siferd, Kelly Thompson and Paul Wolfe. Their hard work and dedication will always be appreciated. I would also like to thank Angus Headley, Mike Webb and Dave McNichol for providing instrumentation and Eureka weather data.

I will always be grateful to the friendly geography staff at McMaster University: Joan, Jude, Darlene, Mettie, Cliff, Bob and Rick who always managed to steer me in the right direction. I also wish to thank the geography staff at York University: Kathy, Carol, Carolyn, Sharon, Susan, Pam and Rick who have now taken over this task and are now steering me in the right (York) direction.

I wish to thank my lab mates who have put up with me for the last few years: Augustine, Sharon, Bob, Shannon, Sean and Ron. We have shared many enthusiastic discussions and "Hok" stories. These happy memories will always be cherished.

Finally, this thesis could not have been completed without the love and support of my family, my good friends in Winnipeg, Calgary and Ontario and the love and wisdom from my little boy, John Rae.

TABLE OF CONTENTS

PREFACE

INFLUENCE OF LOCAL TOPOGRAPHY, SOIL AND VEGETATION ON MICROCLIMATE AND HYDROLOGY AT A HIGH ARCTIC SITE

Authors: Kathy L. Young, Ming-ko Woo and S.A. Edlund

This study which has been submitted to *Arctic & Alpine Research*, March 1995 describes the field programme and data analysis from two intensive summer seasons (1989, 1990) and data from supplemental years (1991–1993) at Hot Weather Creek, Ellesmere Island, N.W.T.. K. Young carried out the field measurements, analyzed the data, drafted the diagrams and wrote the paper. Dr. M.-K. Woo provided snow survey data for the Heather Creek basin (1990–1993), provided guidance on the paper's outline and reviewed the paper several times. The plant response section analyzes field results obtained from Dr. S.A. Edlund at Hot Weather Creek. Dr. S.A. Edlund also reviewed an early draft of the paper.

SIMPLE APPROACHES TO MODELLING SOLAR RADIATION IN THE ARCTIC

Authors: Kathy L. Young, Ming-ko Woo and D. Scott Munro

This study accepted by *Solar Energy* describes the theory and validation of a solar radiation model using limited data input (temperature, cloud). K. Young wrote the programme, carried out the data analysis, drafted the diagrams and wrote the paper. Dr. M.-K. Woo provided guidance on the paper's outline, and reviewed the paper several times. K. Young learned the basic structure of a clear-sky radiation model from Dr. D.S. Munro in a graduate course. Dr. D.S. Munro provided comments on an earlier draft of the paper.

MODELLING NET RADIATION IN AN ARCTIC ENVIRONMENT USING SUMMER FIELD CAMP DATA

Authors: Kathy L. Young, Ming-ko Woo

This paper submitted to *Solar Energy*, July 1995 describes the theory and validation of a surface energy balance model which was used to simulate net radiation in a permafrost environment. K. Young wrote the programme, carried out all the data analysis, drafted the diagrams and wrote the paper. Dr. M.-K. Woo provided guidance on the paper's outline and reviewed the paper several times.

HYDROLOGIC RESPONSES OF A SMALL HIGH ARCTIC BASIN TO GLOBAL CHANGE IMPACTS

Authors: Kathy L. Young, Ming-ko Woo

This study accepted September 1995 by *Geological Survey of Canada Bulletin* describes the application of a surface energy balance model which uses limited input data to model melt and evaporation for a small high arctic basin. K. Young carried out all of the data analysis, drafted the diagrams and wrote the paper. Dr. M.-K. Woo provided guidance on the outline of the paper.

LIST OF TABLES

LIST OF FIGURES

CHAPTER 1

INTRODUCTION

1.1 Background of Study

Arctic regions play an extremely important role in terms of the earth's atmospheric and oceanic circulation systems (LeDrew, 1993). Growing concern about global change has focussed on the Arctic where General Circulation Models (GCMs) suggest that future increases in temperature and precipitation will be the greatest (Hinzman and Kane; Maxwell, 1992). There is also concern that northern regions will experience changes in cloud cover (e.g. Wetherald and Manabe, 1986) and atmospheric pollution (Blanchet, 1989; Harte and Williams, 1988) but rates, levels of change and their possible environmental impacts are virtually unknown at this time.

This heightened scrutiny of arctic environments has led to a shift in the field of arctic hydrology. In the past, studies were largely driven by resource development and utilization but now the emphasis has been placed more on scientific curiosity (Hinzman and Kane, 1992). Research hydrologists are beginning to realize that hydrologic processes—snowmelt, slope runoff, soil moisture, evaporation and basin discharge—do not operate alone, but are driven and modified by interactions with both the atmosphere and ground surface conditions. Arctic hydrology is entering an era where the linkages and feedbacks between hydrologic processes (e.g. snowmelt, soil moisture) have to be considered in terms of microclimate (e.g. temperature, radiation), vegetation (e.g. surface albedo, plant cover), soil (e.g. texture, structure) and topography (e.g. slope angle, aspect). This more holistic approach to investigating northern hydrologic processes is required not only to settle our own scientific curiosity about what effects global change may have on snowmelt patterns and basin runoff but is also required because of our need to maintain an ecological balance in northern environments. For instance, climate warming through soil moisture changes and shifting nutrient supplies, has the potential of restructuring the character of

northern ecosystems through shifts in species composition (e.g. Bazzaz, 1990; Rizzo and Wiken, 1992; Robinson and Finklestein, 1991). This could eventually affect the traditional, social and economic characteristics of northern communities (Rizzo and Wiken, 1992).

A more complete understanding of environmental interactions is also required to further our present knowledge of ground thaw and slope failures in permafrost terrain (Lewkowicz, 1992) and to assess the sensitivity of northern man-made structures (e.g. pipelines, airports, communities) to global changes.

Northern hydrologic research geared to incorporating atmospheric, and terrestrial interactions has just recently begun and some simulated results showing how hydrologic systems may respond to climate warming have been presented (Hinzman and Kane, 1992; Kane *et al.*, 1992). For example, Hinzman and Kane (1992) through utilization of a HBV hydrological model (Bergström, 1976) for a small continuous permafrost basin (2.2 km^2) have, in conjunction with a ground thermal model (Kane *et al.*, 1991) been able to provide simulations showing basin scale hydrologic responses to possible changes in temperature and precipitation (e.g. snow water equivalent, snowmelt, discharge and evaporation). One of their main modelling limitations is that the snowmelt routine is a simple degree-day approach which offers no opportunity to explore the spatial and temporal variations of radiation and its role in slope snowmelt and evaporational losses. They were also not able to assess possible future changes in clouds or aerosols which could influence both snowmelt amounts and evaporation from the basin (Hinzman and Kane, 1992). In addition, a vegetation routine could not be incorporated into their model because of limited field information. Therefore, they were not able to explore possible future changes in plant cover and their affect on melt and evaporation through alterations in surface roughness and radiation loadings through changes in surface albedo.

Xia (1993) and Woo and Drake (1988) have developed a physically based permafrost model (WAD) which incorporates interactions between pedology and hydrology. Its main linkage

with the atmosphere is through measured solar radiation and air temperature measured at a point. Simulated solar radiation could allow this model to be extrapolated to larger surfaces (e.g. slope, basin, region). The WAD model has been used to explore how changes in temperature and precipitation will affect frost table and water levels, but due to its present structure has not been able to assess how future changes in clouds or aerosol levels could modify permafrost hydrology.

There are several obstacles facing arctic hydrologists as we attempt to evaluate environmental interactions and speculate on possible global impacts and one of these is that a rigorous data baseline, tracking environmental variations in space and time, is lacking. This is not surprising considering the short-term record of hydrologic, botanical and climate data collection in the North. For instance, there are only four Canadian Government atmospheric stations in the Canadian Arctic Islands, and only about 50 years of continuous weather data exists.

Clearly, what is presently needed are experimental sites which are representative of large permafrost areas and can provide a range of hydrologic responses to variations in terrain (e.g. topography, surface conditions) and microclimate (e.g. temperature, radiation, precipitation).

Another problem faced by northern hydrologists as we attempt to understand present-day interactions and future changes is scale. A major criticism of GCMs is that they operate at large scales (e.g. several degrees of longitude and latitude) while, hydrological processes operate at much smaller scales (Dooge, 1992) (e.g. point, quadrat, transect, slope, sub-basin, basin, region). GCMs do not consider local variations in topography, plant cover and soils which can influence rain and snow amounts and modify radiation loadings. Subsequently, GCMs cannot provide at present the detailed temporal and spatial information needed for impact assessments (Robisnon and Finklestein, 1991). At this stage, future changes in stream discharges and basin storage cannot be anticipated easily. Regional climate models have begun to address this issue. They provide atmospheric data for hydrologic modelling that begin to reflect the natural heterogeneity at the regional scale (e.g. orographic rainfall) (Hostetler, 1994). Their major

limitations however, are they are still linked with GCMs, computer demand is high and the regional scale is still larger than is of present interest to most northern researchers.

It is the opinion of several researchers (e.g. Church and Woo, 1990 Hostetler, 1994; Running *et al.*, 1987), that scaling-up is required. The variability which exists at the local scale in terms of topography, surface conditions and microclimate needs to be considered, since it influences snow amounts, snowmelt patterns, and evaporation rates. Only by considering variations at the local scale will reasonable responses at higher scales (basin, region) be realized (Church and Woo, 1990; Hostetler, 1994; Running *et al.*, 1987). Hostetler points out further that confirmation of this approach should be met with measured data.

Determination of spatial and temporal variations of hydrologic processes as a response to terrain and microclimate is not an easy task, even at the local scale. Arctic terrain can range from flat, to rolling to mountainous. It is composed of slopes of varying aspects and angles, plant cover and soil characteristics. Instrumentation is expensive and it is often not economically possible to monitor temperature and radiation for a whole suite of environments comprising one's study site. In fact, in many cases the only available data is weather information gathered two times/day by scientific filed camps scattered throughout the Canadian Archipelago. Often, twice-daily cloud, temperature and wind data comprise the minimum amount of data provided by these camps. However, computer modelling offers the possibility of taking these limited data and extrapolating to larger surfaces (slope-basin), thus, offering the potential to describe both present-day hydrologic processes and future impacts of global change.

Several scientists (e.g. Dooge, 1992; Hinzman and Kane, 1991, 1992; Robinson and Finklestein, 1991) have suggested that the surface energy balance approach offers the best alternative for understanding the present-day linkages and feedbacks between terrain, atmospheric and hydrologic processes and accounting for the local variability. Point information can be aggregated and then extrapolated to larger scales (slope, basin, region). These models developed

at the local scale, provide information which is directly applicable to impact assessments (Robinson and Finklestein, 1991).

1.2 Objectives of this study

Considering the above observations, the objectives of this study are:

1) To investigate the present-day spatial and temporal variability of the local microclimate, hydrology and surface conditions (soils, plant cover) at a High Arctic site (both level/sloping) during two contrasting summer seasons (1989-cool/wet; 1990-warm/dry). This will: a) allow the linkages and feedbacks between the atmosphere and land surface processes to be established under present conditions; b) provide a baseline of natural conditions so that future global impacts can be assessed and c) provide field measurements for model input and validation.

2) Given that energy availability is a driving force behind many important land surfaces processes (e.g. melt, evaporation), this study will show the applicability of a cloud-layer solar radiation model which uses limited field camp data (twice-daily cloud and temperature) in providing daily solar radiation.

3) To develop and assess the applicability of a surface energy balance model which applies a cloud-layer solar radiation model, employs limited field camp data (twice-daily cloud, temperature, wind, precipitation) gathered at one point and allows this information to be extrapolated to different terrains (slopes and plateau) so that surface energy fluxes can be simulated.

4) To simulate melt and evaporation for a small High Arctic basin and demonstrate the applicability of the surface energy balance model at the basin level through a simple surface water balance approach.

5) Examine the hydrological responses of a small continuous permafrost basin to selected atmospheric and terrestrial impacts.

To achieve these objectives, the thesis has been broken down into a series of papers which form the different chapters. A literature review and a description of methods pertaining to each aspect of the thesis is contained within each chapter.

Chapter two entitled *Influence of local topography, soil and vegetation on microclimate and hydrology at a High Arctic site* provides information on the study area, and a description of the field measurements used in 1989 and 1990. The chapter provides baseline information on the spatial and temporal variability of the local microclimate, hydrologic processes and their interaction with the terrain surface. This chapter also provides both input and validation data for a solar radiation and a surface energy balance model.

Chapter three entitled *Simple approaches to modelling solar radiation in the Arctic* outlines the theoretical framework of a solar radiation model and shows the performance of the model using different cloud approaches in attenuating incoming clear-sky solar radiation. It shows the performance of the solar radiation model when only twice-daily cloud information is available.

Chapter four entitled *Modelling net radiation in an arctic environment using summer field camp data* applies the solar radiation model within a surface energy balance approach. The ability to translate limited field camp data (twice-daily temperature, wind, cloud) at a point to nearby slopes and plateaus is assessed. The performance of the model at both level and sloping sites is made through a comparison of simulated and measured net radiation.

Chapter five entitled *Hydrologic responses of a small high arctic basin to global change impacts* tests the utility of the surface energy balance model to a larger area (small basin). Snowmelt and evaporation are simulated for different terrain facets within the basin and confirmation of the model's applicability is tested within a simple surface water balance for two contrasting summer seasons (1989, 1990). This chapter also illustrates the hydrologic responses

of a small continuous permafrost basin (6.1 km^2) to selected atmospheric and terrestrial global change impacts.

Chapter six summarizes the conclusions and presents suggestions for future research leading from this study.

CHAPTER TWO

INFLUENCE OF LOCAL TOPOGRAPHY, SOIL AND VEGETATION ON MICROCLIMATE AND HYDROLOGY AT A HIGH ARCTIC SITE

Authors: Kathy L. Young, Ming-ko Woo[1] and S.A. Edlund[2]

Submitted to Arctic and Alpine Research

March 1995

Geography Department, York University, North York, Ontario, M3J 1P3

[1] Geography Department, McMaster University, Hamilton, Ontario, L8S 4K1

[2] Geological Survey of Canada, 601 Booth Street, Ottawa, Ontario, K1A 0E8

ABSTRACT

The spatial variations of soils, microclimate, hydrology and vegetation were studied on four slopes and a plateau site located within a 1 km^2 area in the continuous permafrost zone of Arctic Canada. An understanding of such variability on a local scale is useful when point observations are upscaled to match the dimensions of regional climate models. The field season covered two summers with contrasting climatic conditions. During the warm, dry summer, the between-slope spatial differences in radiation, air and ground temperatures were exaggerated, while during the cloudy summer, diffuse rather than direct solar radiation prevailed and the differential heating between slopes was reduced. While the ground thaw increased in the warm year, maximum thaw depth at any site was also affected strongly by vegetation and soil characteristics, the latter being controlled by local geology and the geomorphic processes. Precipitation on slopes may be influenced by wind and snow accumulation is governed by local topography such as slope concavities. Snow ablation was largely accomplished through radiation melt so that albedo changes were a major consideration. Meltwater runoff was maintained only downslope of deep snowbanks, and only the lower slopes experienced continuous saturation or groundwater flow. In general, the microclimate responds directly to annual fluctuations of the regional climate and to the local terrain. The spatial pattern of snow accumulation, frost table configuration and surface or groundwater flows tend to recur annually. The distribution of vegetation and soil is established through long-term adaption to the microclimate, hydrology and geomorphology of the local sites.

KEY WORDS: Arctic Hydrology, Ecology, Geomorphology, Microclimate, Permafrost

INTRODUCTION

All Global Climate Models (GCMs) suggest a significant warming of the Arctic under an increase of the atmospheric concentration of CO_2 and other greenhouse gases (Maxwell, 1992) and this is expected to have notable effects on the Arctic environment (Roots, 1989; Rizzo and Wiken, 1992). Scenarios of changes in the ecotone have been postulated (Emmanuel et al., 1985; Webb, 1987), but Edlund (1992) pointed out that such factors as soil and topography in addition to the climate, will affect the regional pattern of vegetation response. While some of the relationships between the environmental elements have been studied (e.g. Chapin et al., 1979; Peterson, 1974), there are no comprehensive investigations on the interactions among the local topography, the microclimate, the soil, hydrology and the vegetation. Such investigations are needed to enable the extrapolation of point observations, be it for the purpose of global change monitoring or the interpretation of paleo-records. It is the objective of this study to determine the spatial and temporal variability of the microclimate and hydrology of a small area in the Arctic and to examine their linkages with the local environmental factors. The results will clarify their complex relationships on a local scale, and this may enhance the up-scaling of point data in environmental change studies.

STUDY AREA

A site covering an area of about 1 km^2 and located in the Hot Weather Creek (HWC) basin, Fosheim Peninsula, Ellesmere Island (79°58'N, 84°28'W) was chosen for this study. The Fosheim Peninsula has been designated as a Geological

Survey of Canada (GSC) Global Change Observatory and is the location of several geological, geomorphological, biological, hydrologic and climatic studies. The Eureka weather station, 25 km west of the study site, provides over forty years of climatological data, against which our study period can be compared.

Geologically, the oldest rock unit in the HWC basin is the Expedition Formation of the Palaeocene Eureka Sound Group (Ricketts, 1986; Thorsteinsson, 1969; 1971). A section of it, over 600 m thick, outcrops south of the base camp (Hodgson et al., 1991), consisting of quartz-rich white sandstone, overlain by alternating sandstone, shale and coal beds. Overlying it is the Strand Bay Formation (< 200 m thick) which is composed of thick sandstone, thin coal seams and dark grey shale. The Iceberg Bay Formation is the uppermost unit and is the thickest encountered at HWC (> 200 m). This unit consists almost entirely of sandstone-coal cycles deposited initially under barrier island, deltaic and lagoonal environments. Carbonaceous beds can reach 6 m thick, mostly of lignite. Deformation of these rocks during the Eurekan Orogeny resulted in north-south to northeast-southwest structural trends in the HWC basin.

Remnants of alluvial terrace sediments consisting of unconsolidated sand overlain by gravel occur on top of the Northwest and West-facing slopes. These materials are well-drained and resistant to mass wasting. Weathered bedrocks of folded and faulted sandstone and shale cover large parts of the basin, yielding greyish brown sandy loam. Tills are present, consisting of materials that range from granules to boulder clasts of resistant quartzitic sandstone, dolomite and diabase, lithologies uncommon to the Eureka Sound Formation. However, their age is

uncertain and it is unclear whether the Fosheim region was glaciated in the late Quaternary (Hodgson, 1984).

HWC lies within the early Holocene marine limit so that areas below 140-145 m have a discontinuous cover of weathered marine, estuarine and deltaic deposits, composed of medium to fine-grained sand, silt and minor clayey silt, sandstone granules, coal fragments, detrital plant materials or molluscs. These materials commonly are interbedded 1 mm to 100 mm thick, with a white surface crust of calcium-magnesium sulphate, up to several mm thick, overlying unvegetated zones.

Massive and shallow ground ice is present in the marine sediments but their areal extent is unclear (Robinson, 1994). Thermal contraction cracking is widespread, ranging from fine cracks on the ground surface to larger cracks measuring 0.04 x 0.06 m across and 0.12 m deep. Larger cracks provide infiltration pathways for rain, snow and ice meltwater. Consequently, plants tend to occur at these openings (i.e. Salix arctica) where the ease of root penetration facilitates access to deeper water and nutrient sources. In addition to soil cracks, the lowland is dissected by high-centre polygons measuring over 30 m across, within which are fields of earth hummocks 0.1 to 0.5 m high. The plateau has many ponds formed at the junctions of the polygon troughs. Smaller slope hummocks are common on many steep slopes (Lewkowicz and Gudjonsson, 1992).

Summers are more moderate than most areas of the Queen Elizabeth Islands, with July temperatures of at least 5°C being common. This regional temperature

anomaly is due to the surrounding mountains which block off most cyclones and low level clouds from the Central Arctic Ocean (Edlund and Alt, 1989), allowing higher radiation input to warm the air and the ground. One consequence is a greater vegetation diversity (over 140 vascular plant species in the HWC basin) compared with elsewhere in the Queen Elizabeth Islands (Edlund, 1988).

The study area has rolling topography. Five sites (one plateau and four slopes) were selected for detailed investigation (Fig. 1). The Northwest (NW) facing slope has a gradient of 0.2 (11.5°) and the slope length from the pond edge to the top of the middle pipe is about 44 m. The Southeast (SE) facing slope lies directly across from the NW slope and has a more gentler gradient of 0.12 (6.8°). Its slope length is longer (approx. 73 m) from the pond edge to the upper middle pipe. The East (E) facing slope consists of three sections: two segments with a gradient of 0.2 (11.3°) separated by a gentler slope of 0.03 (1.9°). The entire slope measures about 98 m. The West (W) slope is steep (0.38 or 20.1°) and short with a slope length of only 21 m.

METHODS

Our intensive study spanned two summers, one of which (1989) was cool and wet and the other (1990) was warm and dry. In subsequent years, 1991-1993, supplementary field data (frost and water tables, precipitation totals) were also obtained. An automatic weather station was installed by the Atmospheric Environment Service at the Plateau (P) site (31 m above base camp) to monitor solar

radiation, air, surface and ground temperature, wind speed and direction and relative humidity (Headley, 1990). In addition, net radiation and rainfall, air and near surface temperatures, relative humidity and wind speed and direction were recorded on the four slopes, while spot albedo measurements were made with a single inverting pyranometer. Table 1 lists the instruments used and their level of accuracy and Figure 1 shows the location of their deployment.

Snow surveys were carried out in early to mid-May following a method described by Woo and Marsh (1978). Snow ablation (in water equivalent units) was obtained daily by measuring the rate of surface lowering and multiplying the lowering rate by the snow surface density (Heron and Woo, 1978). Slope runoff from NW and E slopes were measured using methods modified after Lewkowicz and French (1982). Soil moisture was monitored by Time Domain Reflectometry once every few days (Brisco et al. 1992). Probes were inserted vertically to obtain an integrated value of the surface soil moisture in the rooting zone (1-100 mm).

On each study slope, a network of 9 to 12 groundwater wells was installed. Manual water level readings were taken every few days in 1989 and daily in 1990. Single auger hydraulic conductivity measurements were made at several wells using a method described by Luthin (1966).

Soil samples were obtained from the lower, middle and upper sections of the slopes and on the plateau. Soil pits down to a depth of 0.9 m were also dug for sampling. All samples were analyzed for particle size distribution and organic content. In addition, specific yield, specific retention, bulk density, and porosity

were determined for column soils, using methods given by Luthin (1966) and Jumikis (1984).

Frost table measurements were made once every several days near all groundwater wells. Frost depth was obtained by pounding a steel rod into the active layer until the hard frozen substrate was encountered. Voucher specimens of all vascular plants found on the four slopes were identified and deposited with the National Herbarium, Canadian Museum of Nature. Nomenclature follows, as far as possible from Kartez and Kartez (1980) which updated that of Porsilid and Cody (1980). Percentage vegetation cover was measured in 1976 and 1988. Plant communities are designated by the dominant vascular plant and common associates.

RESULTS

SOIL

Pedogenesis

The formation of soil is strongly influenced by present-day slope processes which continuously erode or deposit materials on the slope. The rapidity of change is demonstrated by the measurement of nine erosion pins inserted over an area of 6 m across the lower, middle and upper parts of the NW slope in August 1989. Measurements of these pins following the snowmelt period of 1990 showed that the upper slope lost 1 to 4 mm of soil, the middle slope lost 1 mm at one pin, showed no change at another pin and accumulated 7 mm at the third. On the lower slope, two pins indicated no change while the third pin had an accumulation of 9 mm.

Rapid erosion or deposition has likely prevented the establishment of a plant cover on the soil. Elsewhere, aeolian deposition is common on slopes, usually as windblown materials incorporated with the snow and then left on the ground after the snowmelt (Edlund and Woo, 1992; Lewkowicz and Young, 1991). Where the marine deposits have abundant ground ice, slope failure is common (Lewkowicz and Gudjonsson, 1992). The occurrence of active layer detachment slides completely rearrange the soil profiles.

Soil Characteristics

Organic content, porosity and particle size distribution of the samples obtained from soil pits and from the surface soil layer are presented in Figures 2 and 3. Following Nadelhoffer et al. (1992) these soils can be classified as polar desert soils since they exhibit thin organic mats, thaw relatively deeply and are generally well drained and covered by varying percentages of heath and dwarf shrub vegetation.

Three main features are evident from these soil samples. First, the large amount of fines <0.074 mm in the samples reflects the mechanical weathering of marine deposits and aeolian deposition of fine sand, silt and clay. Only the W slope has much medium sand. This site probably experienced fluvial deposition in the past since it is on an alluvial terrace adjacent to the present-day Hot Weather Creek. On the P, the small depressions have more fines than their adjacent hummock fields,

possibly because of the accumulation of fine materials washed into the depressions during the snowmelt seasons.

Second, the abundance of fines gives rise to relatively high porosites, with the pit samples from the SE slope being the most porous. A third feature is the high organic content in many samples which corresponds with the intercalation of organic-rich layers in some slopes as confirmed by excavation observations. Most noticeable are the profile samples for the E and W slopes. Organic contents obtained at 0.2-0.4 m below the surface on the E slope are much higher than the upper and lower depths. Organic content of samples retrieved at the W slope tends to increase with depth.

Low organic contents were obtained from both vertical and surface samples of the NW slope even though it has a distinctive woody plant dominated community composed of Cassiope tetragona (35% cover) mixed with Dryas integrifolia and Salix arctica (5-20%) at the footslope. Surface samples were obtained on the lower slopes where sediment had been washed into the inter-hummock cracks, thus reducing the overall organic contents.

These soil characteristics may be related to the soil forming processes. The weathered products of the Eureka Sound Formation, marine deposits, fluvial sediments and glacial till provide materials for soil development. The deposition of aeolian materials, and their subsequent transport downslope by slopewash, leads to smothering of the vegetation and the intercalation of clastic layers with organics. The fresh sediments also provide opportunities for newly invading plants such as

Papaver radicatum and graminoids. Mass wasting also plays a significant role by making materials available for wind erosion, burying vegetation and moving materials downslope.

MICROCLIMATE

Albedo

Albedo, defined here as the ratio between reflected and incoming global radiation varied spatially during the snow-covered period. Spot measurements of albedo on the lower, middle and upper section of the experimental slopes showed that when the snow cover was complete, and where the aeolian deposits on the snow were minimal or when new snow fell, the albedo values were large, varying from about 0.80-0.50. After May 30, surface albedos declined rapidly to about 0.20-0.25 when the snowpacks began to thin, particularly where mineral and organic detritus were blown on the slopes (i.e. sections of the W and E slopes).

Following the snowmelt period, the surface albedo for different sections of the slopes showed no significant differences (Table 2). No significant difference in albedo was encountered for different plant types. For instance, the surface albedo for Salix arctica (lower sections of the E and SE slopes) was the same as Cassiope tetragona (lower NW slope).

Net Radiation

Net radiation (Q*) or the radiation balance is

$$Q^* = (1-\alpha) K\downarrow + (L\downarrow - L\uparrow) \quad (1)$$

where α is the albedo; $K\downarrow$ is the incoming short-wave radiation; $L\downarrow$ and $L\uparrow$ are the incoming and outgoing long-wave radiation (all fluxes in W/m^2). Figure 4 shows the seasonal net radiation pattern for a cool, wet year (1989) and a warm, dry year (1990). In both years, net radiation was low at the beginning of the melt season when the snow cover was uniform and clean (high albedo). Continued melting reduced the albedo contrast between different slopes, depending on the rate of snow metamorphism and ablation, and the amount of aeolian materials deposited on the snow. Net radiation was mainly a function of (1) the changing surface albedo and (2) topography (slope and aspect) which controlled the amount of short-wave radiation received by each site.

Net radiation contrast between the slopes after the snowmelt period declined, owing to more uniform albedo values for bare and vegetated sites (see Table 2). Differences between slopes were less in the cool and cloudy year (1989) when overcast conditions (Fig. 5a) elevated the contribution of diffuse radiation which is little influenced by the topography. The prevalence of less cloudiness in 1990 increased the contribution of direct radiation which is topographically controlled. This in turn caused the net radiation to be more variable between sites (Figs. 5b, c).

Temperature

Air temperatures in both 1989 and 1990 rose rapidly to above 0°C by May 30 (Fig. 6). The summer of 1989 was cooler and the predominantly overcast conditions reduced the difference in temperature between slopes. Clear sky and partly cloudy conditions do produce slight temperature differences between slopes (Figs. 7b, c).

Similar to the air temperature patterns (Fig. 6), temperature near the surface (10 mm depth) increased rapidly to above 0°C at the beginning of June during the snowmelt season (Fig. 8). On a daily basis, the surface temperature contrasts among slopes were exaggerated compared with the air temperature differences as can be seen for the E and W slopes (Fig. 7 and 9). Surface temperatures were consistently higher in the warmer year (1990) from June 9 to July 9, after which the trends for both years were comparable (Fig. 8b). Greatest daily variations between the slopes occurred during the snowmelt season and can be attributed to changing soil moisture conditions (see Hydrology section) and variable radiation loadings during a period of low cloud cover.

Both seasonal and daily variation between the slopes are minimized under overcast conditions (Figs. 8a, 9a). Slightly greater differences between the slopes during a warmer, dry season (Fig. 8b) also produced early daily peaks in ground surface temperature on the E slope compared with the W slope.

Precipitation

End-of-winter snow accumulation was obtained by ground surveys in May from 1989 to 1993 (Fig. 10 and Table 3). Total snow water equivalent from 1989 and 1990 for the NW slope and P were significantly higher than the other years but accumulations on the SE, E and W slopes were similar over this five year period. Dominant wind direction at HWC was from the north during the winters (Fig. 10) of 1989 and 1990 but this cannot explain the large snow accumulation on the NW facing slope.

Episodic events of blowing snow from the south together with the local topographic effects on snow deposition may account for that anomaly. The very low accumulation on the W slope measured in 1989 was due to the late snow survey when sublimation had already depleted part of the snow cover. Measured sublimation values obtained by small lysimeters (Ohmura, 1982) in May, 1989 suggest that snow losses before the main melt period could approach between 0.1 to 1.0 mm/d.

On a local scale, the snow distribution pattern on slopes was highly uneven. For 1990, for example, both the E and the SE slopes had large snow accumulations at the concave bottom portion of the slopes (Fig. 11). The large snow accumulation above the middle of the E slope represented the tail end of a semi-permanent snowbank formed in a hollow adjacent to this slope section. For the W slope, a sharp change in gradient on the upper part of the slope coincided with the zone with more snow. The upper part of the NW slope had a substantial amount of

snow and this may be attributed to a drop in windspeed. Figure 12 shows that the daily windspeed recorded at the NW slope was often lower than that on the P, while for the other slopes, the windspeed was comparable. A drop in wind speed during snow events encourages the deposition of the blowing snow which leads to greater snow accumulation (Young and Lewkowicz, 1990).

Total precipitation for June and July measured at the various experimental sites is compared with the record from the Eureka weather station (Fig. 13). Most of this precipitation was rainfall but it also included the occasional snow event. The summers of 1990 and 1992, had low precipitation and there was little difference in the precipitation measured on the slopes at HWC and that reported at Eureka. The summer of 1989 was wetter and the experimental slopes received 5 to 70 mm more precipitation than the Eureka station. Overall, the NW and the E slopes received the greatest amounts. A windrose diagram (Fig. 13) obtained for the summer of 1989 from the P indicates that the prevalence of winds is from the southwest. Reduction in windspeed on the leeward slopes such as the NW and the E slopes may have led to more rainfall deposition.

HYDROLOGY

Snow Ablation

Spring melt releases the water held as snow storage accumulated over the winter. Snowmelt occurred earlier in thin snowpatches (SE, W) than in thicker ones (NW, E) (Table 4).

Snowmelt is controlled by the energy balance at the snow surface:

$$Q_M = Q^* + Q_H + Q_E + Q_P \quad (2)$$

where Q_M is the melt energy flux, Q^* is the net radiative heat flux; Q_H is the sensible heat flux; Q_E is the latent heat flux; Q_P is the heat flux transmitted by rainfall and all fluxes are in W/m^2.

In this study, Q_M was determined by the direct measurement of daily melt ablation

$$Q_M = L_f (\rho_s / \rho_w) M \quad (3)$$

where M is the measured rate of snow surface lowering (m/d), L_f is the latent heat of fusion (0.33 MJ/kg), ρ_s is the measured density of snow and ρ_w is the density of water (1000 kg/m^3).

Rainfall was negligible during the melt period so that Q_p was unimportant. The remaining fluxes are lumped and treated as a single entity (Q_T), obtained as residual of the surface energy balance.

$$Q_T = Q_H + Q_E = Q_M - Q^* \quad (4)$$

where Q_T is considered as the turbulent fluxes. The daily contribution of the net radiation and the turbulent fluxes to snowmelt is presented in Fig. 14. Prolonged snowmelt on the NW slope (> 8 days longer in 1990) was due to its large snow accumulation.

Snowmelt began when mean daily air temperature was still <0°C but increased quickly when the daily mean temperature was above 0°C. In the early part of the ablation seasons, net radiation was small and the turbulent fluxes were negative. The latter was mainly due to the heat required for snow sublimation. As melt progressed, the dust inside the snowpack was exposed at the surface. This, together with the increased water content in the snow, greatly reduced the albedo and raised the net radiation. Continued warming of the air raised its temperature so that sensible heat flux became larger and therefore the turbulent fluxes became positive. Over the melt seasons, net radiation was the dominant energy source for snowmelt on all the slopes. On the P, net radiation was less important as a contributor to melt (Table 4) because its snow cover was cleaner and more continuous than on the slopes.

Snowmelt Runoff

No surface flow occurred on the SE and W slopes in 1989 and 1990. Data from the 1990 field season are presented (Fig. 15) to demonstrate the variable slope runoff pattern occurring at the other slopes. Runoff started on May 31 but the flow

was initially low because of low net radiation receipt and low air temperatures (<0°C), so that the flow did not exceed 0.009 $m^3/m/d$ at the NW slope and 0.004 $m^3/m/d$ at the E slope.

By June 6, the shallow snow at the lower NW slope ripened quickly and runoff increased. Its runoff peaked at 0.6 $m^3/m/h$ on June 7 and declined to 0.05 $m^3/m/h$ on the next day as the shallow snow was depleted and as more meltwater infiltrated the thawing soil. Runoff rose on June 8 at the E slope plot, yielding significant flow for about five days ~0.04-0.18 $m^3/m/h$. Surface flow was maintained by a deep snowpack upslope while the 75% plant cover (Salix arctica community) on this section of the slope retarded ground thaw to curtail meltwater infiltration losses.

Frost Table Development

The storage and movement of water is largely confined to the thawed zone below which the frozen ground is relatively impermeable. Above the frost table is often found a saturated and a non-saturated zone. Where the water supply is ample and where the frost table is near the surface, the saturated zone rises above ground to generate surface runoff (Woo, 1986). In terms of plant growth, thawing of the active layer allows the roots to develop and to access both the moisture and the nutrients in the soil. For these hydrological and botanical reasons, the pattern of frost table development plays an important role.

Frost table development depends on (1) the length of the thawing period which is strongly affected by the timing of snow disappearance on the ground, (2) the slope materials which govern the thermal conductivity and (3) the weather conditions of the summer.

Ground thaw often begins around mid-June as the snow on the ground disappears (Fig. 16). The rate of snowmelt varied, however. For instance, the frost table on the eastern portion of the SE slope remained shallow throughout the season because the snow which accumulated in small depressions was slow to disappear. In contrast, despite the considerable amount of snow on the southern edge of the E slope that delayed frost table development, rapid melting soon depleted the snow and the frost table deepened. Large snow accumulation on the middle section of the NW slope delayed ground thaw, but by the end of summer this section had the deepest thaw because of the large thermal conductivity of its soil (low in both organic content and in porosity) that allowed more heat to be conducted into its active layer.

The frost table tended to be shallower at the lower segments of the NW, SE and E slopes. The lower E slope has a relatively continuous cover of Salix arctica which shades the ground. On the lower NW and the SE slopes, the occurrence of shallow frost tables is due to the presence of peaty materials which have low thermal conductivities that hinder ground thaw.

The spatial pattern of the frost table development remained similar between years, suggesting a persistence of the snow distribution pattern and the strong

influence exerted by soil and vegetation. On the other hand, the rate of ground thaw and the maximum thaw depth attained by the end of summer were different from year to year. Table 5 shows that 1990 experienced the most rapid thaw development, with maximum thaw being attained about two weeks earlier than in the other years. This was due to its warm summer accompanied by low rainfall. Snowmelt in 1992 was about three weeks later than in 1989 and 1990, thus shortening the thawing season and reducing the maximum thaw depth attained.

Soil Moisture

The moisture content at the top 0.1 m of the soil was obtained for the lower, middle and upper portions of the slopes and compared with the range of moisture contents determined at the plateau site (Fig. 17). The replicated plateau measurements demonstrate the considerable variability of moisture within a confined area (10 x 10 m^2) such that the representativeness of single point data cannot be established easily. In the discussion to follow, observation from the P site provides the "control" data against which the slope moisture information can be compared to detect any notable departures from the flat terrain. The general tendencies of spatial and seasonal changes in the soil moisture regime on the slopes may be discerned from the data pooled from their slope segments. The soil moisture contents for all sites was lower during a drier, warmer summer (1990) than during a wetter, cool one (1989). Moisture content was initially high after the snowmelt period of 1990. After that, the decline in the moisture levels may be linked to increased evaporation and lateral drainage in the deepening thawed zone. For instance, the rapid drop in

the moisture content of the NW slope in both years following snowmelt may be attributed to the large amount of fine sand which when thawed provided good drainage (hydraulic conductivity is between 4 x 10^{-3} to 1 x 10^{-2} mm/s). Similarly, the lower segments of the SE and E slopes with high content of fine sand provided good drainage (hydraulic conductivity of 2 x 10^{-3} to 1 x 10^{-2} mm/s). Drainage, together with increased evaporation during a period of high radiation, dried out the soil quickly. Soil moisture values rose gradually at the end of summer as rainfall increased and as evaporation dropped.

Differences in the soil moisture pattern of the slopes and on the plateau were reduced during the wet season of 1989. This was due to the large amount of rainfall and to the similar net radiation regime for all slopes (Fig. 4a). The exception was the NW slope which had lower moisture contents, because of rapid drainage of its sandy soils.

Notable departure of slope moisture values beyond the range of the "control" data from the plateau occurred during the warm, dry summer of 1990, suggesting that the local topography played a more prominent role in modifying the soil moisture under sunnier, drier conditions. For example, the low soil moisture levels on the middle and lower sections of the W slope at the beginning of the thaw season in 1990 was related to the low snow accumulation and early snowmelt which allowed these segments to dry out early. The concavity on the upper W slope accumulated more snow and there was more shading to reduce evaporation; hence its soil was more moist.

Groundwater

Most of the groundwater wells remained dry in 1989 and 1990. Only the lower parts of the slopes (except the W slope) experienced continuous or intermittent saturation. A saturated zone was also maintained on one side of the E slope below the late-lying snowbank.

Where a saturation zone existed, a high water table in the early season was maintained by snow meltwater at the site, or by an ablating late-lying snowbank upslope of the site (e.g. left-hand side of E slope, Fig. 18a). The water table rose during rainfall events (Fig. 18b), but declined as evaporation caused water losses from the slopes. The high water table on the left-hand footslope of the NW slope (Fig. 18c) was caused by the local concavity which collected subsurface drainage in this localized depression.

Groundwater flow (Q_s) was evaluated at several sites along the NW, SE, and E slopes using the Darcy equation:

$$Q_s = kd_s (dh/dx) \quad (5)$$

where k is the hydraulic conductivity (m/d), dh/dx is the hydraulic gradient estimated by the elevation of the water table in adjacent wells, and d_s is the thickness of the saturated zone, obtained daily as the elevation difference between the frost and the water tables.

The NW slope has the greatest total flow. Its flow season was longer and its initial flow was higher than at the E slope (Fig. 19) because the NW slope had more snow and a higher hydraulic conductivity (0.1643 m/d, compared with 0.0432 m/d at the E slope). There was no groundwater flow on the SE slope during the early season because of insufficient snow, but flow appeared later in the season, suggesting the contribution from ground ice melt.

One interesting feature was the reversal of flow on the lower left hand side of the NW slope: from the peaty soil backward toward the more deeply thawed sandy section about 10 m upslope (Fig. 19a). This was due to a deeper and faster thaw of the sandy materials to create a "depression" in the frost table, into which the suprapermafrost groundwater drained. This example demonstrates the importance of soil materials in influencing ground thaw rates and subsurface water movement.

PLANT RESPONSE

Figure 20 summarizes the percentage cover of vascular plants at each study site. Two main vegetation types are prevalent: Dryas integrifolia and Salix arctica. These woody plant-dominated communities are typical of moderately to well drained stable silty soils of the lowlands of Fosheim Peninsula and the inter-montaine zone of the north-central Queen Elizabeth Islands (Edlund and Alt, 1989; Woo et al., 1989). Cassiope tetragona only forms a dominant presence on the lower portion of the NW slope and can be related to the extended meltwater supply afforded by the late-lying snowbank (Woo et al., 1989).

Salix arctica dominates all slopes and the plateau. It generally sends roots in shallow troughs and depressions, and into major cracks between hummocks to tap the moisture from the deeper thawed zones (Edlund et al., 1990). The upper-most part of the NW slope has species more typical of recently disturbed sites (e.g. Papaver radicatum). As mentioned previously (see Soils), this site experiences both aeolian deposition and erosion. Meltwater conveys sediment from upslope to be deposited in low-lying depressions in the Cassiope tetragona heath community. Subsequently, plants cannot establish themselves easily on the upper portions of the NW slope.

The W slope tended to have the lowest coverage of plants, with a continuous plant cover restricted to a meltwater channel located on the upper part of the slope. The abundance of bare ground reflects the lower soil moisture because this slopes usually has less snow and suffers higher losses to evaporation. These conditions provide a xeric environment for plant growth.

Poor drainage in the lowland between the NW and the SE slopes gives rise to a wetland plant community, composed of Carex aquatilis var. stans, Eriophorum scheuchzeri, and Dupontia fisheri, with Salix arctica on a slightly raised swale growing on peat.

Overall, vegetation tended to be more prevalent in sites with greater snow accumulation (e.g. the lower part of the E and the SE slopes). There, the snow affords protection to the plants from strong winds and provides ample moisture. Vegetation cover tended to decrease upslope, likely caused by declining soil moisture

and greater exposure to wind. Frost tables tended to be shallower under vegetated sites than beneath bare zones. Plants provide shade to reduce the ground temperature while the production of biomass increases the organic contents of the soil, to lower its thermal conductivity. In an extreme case, the wetland environment with peaty soils yields the most shallow active layer thaw.

DISCUSSION AND CONCLUSION

This paper documents the local variability of soils, microclimate, hydrology and vegetation within a small area in the continuous permafrost zone. Observations from the HWC area showed the linkages and feedbacks among the environmental variables. Their temporal and spatial responses to the local conditions may be identified as direct, recurrent or long-termed.

(1) **Direct responses:** Microclimate, itself affected by topography and the regional climate, often sets the conditions for other variables to respond. Variations of radiation on slopes, particularly during years with few cloudy periods, have effects on the initiation, duration and intensity of snowmelt, as well as evaporation. Areas with little snow yields no surface runoff while ground thaw is accelerated and soil moisture is low if early melt and warm, dry summer conditions extend the ground heating and the evaporation season (e.g. 1990). This pattern differs from a cold, wet summer (e.g. 1989) where ground thaw is shallower and the soil moisture content is higher.

(2) **Recurrent responses:** Snow distribution, frost table configuration and groundwater flow exhibit recurrent spatial patterns, even through the magnitudes

vary from year to year. Thus, deep snow drifts are frequently expected on slope concavities and shallow ground thaw is expected in soils rich in organic matter, while well-drained slopes with high energy input seldom sustain prolonged groundwater flow.

(3) **Long-term responses:** The spatial distribution of vegetation and soil represents long-term adaption to the microclimate, hydrology and geomorphological activities of the local sites. The evolution of soils and plants is a slow process, that manifests the response to the local conditions averaged over a period of years.

Given the spatial variability and different response rates to the environmental factors, limited samples in space and time may not yield a representative set of conditions even for a small area. Our field results therefore cautions that the spatial and temporal variations of local environments must be considered before point measurements of frost depth, snow amount, vegetation cover, soil moisture etc. are upscaled for use in climate change detection.

ACKNOWLEDGEMENTS

This work was funded by a research agreement with the Department of Energy, Mines and Resources and a grant from Natural Sciences and Engineering Research Council to M.-K. Woo and a northern training grant from the Department of Indian and Northern Affairs. The logistical support of the Polar Continental Shelf Project is gratefully acknowledged. We wish to thank Dr. Bea Alt, Shannon

Glenn, Sharon Reedyk, Tim Siferd, Kelly Thompson, Paul Wolfe for their assistance in the field, and Angus Headley for the loan of instruments. Diagrams were skillfully prepared by R. Hamilton and C. King while K. Armstrong carefully typed the final draft of this paper. We acknowledge the A.E.S. Canadian Climate Centre through Mike Webb for providing Eureka station data.

REFERENCES CITED

Brisco, B., Pultz, T.J., Topp, G.C., Hares, M.A., and Zebchuk, W.D. 1992. Soil moisture measurements using portable dielectric probes and time domain reflectometry. Water Resources Research 28(5): 1339-1346.

Chapin, F.S., Cleve, K.V., and Chapin, M.C. 1979. Soil temperature and nutrient cycling in the tussock growth form of Eriophorum vaginatum, Journal of Ecology 67: 169-189.

Edlund, S.A. 1992. Climate change and its effects on Canadian Arctic plant communities. In: Woo, M.K. and Gregor, D.J., eds. Arctic Environment: Past, Present and Future. Proceedings of a Symposium held at McMaster University November 14-15, 1991, 121-138.

Edlund, S.A. and Woo, M.-K. 1992. Eolian deposition on western Fosheim Peninsula, Ellesmere Island, Northwest Territories during the winter of 1990-91. In: Current Research, Part B; Geological Survey of Canada Paper 92-1B. 91-96.

Edlund, S.A. and Alt, B.T. 1989. Regional congruence of vegetation and summer climate patterns in the Queen Elizabeth Islands, Northwest Territories, Canada. Arctic, 42(1): 3-23.

Edlund, S.A. 1988. Effects of climate change on diversity of vegetation in Arctic Canada. In: Preparing for Climate Change, Proceedings of the First North

American Conference on Preparing for Climate Change: A Cooperative Approach, October 27-29, 1987, Washington, D.C., 186-193.

Emmanuel, W.R., Shugart, H.J. and Stevenson, M.P. 1985. Climatic change and broad scale distribution of terrestrial ecosystem complexes. Climatic Change 7: 29-43.

Headley, A. 1990. A comparison of wind speeds recorded simultaneously at three metres and ten metres above ground. Canadian Climate Centre Report No. 90-1. Atmospheric Environment Service, Downsview, Ontario, 36 pp.

Heron, R., and Woo, M.-K. 1978. Snowmelt computations for a High Arctic site. In: Proceedings of the 35th Eastern Snow Conference, Hanover, New Hampshire. 162-172.

Hodgson, D.A., St-Onge, D.A., and Edlund, S.A. 1991. Surficial materials of Hot Weather Creek basin, Ellesmere Island, Northwest Territories. In: Current Research, Part E; Geological Survey of Canada Paper, 91-1E. 157-163.

Hodgson, D.A. 1985. The last glaciation of west-central Ellesmere Island, Arctic Archipelago, Canada. Canadian Journal of Earth Sciences 22(3): 347-368.

Jumikis, A.R. 1984. Soil Mechanics. Malabar, Florida: Robert E. Krieger Publishing Company Incorporated.

Kartez, J.T. and Kartez, R. 1980. A Synonymized Checklist of the Vascular Flora of the United States, Canada, and Greenland. Chapel Hill: University of North Carolina Press.

Lewkowicz, A.G. and Gudjonsson, K.A. 1992. Slope hummocks on Fosheim Peninsula, Ellesmere Island, Northwest Territories. In: Current Research, Part B; Geological Survey of Canada Paper 92-1B. 97-102.

Lewkowicz, A.G. and Young, K.L. 1991. Observations of aeolian transport and niveo-aeolian deposition at three lowland sites, Canadian Arctic Archipelago. Permafrost and Periglacial Processes 2: 197-210.

Lewkowicz, A.G. and French H.M. 1982. The hydrology of small runoff plots in an area of continuous permafrost, Banks Island, N.W.T. In: French, H.M., ed. Proceedings, Fourth Canadian Permafrost Conference, March 2-6, 1981, Calgary, Alberta. Ottawa: National Research Council of Canada. 151-162.

Luthin, J.N. 1966. Drainage Engineering. London: Wiley.

Maxwell, B. 1992. Arctic climate: Potential for change under global warming. In: Chapin III, F.S., Jefferies, R.L., Reynolds, J.F., Shaver, G.R., Svoboda, J., Chu, E.W., eds. Arctic Ecosystems in a Changing Climate - An Ecophysiological Perspective. New York: Academic Press Incorporated. 11-31.

Nadelhoffer, K.J., Giblin, A.E., Shaver, G.R., and Linkins, A.E. 1992. Microbial processes and plant nutrient availability in arctic soils. In: Chapin III, F.S., Jefferies, R.L., Reynolds, J.F., Shaver, G.R., Svoboda, J., Chu, E.W., eds. Arctic Ecosystems in a Changing Climate - An Ecophysiological Perspective. New York: Academic Press Incorporated. 281-295.

Ohmura, A. 1982. Evaporation from the surface of the arctic tundra on Axel Heiberg Island. Water Resources Research 18(2): 291-300.

Peters, B. and Headley, A. 1992. A comparison of winds at Hot Weather Creek and Eureka, N.W.T. Canadian Climate Centre Report No. 90-1. Atmospheric Environment Service, Downsview, Ontario, 22 pp.

Peterson, N.J.K. 1974. Physical characteristics of snowbeds in The Richardson Mountains, Northwest Territories. Environmental-Social Committee Northern Pipelines Task Force on Northern Oil Development Report Number 74-12. 109-202.

Porsild, A.E. and Cody, W.J. 1980. Vascular Plants of Continental Northwest Territories, Canada. Ottawa: National Museum of Natural Sciences.

Ricketts, B.D. 1986. New formations in the Eureka Sound Group, Canadian Arctic Islands In: Current Research, Part B; Geological Survey of Canada Paper 86-1B. 363-374.

Rizzo, B. and Wiken, E. 1992. Assessing the sensitivity of Canada's ecosystems to climatic change. Climatic Change 21: 37-55.

Robinson, S.D. 1994. Geophysical studies of massive ground ice, Fosheim Peninsula, Ellesmere Island, Northwest Territories. In: Current Research, Geological Survey of Canada Paper 94-1B. 11-18.

Roots, E.F. 1989. Climatic change: High-latitude regions. Climatic Change 15: 223-253.

Thorsteinsson, R. 1969. Geology, Greely Fiord West, District of Franklin. Geological Survey of Canada Map 1311A.

Thorsteinsson, R. 1971. Geology, Eureka Sound North, District of Franklin. Geological Survey of Canada Map 1302A.

Webb, T. 1987. The appearance and disappearance of major vegetational assemblages; long term vegetation dynamics in Eastern North America. Vegetation 69: 177-187.

Woo, M.-K. 1986. Permafrost hydrology in North America. Atmosphere-Ocean 24(3): 201-234.

Woo, M.-K., Young, K.L., and Edlund, S.A. 1990. 1989 Observations of soil, vegetation and microclimate, and effects on slope hydrology, Hot Weather Creek basin, Ellesmere Island, Northwest Territories. In: Current Research Part 1-D, Geological Survey of Canada Paper 90-1D. 85-93.

Woo, M.-K. and Marsh, P. 1978. Analysis of error in the determination of snow storage for small High Arctic basins. Journal of Applied Meteorology 17: 1537-1541.

Young, K.L. and Lewkowicz, A.G. 1990. Surface energy balance of a perennial snowbank, Melville Island, Northwest Territories, Canada. Arctic and Alpine Research 22(3): 290-301.

TABLE 1
Climatologic and hydrologic instrumentation employed on the slopes and plateau

CLIMATOLOGICAL VARIABLES	INSTRUMENT[a]	LOCATION & HEIGHT[b]	ACCURACY
Solar Radiation	Pyranometer (Kipp and Zonen Cm-6[c])	Plateau (P) (2m)	>± 1% or 0.01MJ/m²h
Net Radiation	Pyrradiometer (Swissteco[c])	(P) (1m)	>± 1% or 0.01 MJ/m²h
	Pyrradiometer (Middleton[c])	Slope (S) (1m)	>± 1% or 0.01 MJ/m²h
Surface Albedo	Davos type PDI-QK	P(1m), S(1m)	± 5%
Wind Speed	Campbell Scientific (CSI) Met-One Anemometer	P(2m, e, f), S[e] (0.5m)	± 0.25 m/s
	Anemometer (cup-type) Run-of-wind	S(0.5m)	± 10%
Wind Direction	Campbell Scientific (CSI)[e,f] Met-One Wind Vane[e,f]	P(2m), S(1m)	± 5°
Air Temperature and Relative Humidity	CSI 207 Probe[f]	Plateau (1.5m)	± 2° C and 5% respectively
	CSI 201 Probe[d]	Slope (0.5m)	± 0.3° and 5% respectively
Surface Soil Temp.	CSI 101 Probe[e]	P&S	±0.2°C
Precipitation	Weathermeasure Tipping Bucket	Valley between NW-SE Slopes	± 0.25 mm
	Atmospheric Environment Raingauge	S & P & Base Camp (BC)	± 0.25 mm
Water Table - Daily	Groundwater Well Sensor and Tape Measure	P & S	± 1 mm
Soil Moisture	Time Domain Reflectometer Textronix 1502	P & S	0.006 m³/m³
Stage of Surface Flow	Leupold-Stevens Type F Water Level Recorder	S	± 1 mm

[a] Readings were taken every 10s and averaged over 60-min. intervals using Campbell Scientific CR2l dataloggers on the slopes and a CSI CR10 datalogger on the plateau.

[b] During the snowmelt period heights above the snowpack were adjusted daily.

[c] Calibrated prior to fieldwork by the Radiation Department of the Atmospheric Environment Service, Environment Canada.
Accuracy in field (± 15%)

[d] Calibrated during the field season with a Bendix Electric Psychrometer.

[e] Calibrated following the field season by Atmospheric Environment Service, Environment Canada.

[f] Calibrated prior to fieldwork by Atmospheric Environment Service, Environment Canada.

TABLE 2
Mean surface albedos for the snowfree season, 1990

SLOPE	LOWER	MIDDLE	UPPER	NUMBER OF SAMPLES
Northwest	0.15 ± 0.03 *(C. tetragona)*	0.19 ± 0.06 *(Bare)*	0.19 ± 0.06 *(Bare)*	(22)
Southeast	0.15 ± 0.02 *(S. arctica)*	0.16 ± 0.03 *(Partial S. arctica-Bare)*	0.18 ± 0.03 *(Partial S. arctica-Bare)*	(20-21)
East	0.15 ± 0.04 *(Bare)*	0.14 ± 0.02 *(S. arctica)*	0.16 ± 0.02 *(S. arctica)*	(20)
West	0.16 ± 0.04 *(Bare)*	0.16 ± 0.05 *(Bare)*	0.14 ± 0.06 *(Bare)*	(17)
Plateau	HUMMOCK TOPS 0.17 ± 0.02 *(S. arctica)*	DEPRESSIONS 0.15 ± 0.02 *(Bare)*		(19-20)

[1] Three measurements/section at each sampling period

[2] Measurements were staggered over time (daily) and under various cloud conditions

TABLE 3

Snow accumulation at experimental sites in May

SITE	1989	1990	1991	1992
Northwest				
Mean Depth (m)	0.46 ± 0.44[1]	0.70 ± 0.46	0.17 ± 0.18	0.24 ± 0.13
Mean Density (kg/m³)	393 ± 47	358 ± 61	301 ± 61	227 ± 54
W.E.[2] (mm)	181 ± 21	249 ± 28	51 ± 11	54 ± 7
Southeast				
Mean Depth (m)	0.15 ± 0.15	0.18 ± 0.15	0.11 ± 0.10	0.19 ± 0.08
Mean Density (kg/m³)	342 ± 4	358 ± 54	330 ± 40	198 ± 26
W.E. (mm)	51 ± 6	63 ± 8	36 ± 4	38 ± 2
East				
Mean Depth (m)	0.33 ± 0.39	0.23 ± 0.18	0.22 ± 0.23	0.33 ± 0.22
Mean Density (kg/m³)	339 ± 21	314 ± 41	286 ± 35	239 ± 28
W.E. (mm)	112 ± 8.0	72 ± 7	63 ± 8	79 ± 6
West				
Mean Depth (m)	0.075 ± 0.15	0.21 ± 0.26	0.10 ± 0.13	0.20 ± 0.14
Mean Density (kg/m³)	309 ± 23	297 ± 49	297 ± 38	281 ± 92
W.E. (mm)	23 ± 3	62 ± 13	30 ± 5	56 ± 13
Plateau				
Mean Depth (m)	0.26 ± 0.11	0.31 ± 0.10	0.16 ± 0.08	0.32 ± 0.11
Mean Density (kg/m³)	337 ± 106	383 ± 44	267 ± 92	274 ± 117
W.E. (mm)	89 ± 12	118 ± 4	43 ± 7	88 ± 13

[1] Standard Deviation
[2] W.E. = Snow Water Equivalent

TABLE 4

Snow ablation comparison - 1989 versus 1990

	PLATEAU		NORTHWEST		SOUTHEAST		EAST		WEST	
Year	1989	1990[1]	1989[2]	1990	1989	1990	1989	1990	1989[3]	1990
Initial Snow Water Equiv. (mm)	89	118	181	247	51	63	109	72	26	62
Starting Date of Melt	May 26	May 16	May 26	May 16	May 28	May 16	May 27	May 16	—	May 16
Duration of Melt (Days)	11	24	8	32	8	24	10	24	—	19
Total Melt Energy (MJ/m^2)	+17.69	38.37	+14.33	+201.12	+64.33	+48.54	+35.7	+40.93	—	35.39
Q^* Total (MJ/m^2)	+11.58	—	57.0	+210.18	+75.06	+55.96	+62.7	+56.29	—	153.4
Q_T Total (MJ/m^2)	+6.11	—	-42.69	-9.06	-10.73	-7.42	-27.0	-15.36	—	-118.01

[1] Totals for 1990 are for days when Q^* values occur
[2] Lower part of slope
[3] Sublimation values only

TABLE 5

Maximum frost table development for the middle line of pipes running from downslope - upslope

PIPE LOCATION	NORTHWEST				SOUTHEAST				EAST				WEST			
YEAR	89[1]	90[2]	91[3]	92[4]	89	90	91	92	89	90	91	92	89	90	91	92
Footslope	—	.49	—	.45	—	.64		.50	—	.69		.56	—	—	—	—
Lower	.65	.82	—	.68	.69	.80		.63	.65	.68		.57	.74	.80	—	.66
Middle	.91	.90	.92	.79	.70	.78	.73	.57	.63	.83	.71	.61	.78	.92	.89	.75
Upper	.74	.78	—	.64	.76	.82		.61	.60	.59		.53	.78	.96	—	.69

[1] Max Thaw = August 22
[2] Max Thaw = August 4
[3] Max Thaw = August 18
[4] Max Thaw = August 23

LIST OF FIGURES

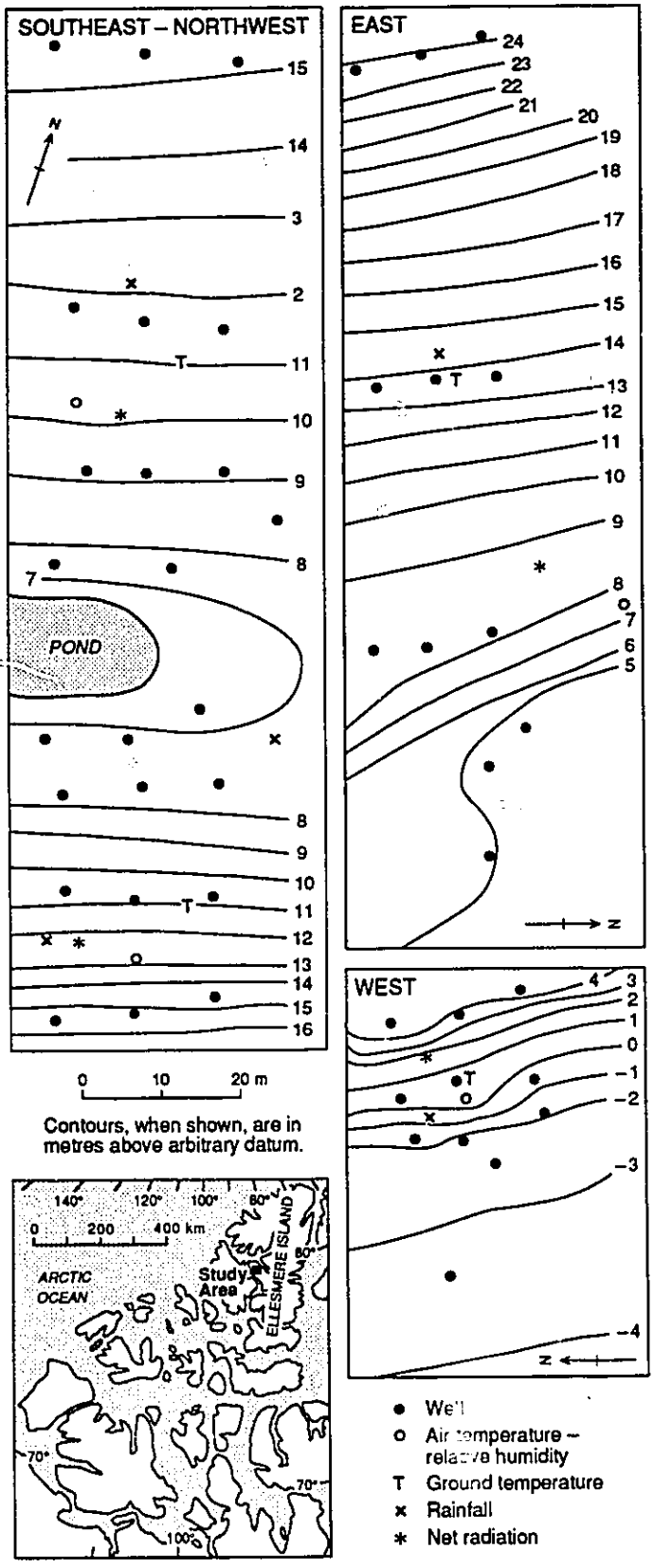

Contours, when shown, are in metres above arbitrary datum.

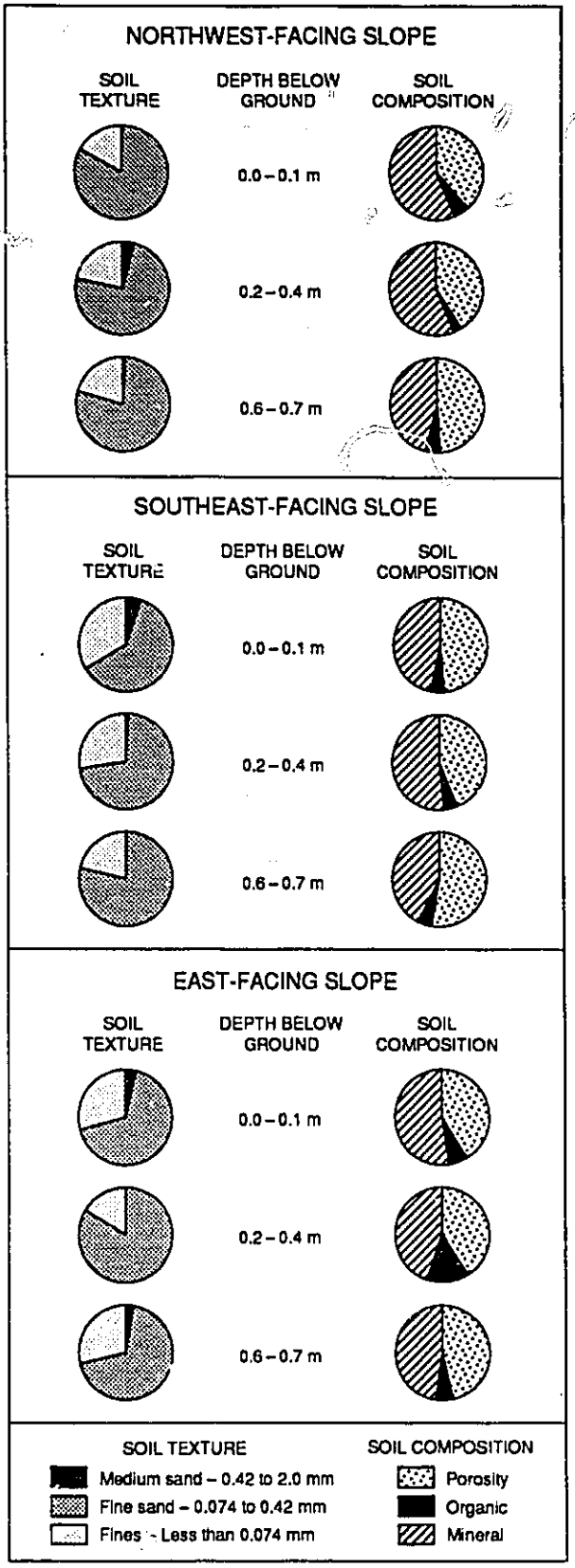
NORTHWEST-FACING SLOPE
SOIL TEXTURE
DEPTH BELOW GROUND
SOIL COMPOSITION
0.0 – 0.1 m
0.2 – 0.4 m
0.6 – 0.7 m
SOUTHEAST-FACING SLOPE
SOIL TEXTURE
DEPTH BELOW GROUND
SOIL COMPOSITION
0.0 – 0.1 m
0.2 – 0.4 m
0.6 – 0.7 m
EAST-FACING SLOPE
SOIL TEXTURE
DEPTH BELOW GROUND
SOIL COMPOSITION
0.0 – 0.1 m
0.2 – 0.4 m
0.6 – 0.7 m
SOIL TEXTURE
Medium sand – 0.42 to 2.0 mm
Fine sand – 0.074 to 0.42 mm
Fines – Less than 0.074 mm
SOIL COMPOSITION
Porosity
Organic
Mineral

Fig. 2 cont.

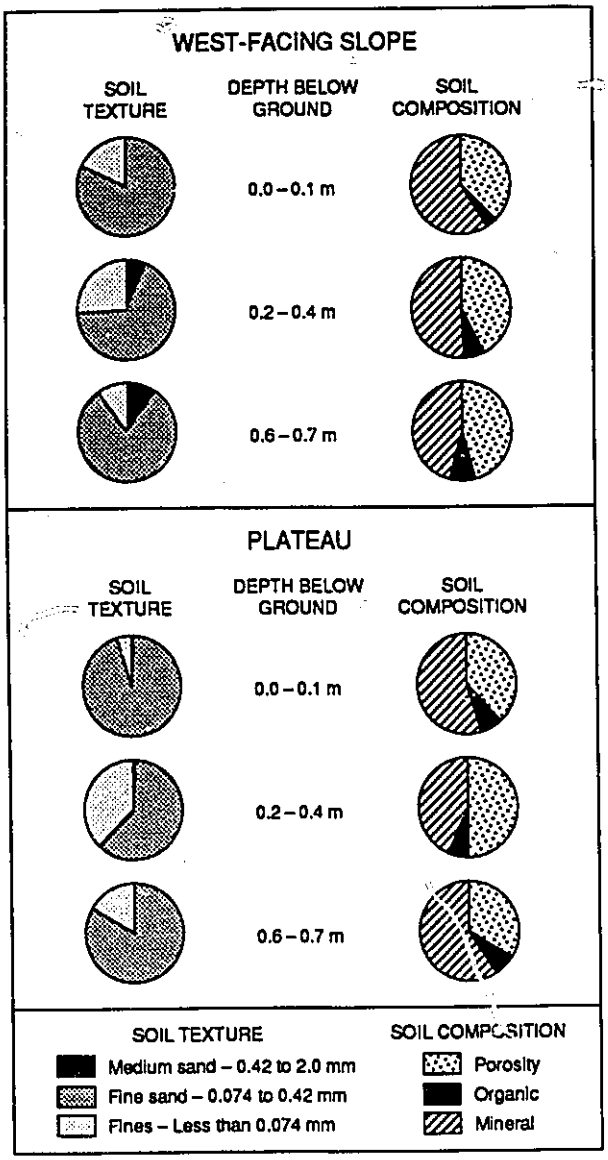
WEST-FACING SLOPE
SOIL TEXTURE
DEPTH BELOW GROUND
SOIL COMPOSITION
0.0 – 0.1 m
0.2 – 0.4 m
0.6 – 0.7 m
PLATEAU
SOIL TEXTURE
DEPTH BELOW GROUND
SOIL COMPOSITION
0.0 – 0.1 m
0.2 – 0.4 m
0.6 – 0.7 m
SOIL TEXTURE
Medium sand – 0.42 to 2.0 mm
Fine sand – 0.074 to 0.42 mm
Fines – Less than 0.074 mm
SOIL COMPOSITION
Porosity
Organic
Mineral

Fig. 2

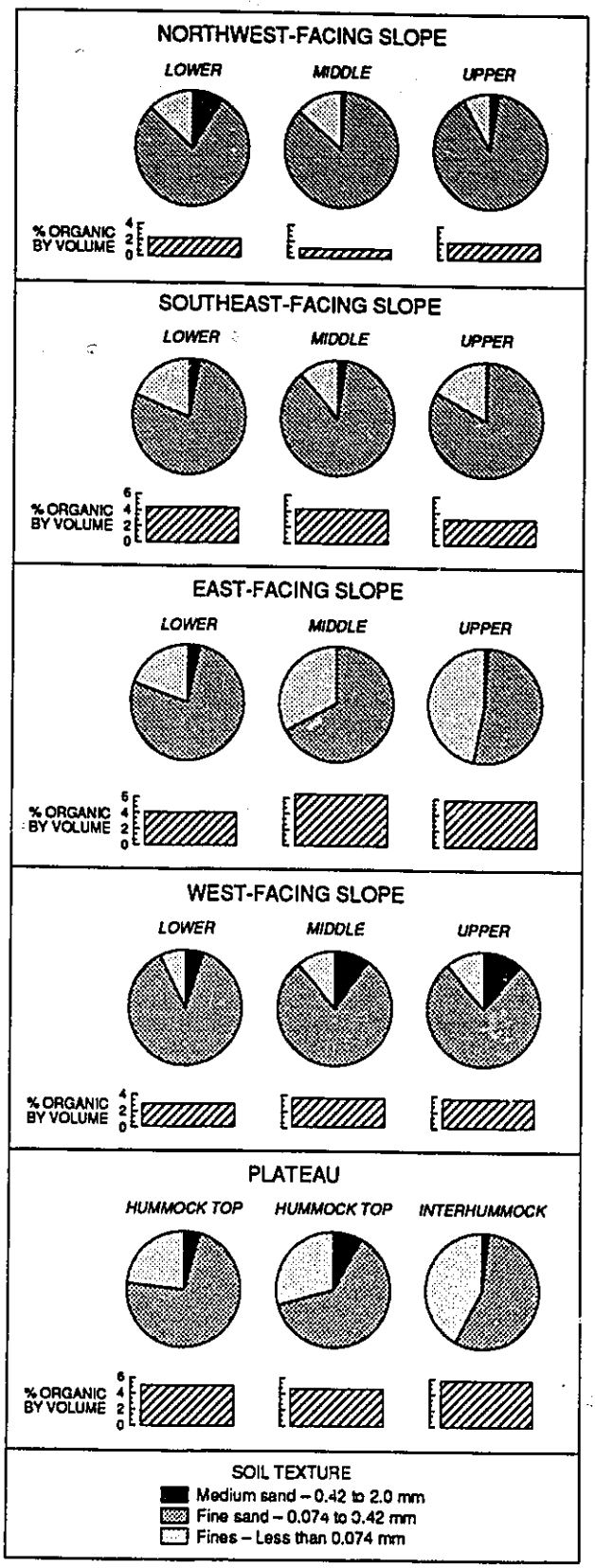
NORTHWEST-FACING SLOPE
LOWER
MIDDLE
UPPER
% ORGANIC BY VOLUME
4
2
0
SOUTHEAST-FACING SLOPE
LOWER
MIDDLE
UPPER
% ORGANIC BY VOLUME
6
4
2
0
EAST-FACING SLOPE
LOWER
MIDDLE
UPPER
% ORGANIC BY VOLUME
6
4
2
0
WEST-FACING SLOPE
LOWER
MIDDLE
UPPER
% ORGANIC BY VOLUME
4
2
0
PLATEAU
HUMMOCK TOP
HUMMOCK TOP
INTERHUMMOCK
% ORGANIC BY VOLUME
6
4
2
0
SOIL TEXTURE
Medium sand – 0.42 to 2.0 mm
Fine sand – 0.074 to 0.42 mm
Fines – Less than 0.074 mm

Fig.4

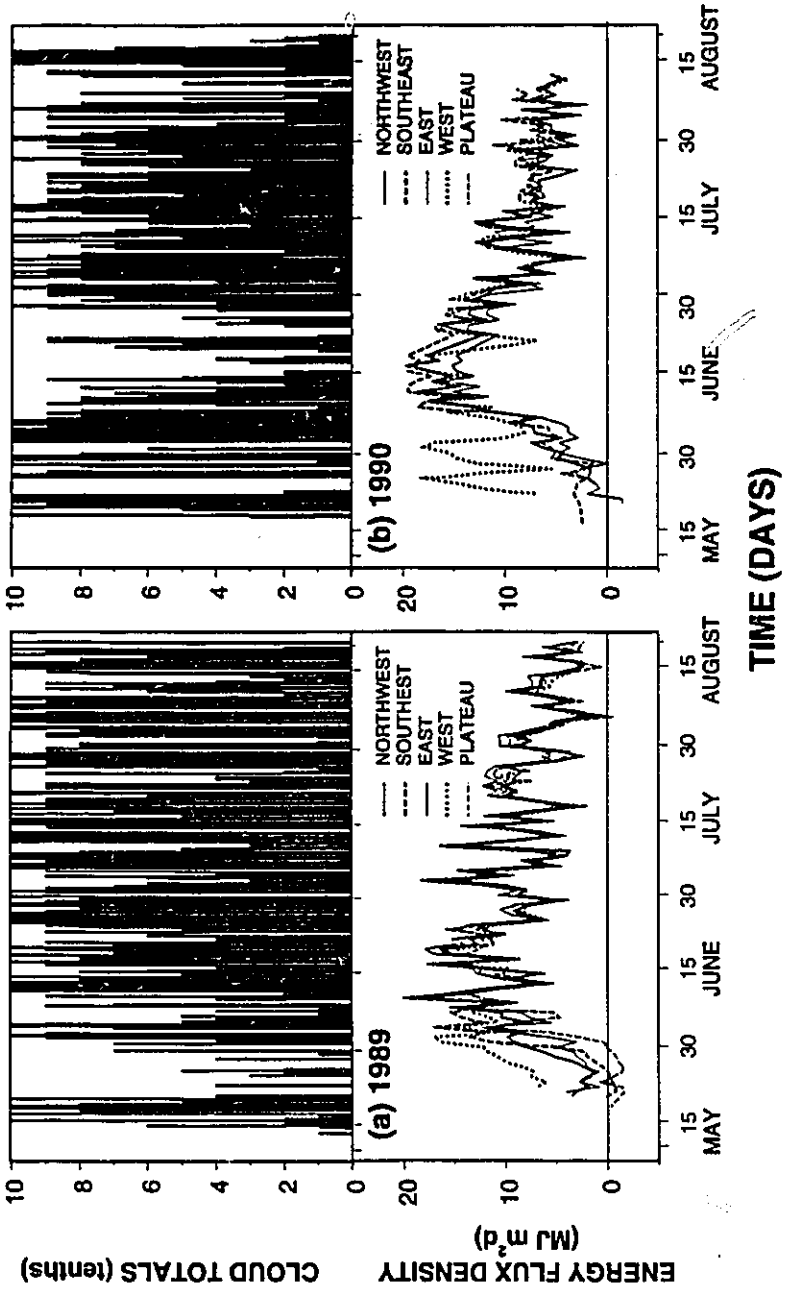
(a) 1989
(b) 1990
NORTHWEST
SOUTHEAST
EAST
WEST
PLATEAU
ENERGY FLUX DENSITY (MJ m²d)
CLOUD TOTALS (tenths)
TIME (DAYS)
15 MAY
30
15 JUNE
30
15 JULY
30
15 AUGUST

Fig 5

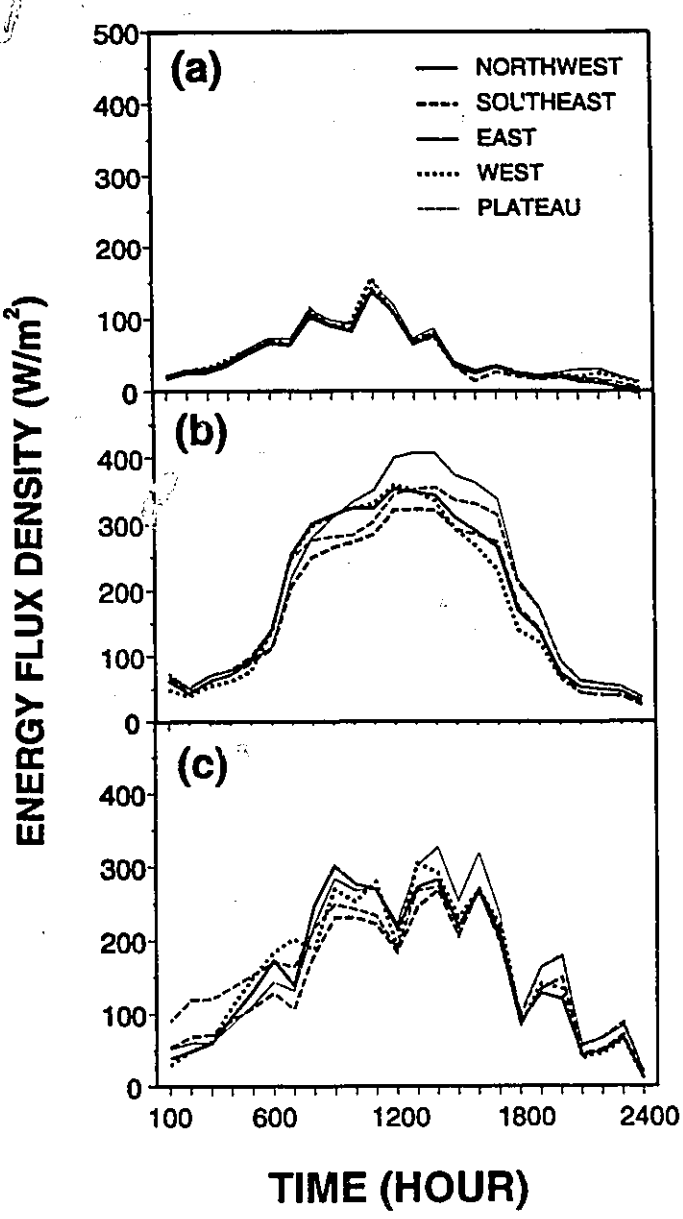
(a)
(b)
(c)
NORTHWEST
SOUTHEAST
EAST
WEST
PLATEAU
ENERGY FLUX DENSITY (W/m²)
TIME (HOUR)
0
100
200
300
400
500
100
600
1200
1800
2400

Fig. c

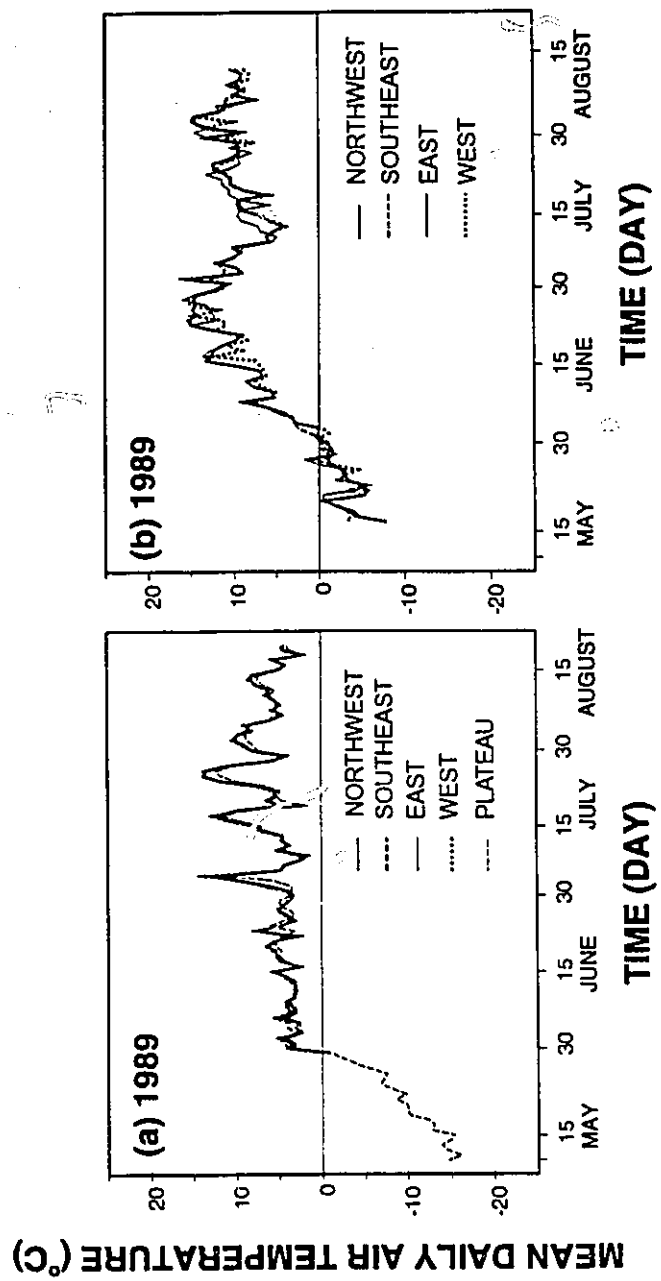
MEAN DAILY AIR TEMPERATURE (°C)
(a) 1989
(b) 1989
NORTHWEST
SOUTHEAST
EAST
WEST
PLATEAU
20
10
0
-10
-20
15 MAY
30
15 JUNE
30
15 JULY
30
15 AUGUST
TIME (DAY)

Fig.7

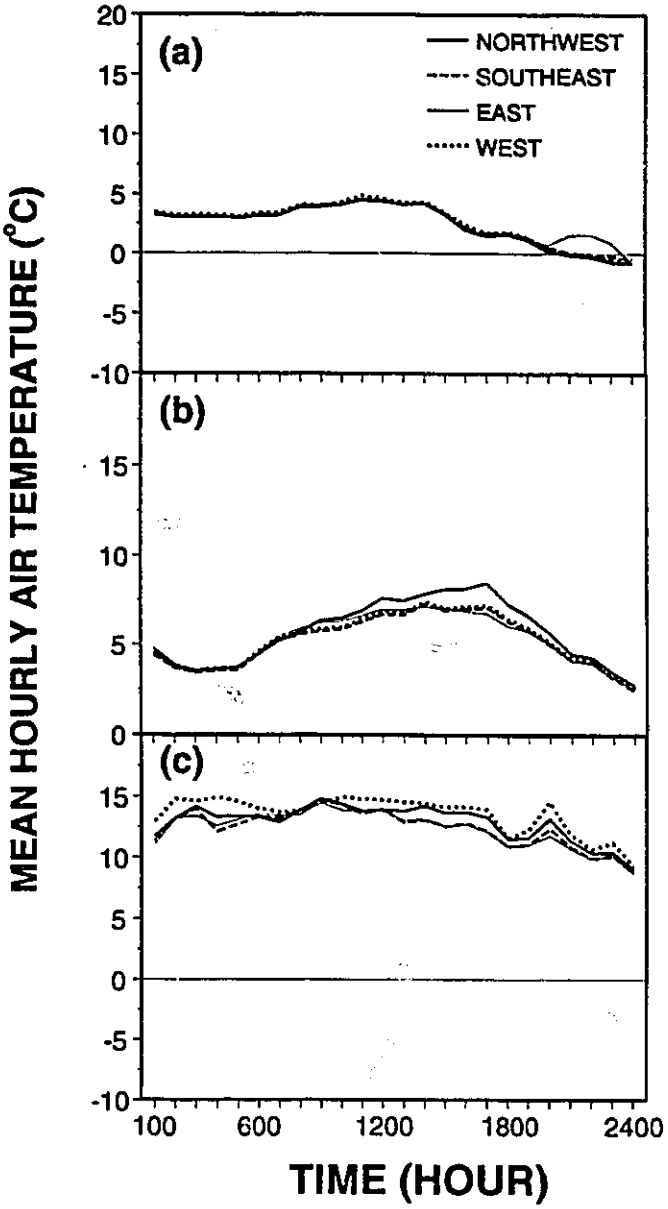
(a)
(b)
(c)
NORTHWEST
SOUTHEAST
EAST
WEST
MEAN HOURLY AIR TEMPERATURE (°C)
TIME (HOUR)
20
15
10
5
0
-5
-10
100
600
1200
1800
2400

Fig. 8

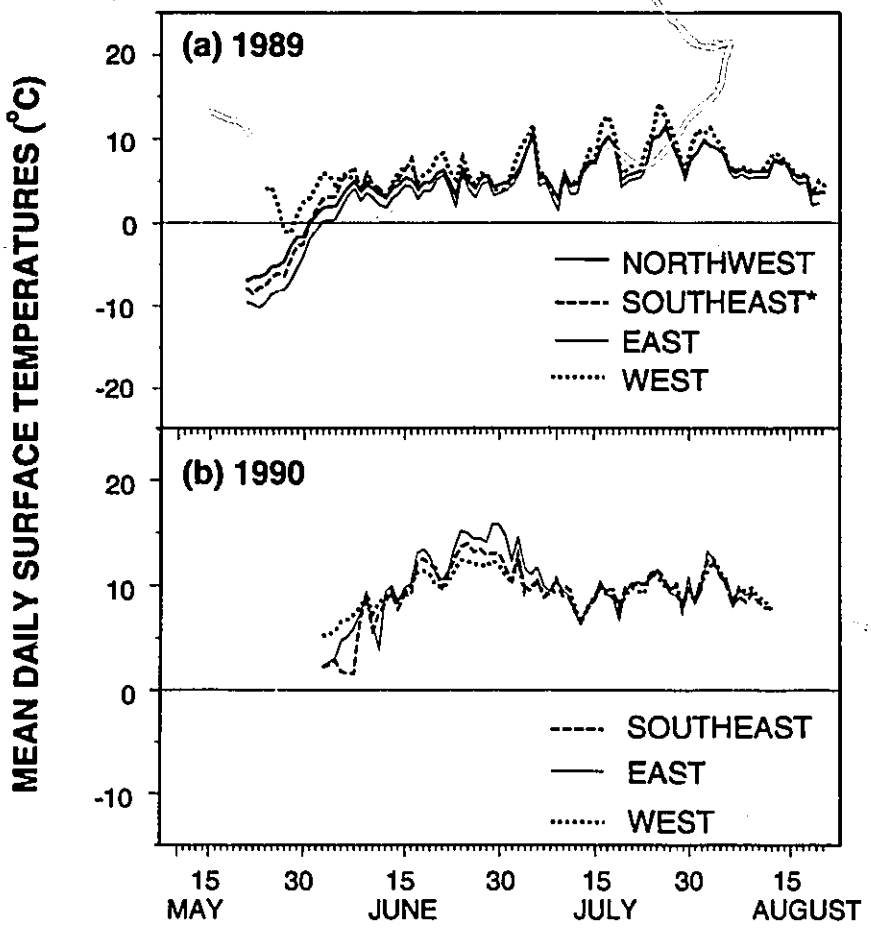

* after June 17, thermister placed at 0.1 m

Fig. 9

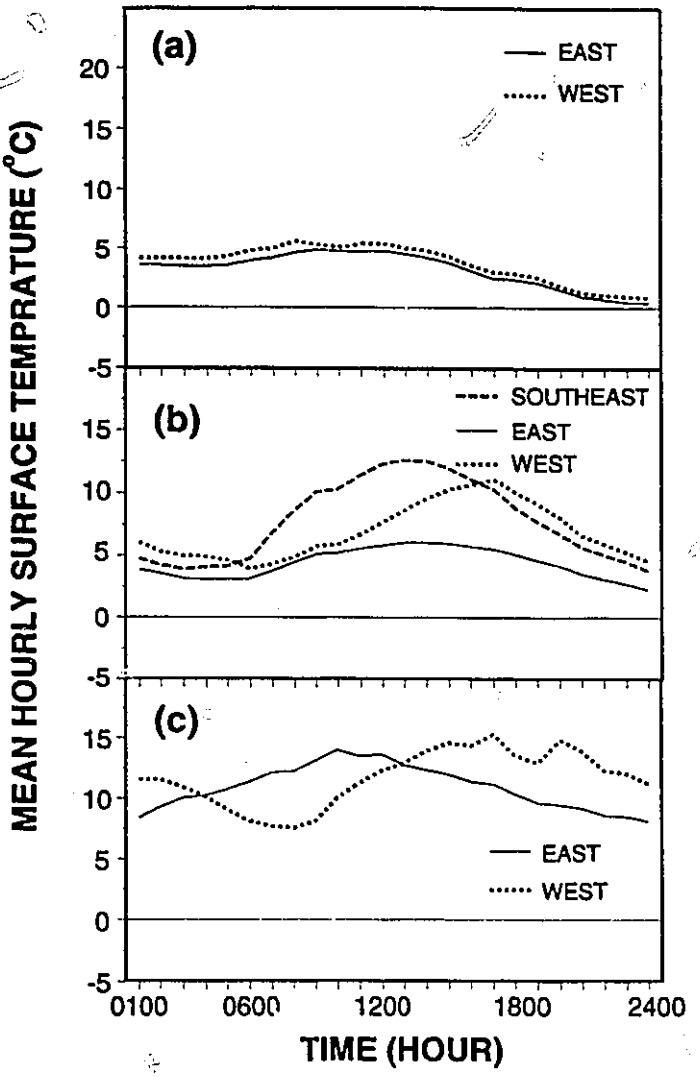
(a)
EAST
WEST
(b)
SOUTHEAST
EAST
WEST
(c)
EAST
WEST
MEAN HOURLY SURFACE TEMPRATURE (°C)
20
15
10
5
0
-5
0100
0600
1200
1800
2400
TIME (HOUR)

Fig. 10

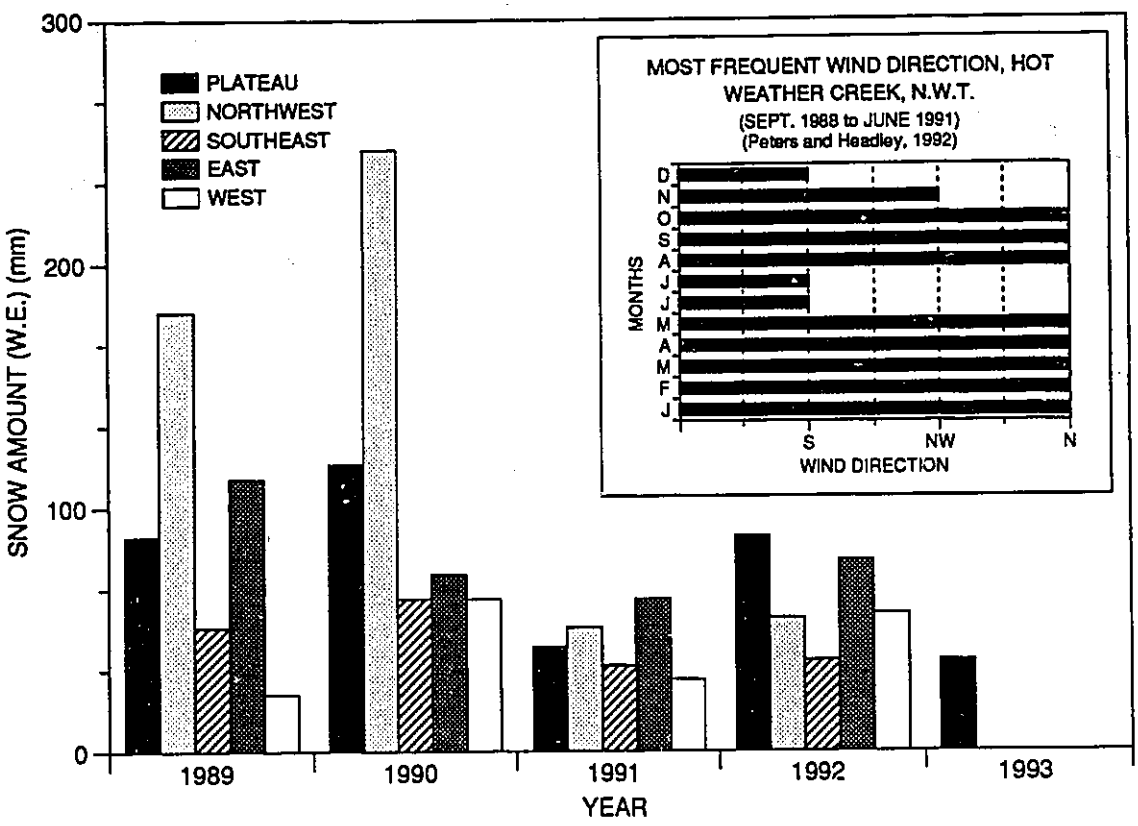
300
200
100
0
SNOW AMOUNT (W.E.) (mm)
PLATEAU
NORTHWEST
SOUTHEAST
EAST
WEST
1989
1990
1991
1992
1993
YEAR
MOST FREQUENT WIND DIRECTION, HOT WEATHER CREEK, N.W.T.
(SEPT. 1988 to JUNE 1991)
(Peters and Headley, 1992)
MONTHS
D
N
O
S
A
J
J
M
A
M
F
J
S
NW
N
WIND DIRECTION

NORTHWEST

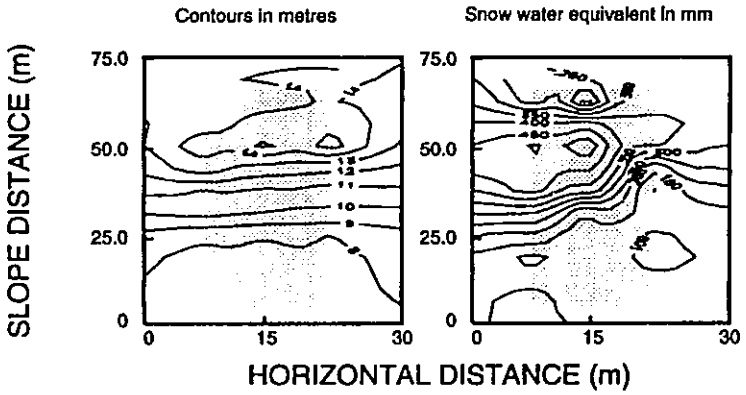

EAST

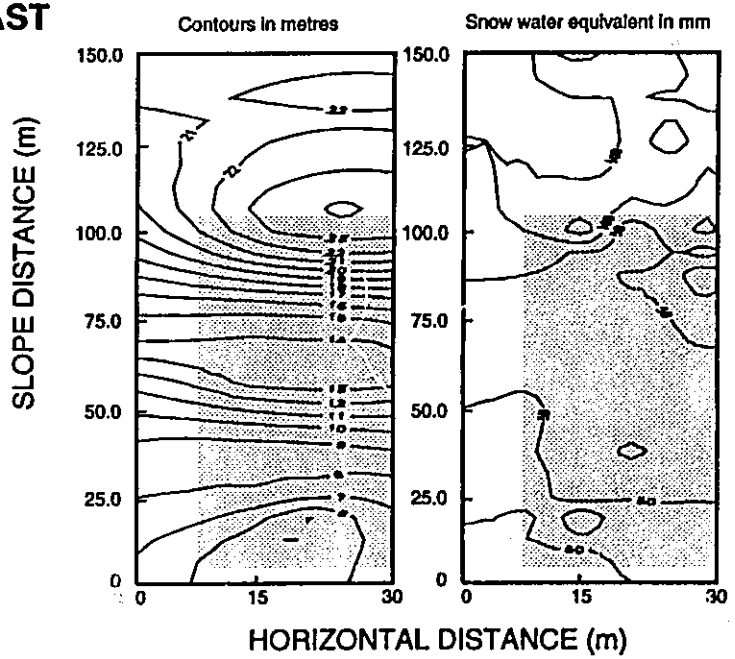

SOUTHEAST

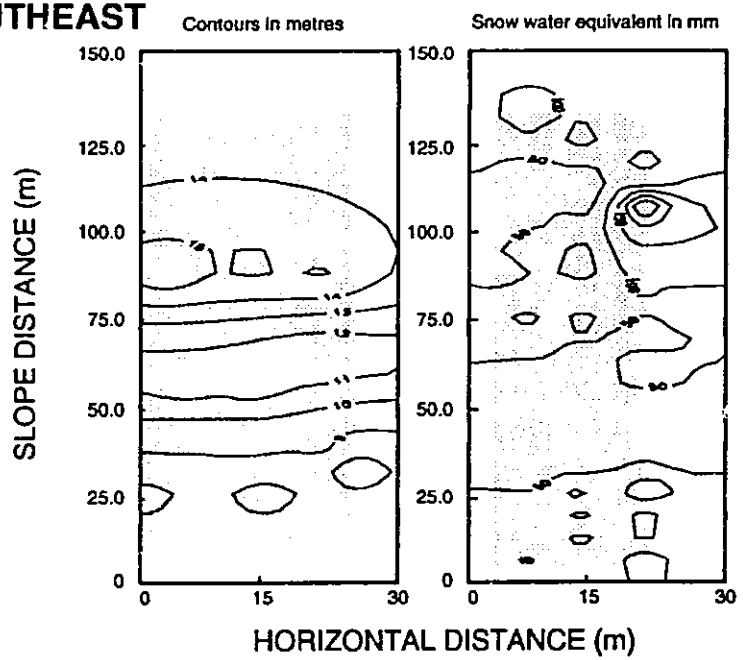

WEST

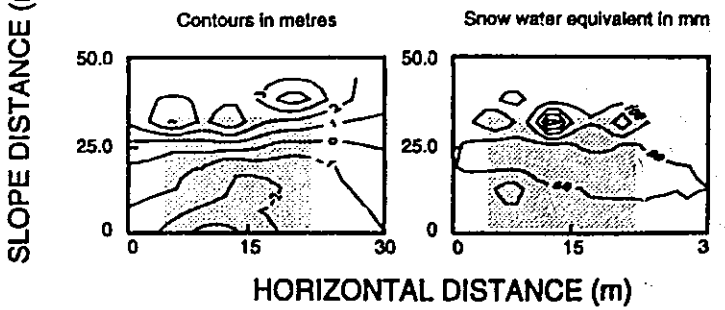

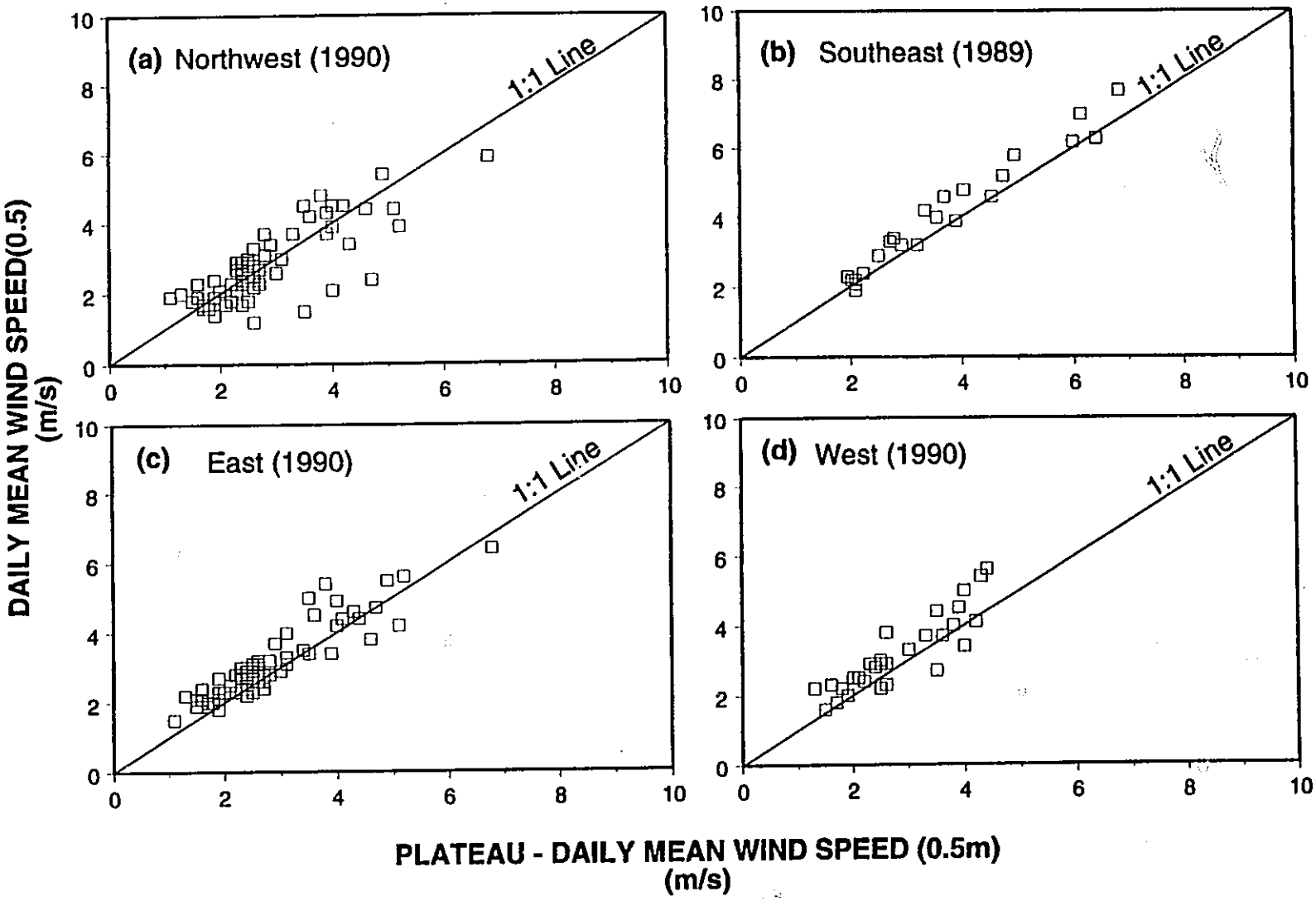
(a) Northwest (1990)
(b) Southeast (1989)
(c) East (1990)
(d) West (1990)
1:1 Line
DAILY MEAN WIND SPEED(0.5) (m/s)
PLATEAU - DAILY MEAN WIND SPEED (0.5m) (m/s)

Fig. 1

Fig. 13

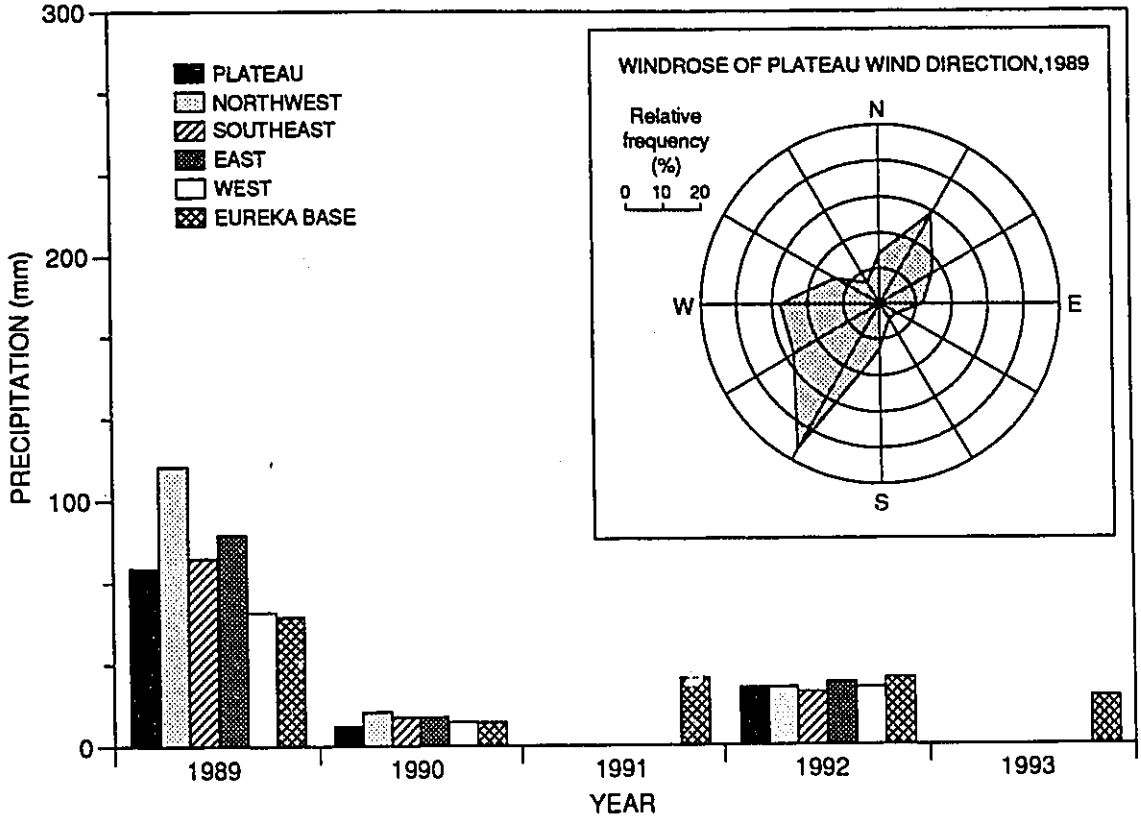
PLATEAU
NORTHWEST
SOUTHEAST
EAST
WEST
EUREKA BASE
PRECIPITATION (mm)
300
200
100
0
1989
1990
1991
1992
1993
YEAR
WINDROSE OF PLATEAU WIND DIRECTION,1989
Relative frequency (%)
0 10 20
N
W
E
S

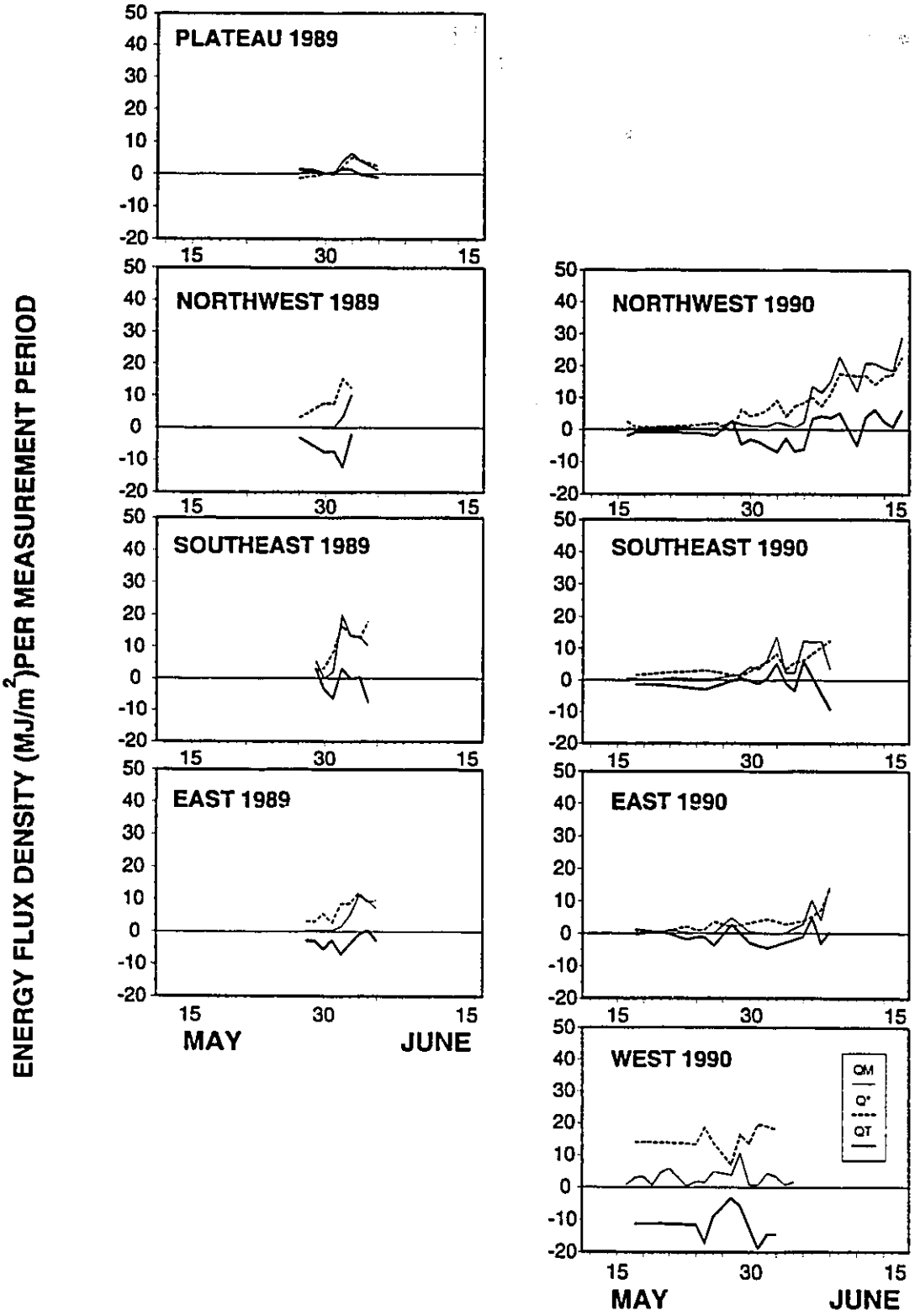
ENERGY FLUX DENSITY (MJ/m²)PER MEASUREMENT PERIOD
PLATEAU 1989
NORTHWEST 1989
SOUTHEAST 1989
EAST 1989
NORTHWEST 1990
SOUTHEAST 1990
EAST 1990
WEST 1990
QM
Q*
QT
50
40
30
20
10
0
-10
-20
15
30
15
MAY
JUNE

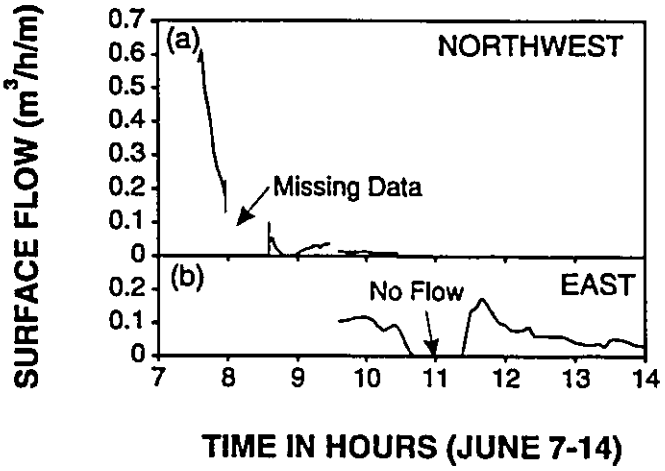
SURFACE FLOW ($m^3/h/m$)
0.7
0.6
0.5
0.4
0.3
0.2
0.1
0
(a)
NORTHWEST
Missing Data
(b)
No Flow
EAST
0.2
0.1
0
7
8
9
10
11
12
13
14
TIME IN HOURS (JUNE 7-14)

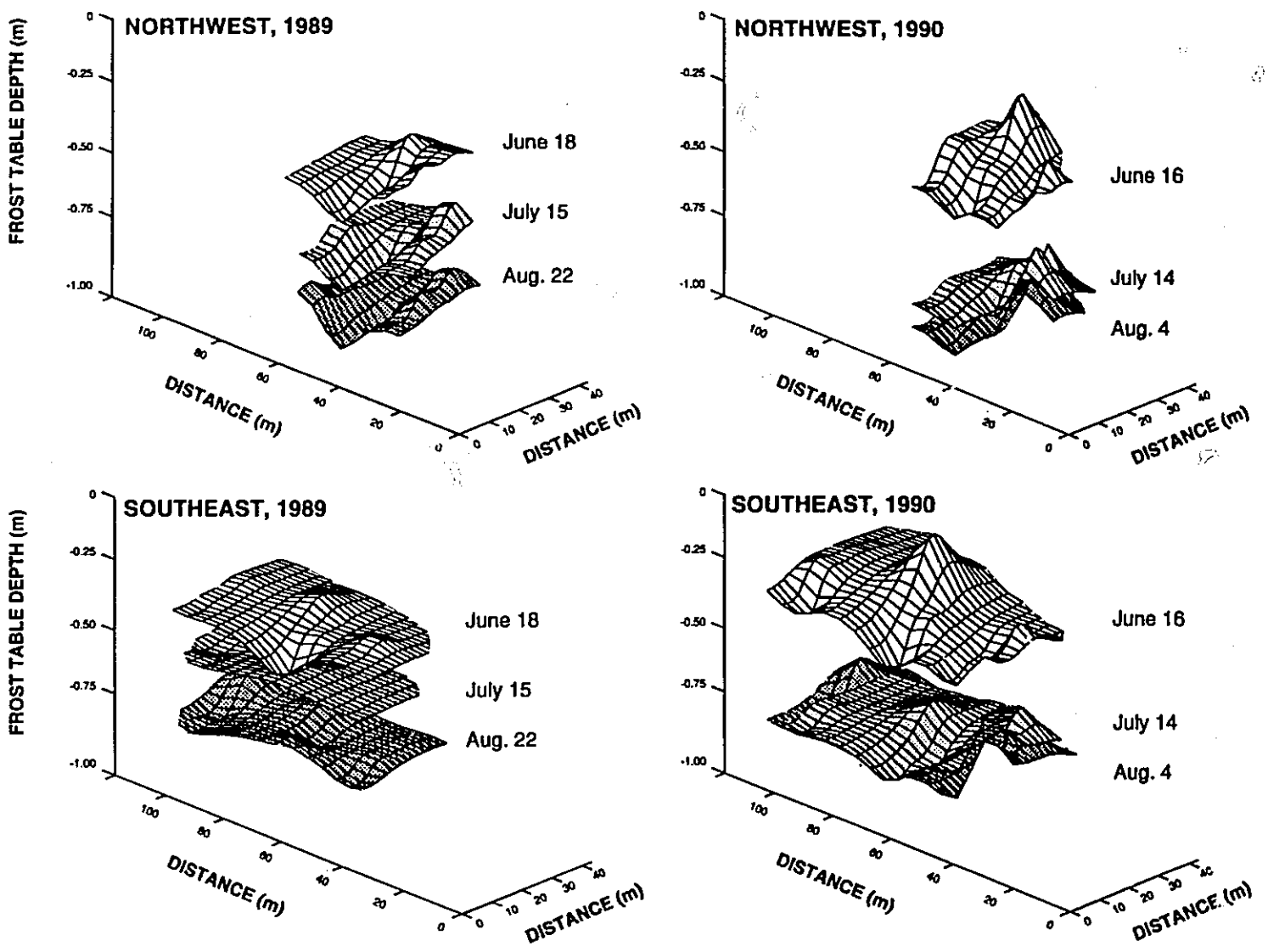
NORTHWEST, 1989
FROST TABLE DEPTH (m)
0
-0.25
-0.50
-0.75
-1.00
June 18
July 15
Aug. 22
100
80
60
40
20
0
DISTANCE (m)
0
10
20
30
40
DISTANCE (m)
NORTHWEST, 1990
June 16
July 14
Aug. 4
SOUTHEAST, 1989
SOUTHEAST, 1990

Fig. 1

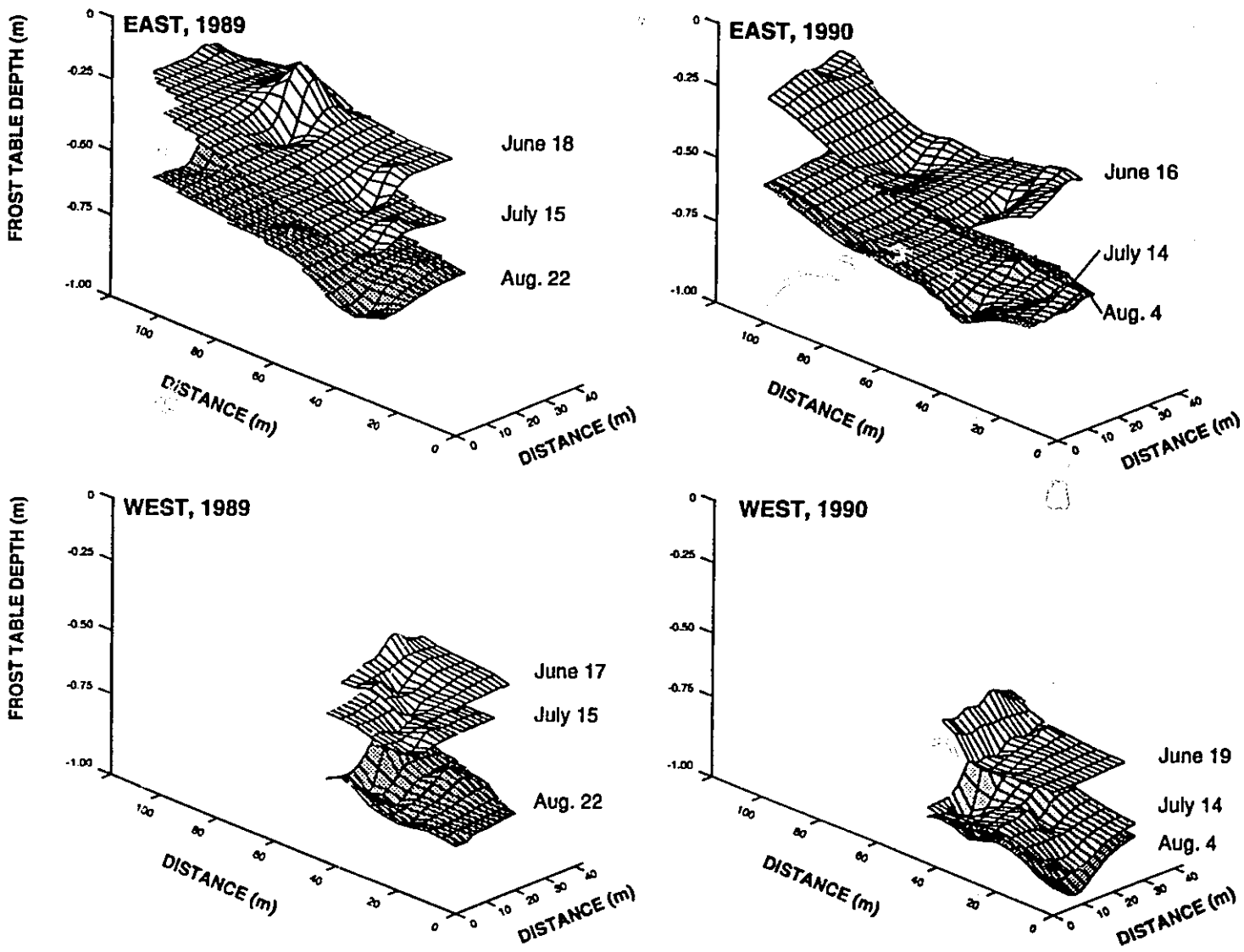
EAST, 1989
FROST TABLE DEPTH (m)
0
-0.25
-0.50
-0.75
-1.00
June 18
July 15
Aug. 22
DISTANCE (m)
100
80
60
40
20
0
0
10
20
30
40
DISTANCE (m)
EAST, 1990
June 16
July 14
Aug. 4
WEST, 1989
June 17
July 15
Aug. 22
WEST, 1990
June 19
July 14
Aug. 4

Fig. 14
CONT.

Fig.

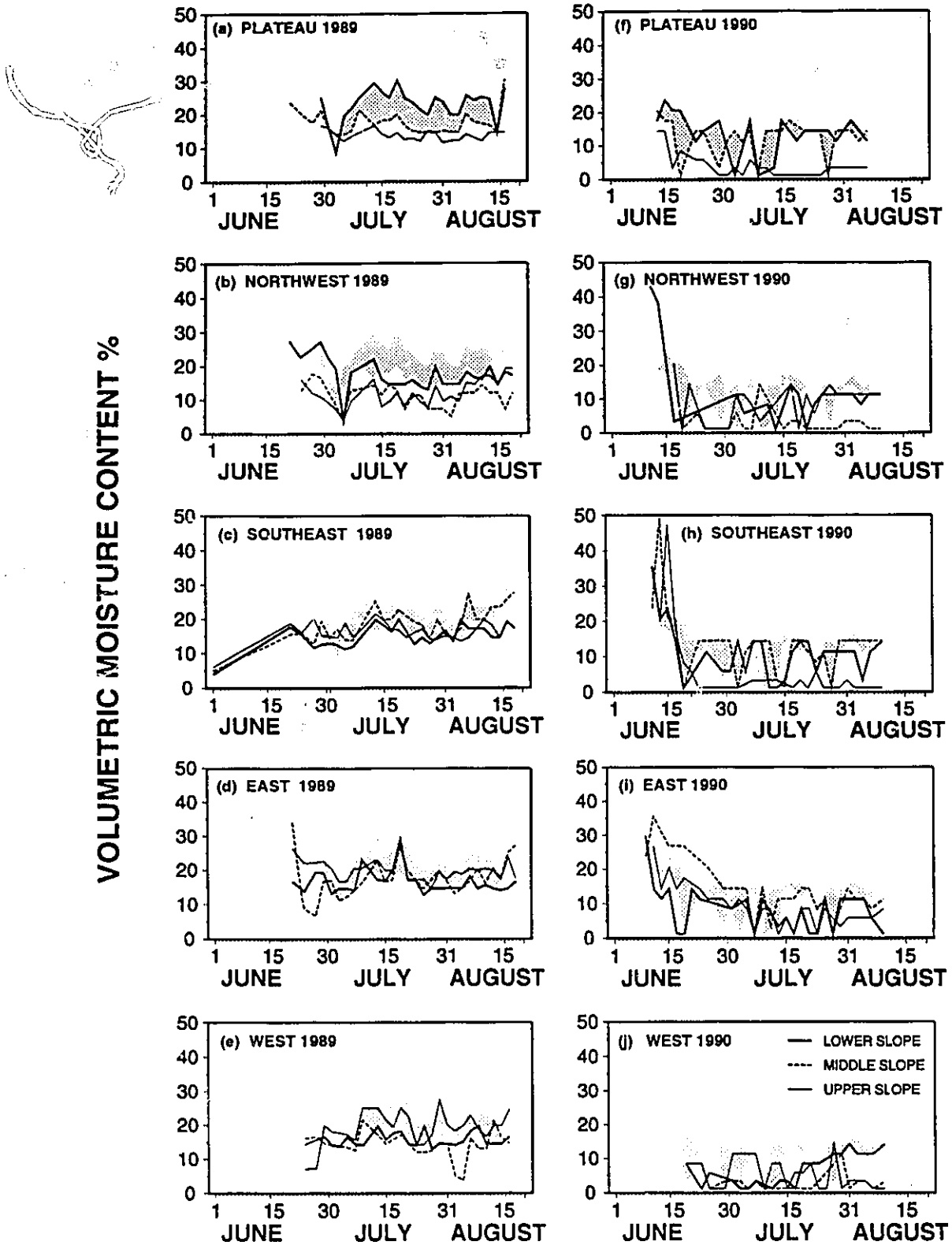
VOLUMETRIC MOISTURE CONTENT %
(a) PLATEAU 1989
(f) PLATEAU 1990
(b) NORTHWEST 1989
(g) NORTHWEST 1990
(c) SOUTHEAST 1989
(h) SOUTHEAST 1990
(d) EAST 1989
(i) EAST 1990
(e) WEST 1989
(j) WEST 1990
LOWER SLOPE
MIDDLE SLOPE
UPPER SLOPE
0
10
20
30
40
50
1
15
30
15
31
15
JUNE
JULY
AUGUST

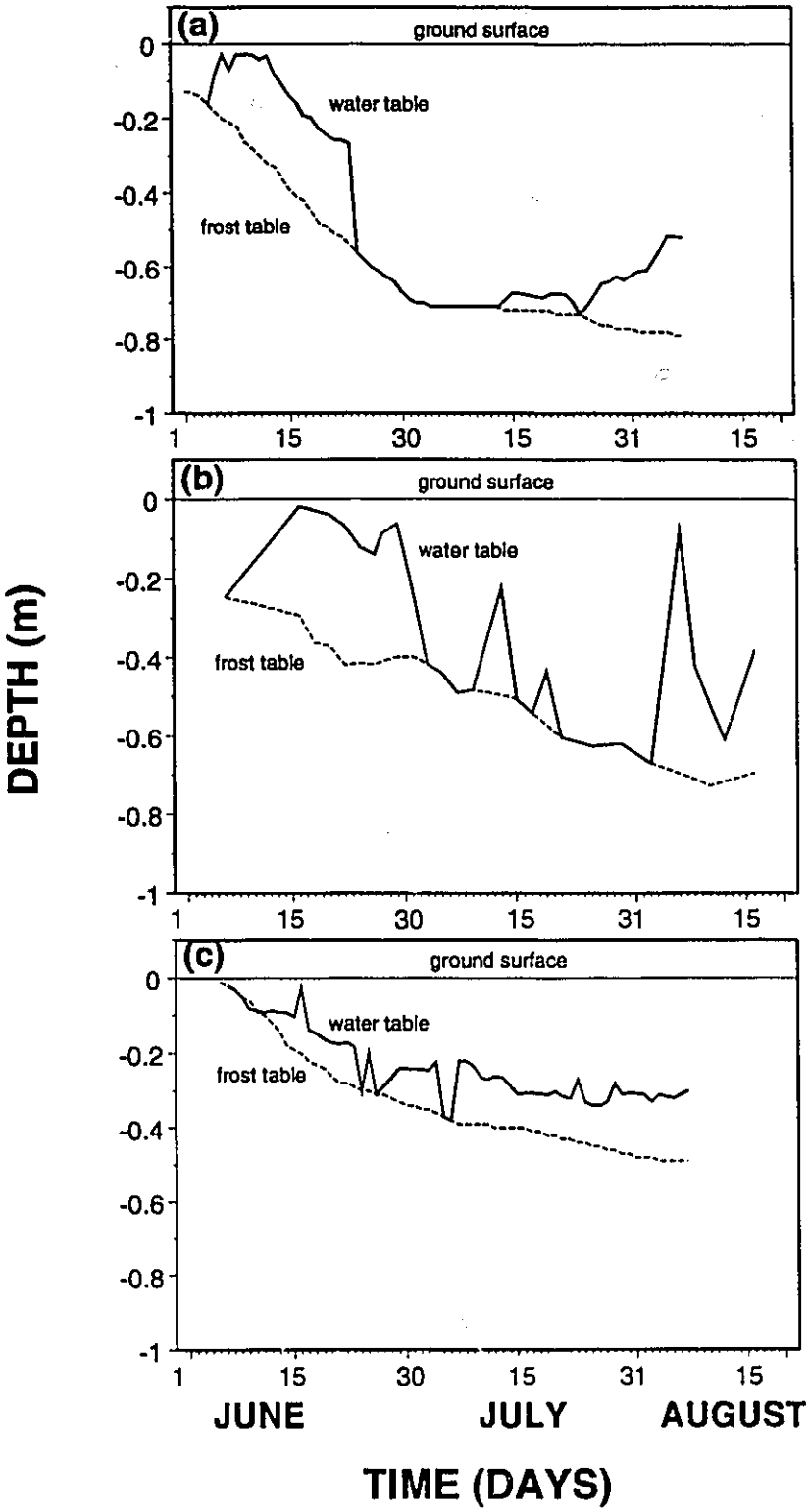
(a)
ground surface
water table
frost table
(b)
ground surface
water table
frost table
(c)
ground surface
water table
frost table
0
-0.2
-0.4
-0.6
-0.8
-1
1
15
30
15
31
15
JUNE
JULY
AUGUST
DEPTH (m)
TIME (DAYS)

Fig. 19

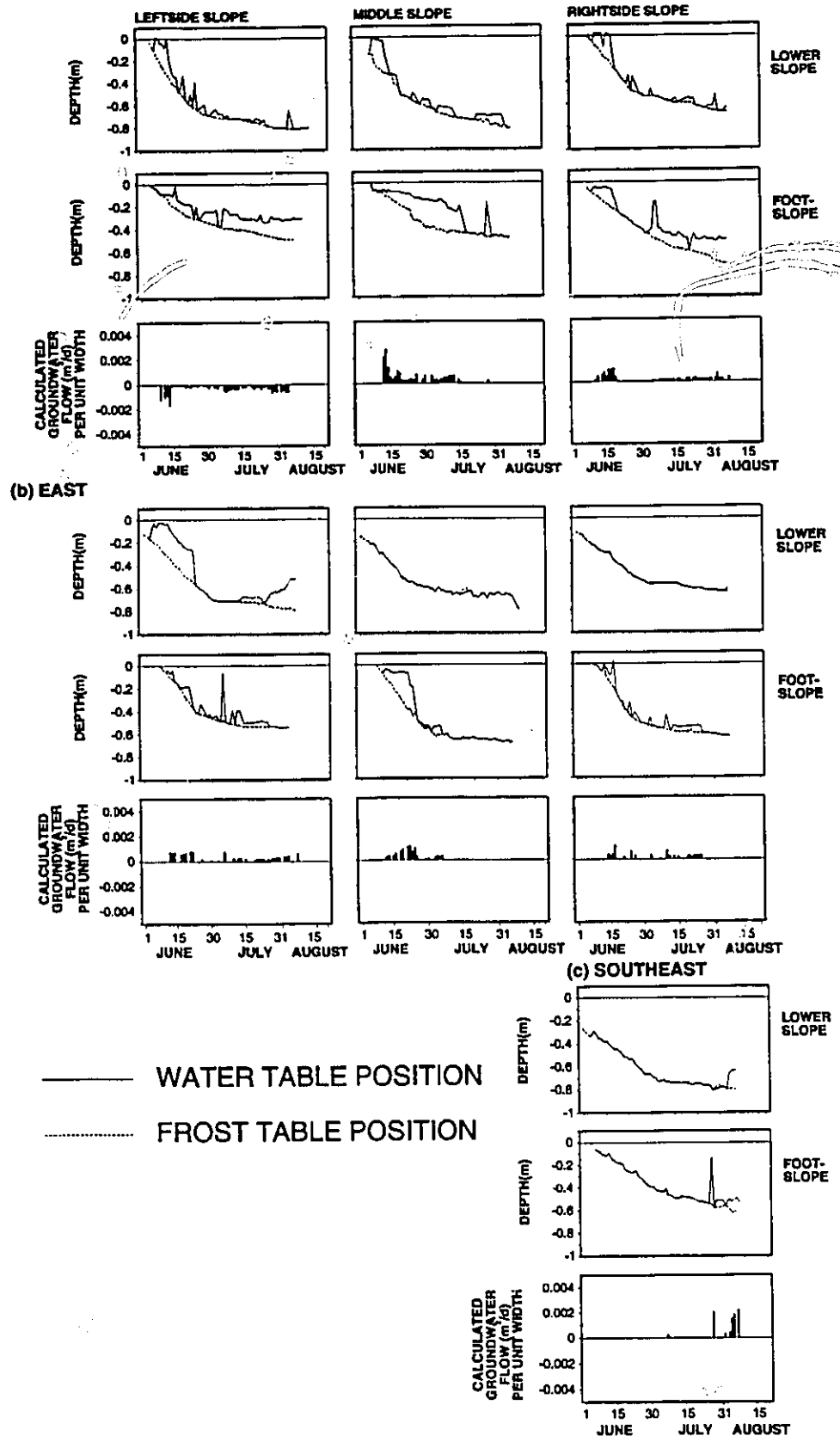
(a) NORTHWEST
LEFTSIDE SLOPE
MIDDLE SLOPE
RIGHTSIDE SLOPE
LOWER SLOPE
FOOT-SLOPE
DEPTH(m)
0
-0.2
-0.4
-0.6
-0.8
-1
CALCULATED GROUNDWATER FLOW (m²/d) PER UNIT WIDTH
0.004
0.002
0
-0.002
-0.004
1 15 30 15 31 15
JUNE JULY AUGUST
(b) EAST
(c) SOUTHEAST
WATER TABLE POSITION
FROST TABLE POSITION

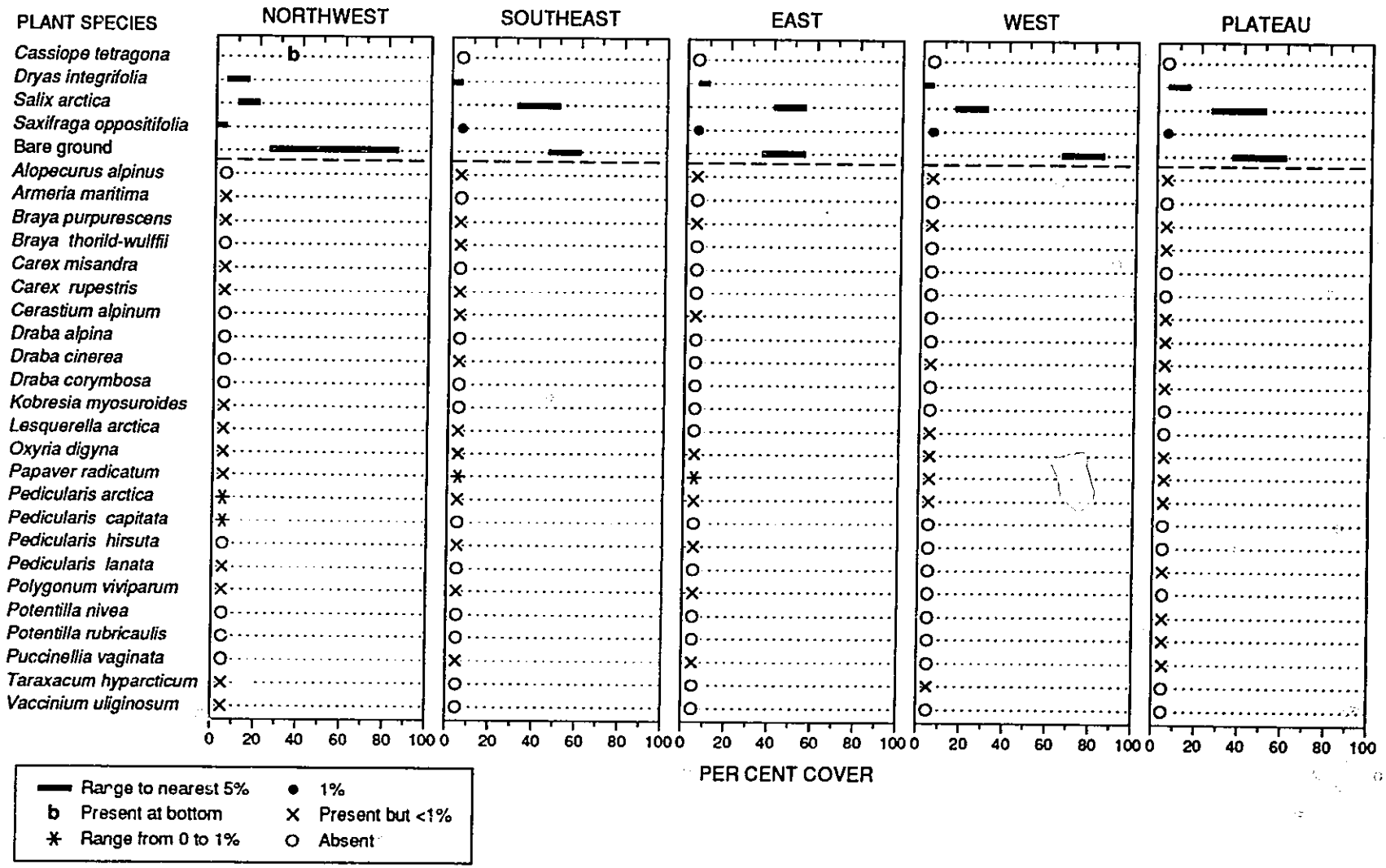
PLANT SPECIES
NORTHWEST
SOUTHEAST
EAST
WEST
PLATEAU
Cassiope tetragona
Dryas integrifolia
Salix arctica
Saxifraga oppositifolia
Bare ground
Alopecurus alpinus
Armeria maritima
Braya purpurescens
Braya thorild-wulffii
Carex misandra
Carex rupestris
Cerastium alpinum
Draba alpina
Draba cinerea
Draba corymbosa
Kobresia myosuroides
Lesquerella arctica
Oxyria digyna
Papaver radicatum
Pedicularis arctica
Pedicularis capitata
Pedicularis hirsuta
Pedicularis lanata
Polygonum viviparum
Potentilla nivea
Potentilla rubricaulis
Puccinellia vaginata
Taraxacum hyparcticum
Vaccinium uliginosum
b
0 20 40 60 80 100
PER CENT COVER
Range to nearest 5%
1%
b Present at bottom
× Present but <1%
✳ Range from 0 to 1%
○ Absent

Pergamon

CHAPTER THREE

Solar Energy, Vol. 54, No. 1, pp. 33–40, 1995

0038-092X/95 $9.50 + .00

0038-092X(94)00106-5

SIMPLE APPROACHES TO MODELLING SOLAR RADIATION IN THE ARCTIC

KATHY L. YOUNG,† MING-KO WOO, and D. SCOTT MUNRO*
Department of Geography, McMaster University, Hamilton, Ontario, Canada L8S 4K1; *Department of Geography, Erindale College, University of Toronto, Mississauga, Ontario, Canada L5L 1C6

Abstract—Solar radiation was modelled for an Arctic location using hourly and twice daily meteorological data. Results indicate that a total cloud model (TC_o) employing cloud opacity data and cloud layer models (CL_o) utilizing cloud opacity and cloud amount data (CL_a) perform equally well; and they are better than a total cloud model (TC_a) employing cloud amount data. The performance of TC_o, CL_o, and CL_a models improve greatly when averaged over 4 days, indicating the feasibility of utilizing rudimentary meteorological observations to broaden the radiation database for the vast Arctic region of North America.

1. INTRODUCTION

The Canadian Arctic covers an area of 2.6×10^6 km^2 (Rizzo and Wiken, 1992) and represents about one-quarter of the terrestrial surface of Canada. There is often a demand for Arctic solar radiation data from researchers in ecology (Edlund and Alt, 1989; Oberbauer and Dawson, 1992), climatology (Kane *et al.*, 1992; Rouse *et al.*, 1992), hydrology (Woo *et al.*, 1990; Young and Lewkowicz, 1990) and glaciology (Munro and Young, 1982). Yet, there are few weather stations that measure radiation in this vast territory (e.g., only four in the Queen Elizabeth Islands). There exists a need to model solar radiation using a limited amount of auxillary information that is easily obtainable from summer scientific field camps.

Presently, several methods are available to model solar radiation under cloudy skies (Atwater and Ball, 1978; Davies and McKay, 1982, 1989; Davies *et al.*, 1984; Lyons and Edwards, 1982a, 1982b; Munro and Young, 1982; Revfeim, 1981; Rietveld, 1978; Suckling and Hay, 1977). Davies *et al.* (1984) identified them into five groups, depending on the type of input data used for the models: (a) Cloud layer based models, (b) Total cloud based models, (c) Sunshine based models, (d) Satellite data based models, and (e) Liu-Jordan (1960) type models which partition global radiation into direct and diffuse components. A selected list of solar radiation models and their required input variables are given in Table 1.

In this study, cloud layer and total cloud model approaches are employed because the information is easily obtainable by scientific field camps without expensive instrumentation. The purpose of this paper is to test the applicability of several solar radiation models to the Arctic and quantify their error in comparison with radiation measurements. Table 1 outlines the variety of models used in this study and their required inputs.

† The current address of Kathy L. Young is Department of Geography, York University, North York, Ontario, Canada M3J 1P3.

2. THEORY

The approach adopted is to model radiation under clear sky conditions and then modify the radiation thus obtained through various cloud models.

2.1 *Radiation under clear sky conditions*

Global radiation (G_o) under clear sky conditions is modelled using a single-band approach (Munro, 1991; Munro and Young, 1982). Here,

$$G_o = G_b + G_d \tag{1}$$

where G_b and G_d are the direct and diffuse components of clear sky radiation respectively, and follows from Paltridge and Platt (1976) with

$$G_b = I_{sc} R^{-2} \mu (\psi_{oz} \psi_r - a_w) \psi_{da} \psi_{ds} \tag{2a}$$

$$G_d = I_{sc} R^{-2} \mu \{0.5 \psi_{oz} (1 - \psi_r) + f \psi_{da} (1 - \psi_{ds}) [\psi_{oz} \psi_r - a_w]\} \tag{2b}$$

I_{sc} is the solar constant (1370 ± 3 Wm^{-2}; Lean, 1991), R is the squared ratio between the actual and average sun–earth distance, μ is the cosine of the solar zenith angle. The transmittances, ψ_{oz}, ψ_r, ψ_{da}, and ψ_{ds}, account for ozone absorption, Rayleigh scattering, aerosol absorption, and aerosol scattering, respectively, and a_w is absorptance by water vapour. The values 0.5 and f (here taken to be 0.8) are the downward scattering ratios for Rayleigh and Mie scattering (Munro and Young, 1982). Procedures using latitude and time to determine μ and R are found in Paltridge and Platt (1976), and so are the various transmittances, ψ_{oz}, a_w, and ψ_r. Aerosol transmittances are treated by assuming that $\psi_{da} = \psi_{ds} = \kappa^m$ (Houghton, 1954), where m is the optical air mass and κ is a coefficient. A value of 0.96 is adopted for κ (Munro and Young, 1982; Suckling and Hay, 1976).

Assuming an atmosphere of finite curvature, the optical air mass was calculated using the method found in Paltridge and Platt (1976),

Table 1. Selected models for review and for this study

Model type	Input variables								
	C_i	CT_i	C_a	C_o	N_s	T	T_d	S_p	P_w
Total cloud									
Won (1977)[1]			X			X	X	X	
Davies *et al.* (1984)			X			X	X	X	
Sunshine									
Rietveld (1978)[1]									
Revfeim (1981)[1]									
Cloud layer									
Davies *et al.* (1984)	X	X		X		X	X	X	
Lyons and Edwards (1982a)	X	X	X						X
Atwater and Ball (1978)	X	X	X					X	X
Sucking and Hay (1977)	X	X	X		X				X
Total cloud									
TC_a			X			X			
TC_o				X		X			
Cloud layer									
CL_o	X	X		X		X			
CL_a	X	X	X			X			

C_i = cloud layer amount; CT_i = cloud layer type; C_a = total cloud amount; C_o = total cloud opacity amount; N_s = number of sunshine hours; T = air temperature; T_d = dew-point temperature; S_p = surface pressure; P_w = precipitable water.
[1] Found in Davies *et al.* (1984).

$$m = \{[(RE/H)\mu]^2 + 2(RE/H) + 1\}^{1/2} - (RE/H)\mu \quad (3)$$

where RE is the radius of the earth (6.370×10^6 m) and H is the height (m) of the homogeneous atmosphere of constant density. H (here taken as 8436 m) has been adjusted for the effects of atmospheric pressure using an empirical relationship between air pressure and elevation (Williams *et al.*, 1972).

The precipitable water (P_w in 10^{-2} m) required for a_w computations is based solely upon average air temperature (t_a in K), and elevation (in m a.s.l) according to expressions formulated by Deacon (1970) and is as follows:

$$P_w = 10^{[16.8 \log(t_a) - 40.97]} \exp(-Z/2700) \quad (4)$$

2.2 *Radiation under cloudy skies*

Clouds play an important role in modifying radiation but our understanding of them is far from complete (Davies *et al.*, 1975; Kondratyev, 1969; Suckling and Hay, 1977). They affect the reflectance, absorptance, and transmittance of the incident radiation (Kondratyev, 1969). Two sets of radiation models that incorporate the cloud effects are used in the present study because they require only a limited amount of easily obtainable information.

2.2.1 *Models using total cloud amount (TC_a, TC_o).* These models are based upon cloud reflectance and treat all clouds as though they are confined to one layer (Munro, 1991). Hence, direct radiation under cloudy skies, G_{bc}, is simply a function of total cloud amount (n):

$$G_{bc} = G_b(1 - n) \quad (5)$$

where G_b is direct radiation under clear skies (eqn 2a). In this study, n is evaluated in two ways using total cloud amount (n_{ca}) and total cloud opacity amount (n_{co}), hence the difference between the TC_a and the TC_o models.

Total cloud amount is expressed as cloud-covered fraction of the sky hemisphere. Total cloud opacity is a visual estimate of the effective cloud cover of the sky (Davies and McKay, 1989) and it is the non-transparent cloud amount that can be seen by the ground-based observer. Consequently, cloud amount totals using cloud opacity values tend to be lower than total cloud estimates. Cloud opacity totals have also been used by Kimura and Stephenson (1969) in their irradiation model.

Diffuse radiation under cloudy skies (G_{dc}) follows from Monteith (1962) and Munro and Young (1982),

$$G_{dc} = D_1 + D_2 \quad (6a)$$

where

$$D_1 = G_d(1 - n) + nG_b(1 - a_n - \alpha_n) \quad (6b)$$

and

$$D_2 = (G_{bc} + D_1)n\alpha_b\alpha(1 - \alpha_b\alpha)^{-1} \quad (6c)$$

with, a_n being the absorptance of cloud; α_n, α_b, and α being the reflectance of the cloud top, the cloud base, and the average reflectance of the ground, respectively. Here, D_1 represents diffuse radiation from the cloudless portion of the sky plus that passing through the cloud layer, while D_2 represents diffuse radiation due to multiple reflection between the cloud base and the ground.

Following Munro and Young (1982), a saturation value of 0.18 is adopted for a_n and α_b is taken to be 0.6. The cloud top reflectance α_n varies according to air mass number and cloud thickness (Paltridge and Platt, 1976),

$$\alpha_n = 1 + \{\exp(-0.5656mx)[x(1 - 1.48m) + 3.54m^{-1} - 2.62] - 3.54m^{-1} - 2.62\}(x + 5.2)^{-1} \quad (7)$$

in which m is the optical air mass and χ is the ratio of cloud thickness to the mean free path of light through the cloud. Thus eqn 7 allows α_n to decrease as m becomes small, yielding relatively high values of diffuse radiation near local noon. Following the practice of Munro and Young (1982) the value $\chi = 1.5$ was obtained empirically by comparing the predicted and measured radiation under an overcast sky at Hot Weather Creek, a field camp 25 km east of Eureka.

Using field measurements made at Hot Weather Creek during the snow-free period in 1990, the mean surface reflectance was found to be 0.16. This value falls within the range reported for tundra surfaces of the alpine, sub-arctic, and arctic environments (Bowers and Bailey, 1989; Lafleur *et al.*, 1993; Oke, 1987). When both direct and diffuse radiation are obtained, global radiation under cloudy skies (G) is given by

$$G = G_{bc} + G_{dc} \tag{8}$$

2.2.2 *Modelling using a cloud layer approach* (CL_a, CL_o). Cloud layer models take into consideration the variations in cloud transmittance with cloud type. They have the general form

$$G = G_o \prod_{i=1}^{j} (1 - C_i + CT_iC_i)/(1 - \alpha b) \tag{9}$$

where G is global radiation, G_o is a theoretical estimate of cloudless sky irradiance, C_i and CT_i are the cloud amount and the transmittance of an individual layer, j is the number of cloud layers, and b is an atmospheric backscatter coefficient for surface reflected radiation. The denominator incorporates the effect of multiple reflections between the surface and the atmosphere (Davies and McKay, 1989; Wendler *et al.*, 1981). Dominant cloud type in each layer determines the transmittances (Davies *et al.*, 1985; Suckling and Hay, 1977). Following the recommendations of Davies *et al.* (1985), three transmittances were incorporated into our study: 0.32 for low clouds, 0.42 for middle layer clouds, and 0.78 for high clouds. The back scattering coefficient (b) is evaluated by Davies and McKay (1982):

$$b = 0.0658(1 - n) + 0.0124 + \alpha_b n \tag{10}$$

Here, the first term is molecular scattering, assumed to apply only to the cloudless portion of the sky, the second term is scattering by aerosol in the atmosphere below the cloud base, and the third term is the cloud base reflectance, the product of average cloud reflectance (α_b) and cloud amount. Total cloud amount $n = n_{co}$ is the total cloud opacity amount in the CL_o model and $n = n_{ca}$ is the total cloud amount in the CL_a model.

Since cloud layer amounts are reported from surface-based observations, a correction is applied to the amount of upper layer clouds to offset the obscuring effect of the layers below,

$$n_i = n_i'/(1 - sum_{nr}) \tag{11}$$

where n_i is the corrected cloud layer amount and n_i' is the reported cloud layer amount. The variable, sum_{nr} is the simple sum of reported cloud amount for the layers beneath (Suckling and Hay, 1977). Direct solar radiation under cloudy skies (G_{bc}) using the cloud-layer model is,

$$G_{bc} = G_o(1 - n) \tag{12}$$

where $n = n_{co}$ is total cloud opacity amount in CL_o; and $n = n_{ca}$ is total cloud amount in the CL_a model. Diffuse radiation (G_{dc}) is then obtained by subtracting G_{bc} from global radiation (G) (Davies *et al.*, 1984).

3. DATA

For model computation and confirmation, we used meteorological data (Table 1) from Eureka weather station (80°00'N, 85°56'W, elevation 10.4 m). The TC_a, TC_o, and CL_o models were evaluated using cloud opacity data from the summer of 1989. The summer of 1973 was the only year at Eureka where there was continuous measurements of cloud amounts to analyse the performance of the CL_a model.

Pyranometers used by official weather stations are checked daily to ensure that they are level and free of condensation, rime, and dust. These instruments are also re-calibrated once every 2 years. The Atmospheric Environment Service (AES) guidelines estimate uncertainty in global radiation values to be the greater of ±1% or ±0.01 $MJm^{-2}h^{-1}$ (AES, 1989). Air temperature values have an uncertainty of ±0.1°C (AES, 1989).

Cloud observations were made following the standard Environment Canada procedures, specifying

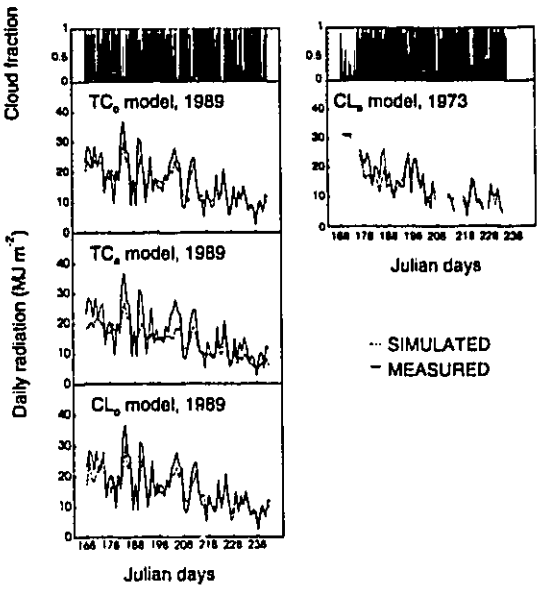

Fig. 1. Measured daily global radiation compared with values estimated by four models using hourly meteorological data at Eureka.

cloud layer heights, amounts, and the types of clouds in each layer. Twice daily observations were also obtained during the snowfree period. The cloud data taken at 0700 h (LST) are considered to be representative of the period 0100–1200 h, and the values obtained at 1900 h (LST) were used to represent cloud conditions from 1200 h to 2400 h. These types of data replicate those which can be obtained easily by field camps scattered in the Arctic during the summer.

4. RESULTS

The radiation models were run using hourly or twice daily cloud data (2×/day). The root mean square error (RMSE) and the mean bias error (MBE) were used as indicators of model performance:

$$\mathrm{RMSE} = \left[\sum_{i=1}^{k} (P_i - O_i)^2/k\right]^{0.5} \qquad (13)$$

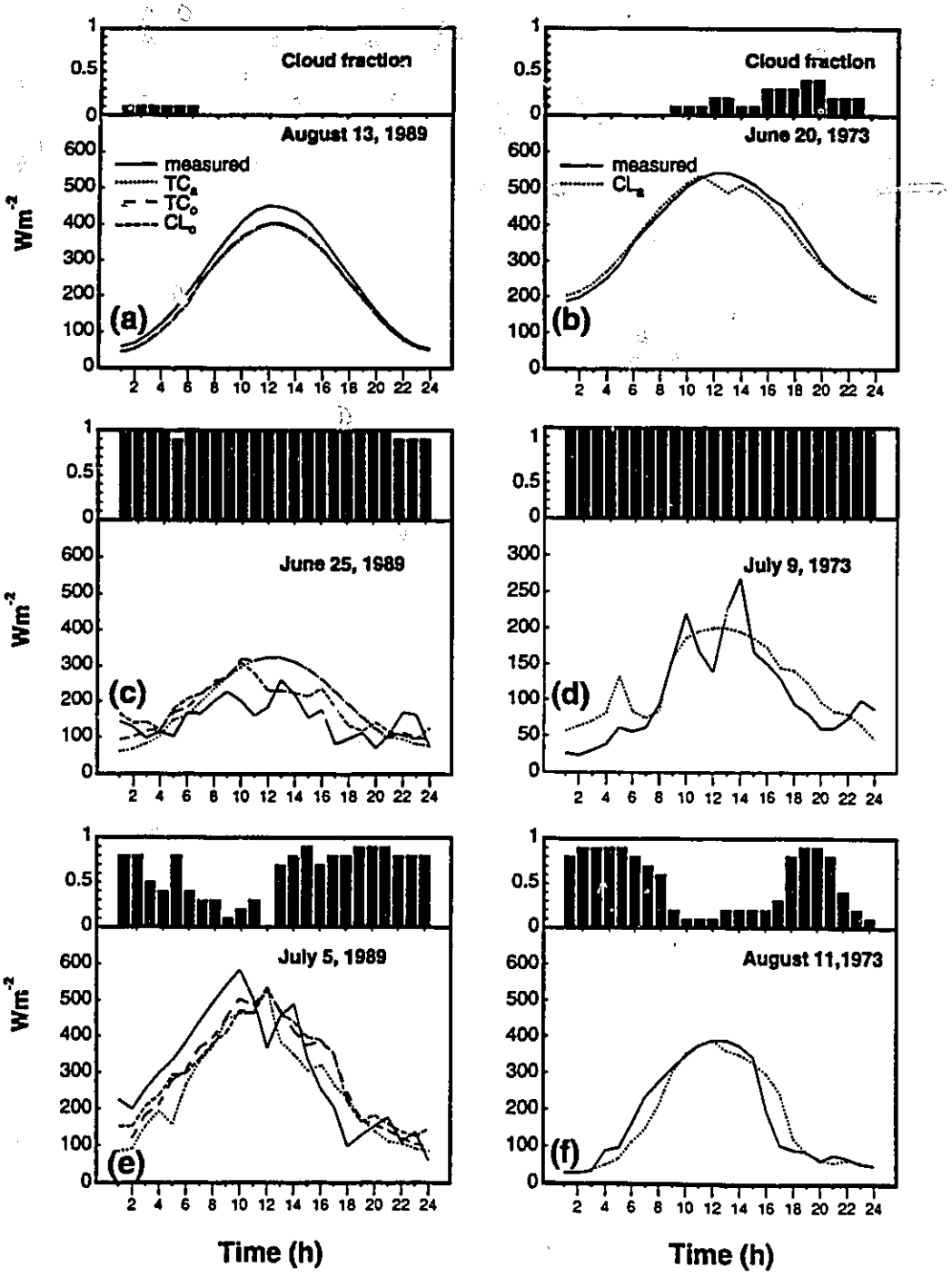

Fig. 2. Hourly global radiation for Eureka compared with values estimated by four models under varying cloud cover conditions.

and

$$\text{MBE} = \sum_{i=1}^{k} (P_i - O_i)/k \qquad (14)$$

where P and O are computed and observed values and k is the number of data points. RMSE was also expressed as a percentage of the mean for different averaging periods (from hourly to 10-day intervals).

4.1 *Calculations using hourly data*

Figure 1 plots the estimates of daily global radiation from four models (TC_a, TC_o, CL_o and CL_a) using hourly meteorological data, compared against measured global radiation at Eureka. Both the TC_o and the CL models perform better than the TC_a model, reproducing the seasonal trend and the shorter term fluctuations. The CL_a model using 1973 data underestimates high peaks early in the season. The TC_a, TC_o, and CL_o models tend to underestimate extreme high peaks and overestimate extreme low troughs in 1989. To examine this phenomenon in greater detail, hourly values for clear, overcast and partly cloudy days are presented in Fig. 2. The underestimation of global radiation during the clear days (Figs. 2a, b) may indicate that the aerosol factor (κ) needs to be elevated from 0.96 to a higher value, as the arctic atmosphere has lower aerosol content than that found in Western Canada. The overestimation during the overcast days (Fig. 2c, d) may be partly explained by the optimized value of $\chi = 1.5$ used throughout the summer period. The CL models which do not use any optimization technique also overestimate radiation under overcast conditions, with the CL_o model overestimating more frequently than the CL_a. On days with partly cloudy skies, (Fig. 2e, f) the models again tend to underestimate during the hours of low cloud cover possibly due to observer overestimate of total cloud and overestimate during the hours with large cloud amounts.

Despite the above limitations, the overall performance can be evaluated against other models currently available. The average %RMSE over 1-day, 5-day, and 10-day periods are plotted in Fig. 3 for all the models (TC_a, TC_o, CL_o, and CL_a) and compared against the %RMSE reported by other radiation models for these same time periods but for more southerly latitudes.

On a daily basis, the TC_a model performs poorly. TC_o, CL_o, and CL_a perform as well as Rietveld's (1978) sunshine model and a cloud layer model by Suckling and Hay (1977) and one by Atwater and Ball (1978). They also provide better results than the Davies *et al.* (1984) total cloud approach and Revfeim's (1981) sunshine model. However, the TC_o, CL_o, and CL_a models yield higher %RMSEs than the cloud layer method by Davies *et al.* (1984), one by Lyons and Edwards (1982a), and a total cloud approach utilized by Won (1977). This is attributed to the fact that the TC_o, CL_o, and CL_a models use only a limited amount of input data compared with the other models mentioned (Table 1).

Over a 5-day period, the %RMSE drops for all models, and the TC_o, CL_o, and CL_a models show greater improvement relative to the other methods. Although still weaker than the models of Davies *et al.* (1984) and Won (1977), the TC_o, CL_o, and CL_a models are as good as the models cited. Over a 10-day basis, the %RMSE of TC_o and CL_o falls below 10%, while CL_a falls below 11%. Here, CL_o and CL_a compare well with four radiation models and perform better than one sunshine model (Revfeim, 1981) whereas TC_o compares well with the Davies *et al.* (1984) and the Won (1977) model which benefit from more input information.

The daily %MBE of the TC_a, TC_o, CL_o, and CL_a models are plotted against the range of %MBE values of several other models (Fig. 4). The bias errors of the CL_o and CL_a models are equivalent to those of the total cloud method used by Davies *et al.* (1984) and Reitveld's (1978) sunshine model. Revfeim's sunshine model has a greater %MBE than both the TC_o and the

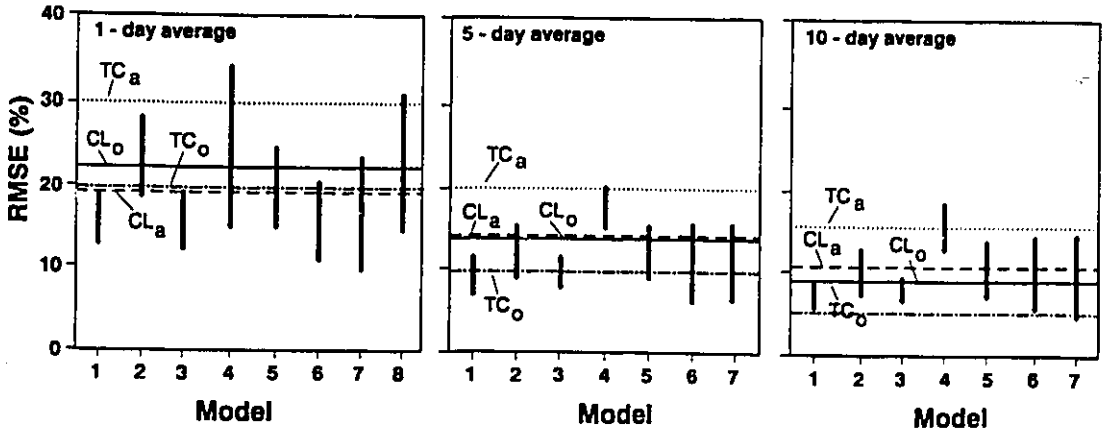

Fig. 3. Percentage root mean square error (RMSE) of the four modelled results (horizontal lines) compared with the ranges of error for other reported models (vertical bars). Three data averaging periods (1 day, 5 days, and 10 days) are represented. Hourly data were used in the computations. 1: Davies *et al.* (1984), CL Model; 2: Davies *et al.* (1984), TC Model; 3: Won (1977); 4: Revfeim (1981); 5: Reitveld (1978); 6: Lyons and Edwards (1982); 7: Suckling and Hay (1977); 8: Atwater and Ball (1978).

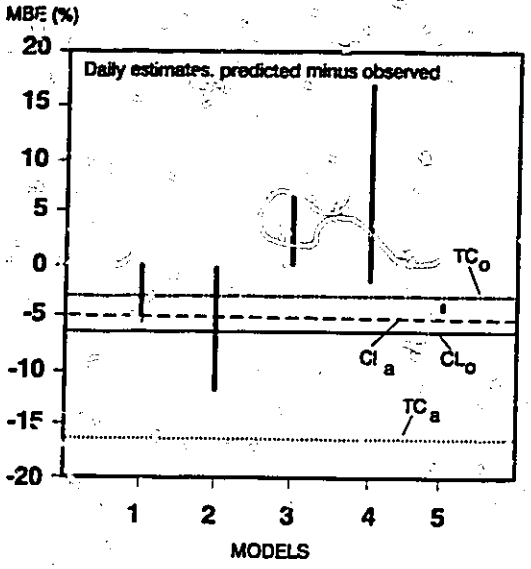

Fig. 4. Percentage mean bias error (MBE) of the four modelled results (horizontal lines) compared with the ranges of error reported by other studies (vertical bars). Hourly data were used in the computations. 1: Davies *et al.* (1984), CL Model; 2: Davies *et al.* (1984), TC Model; 3: Won (1977); 4: Revfeim (1981); 5: Reitveld (1978).

CL models. The TC_o model has a %MBE within the range found by the Davies *et al.* (1984) cloud layer model and Won's (1977) total cloud model.

It is evident from Figs. 3 and 4 that the error associated with the TC_o, CL_o, and CL_a models fall within the range of error experienced by other radiation models, even though the latter models may require more input data. Given the lesser demand for a data base, the total cloud model (TC_o) and the cloud layer models (CL_o and CL_a) offer reasonable alternatives to measuring solar radiation in the Arctic. We further explore the manner in which the %RMSE declines as the averaging time lengthens.

Figure 5 shows that there is a rapid decrease in %RMSE for all four models (TC_a, TC_o, CL_o, and CL_a), as the time base increases from an hourly to a ten-day period. For both the TC_o and CL models, the %RMSE is reduced to less than 15% after 4 days. Thus, for arctic ecologists or geomorphologists (e.g., Keller, 1992) who may require radiation data for only 5–10-day intervals, the TC_o and the CL models are adequate.

4.2 *Calculations using twice daily data*

For many arctic field stations, meteorological and cloud data are obtained only two times per day. Solar radiation was re-calculated using only twice-daily data inputs. Results show that the twice daily totals are comparable to those obtained using hourly data (see Fig. 1). One possible reason is the persistance of high cloud cover during the summers of 1973 and 1989. Davies and McKay (1988, 1989) also observed that the good performance of their cloud layer model using 3-hourly or 6-hourly cloud data is due largely to the persistance of the cloud cover during these times.

The %RMSE of these models using twice daily cloud data can be compared with the same model computation, using hourly data (Fig. 5). The %RMSE for the two times per day version also decline rapidly and

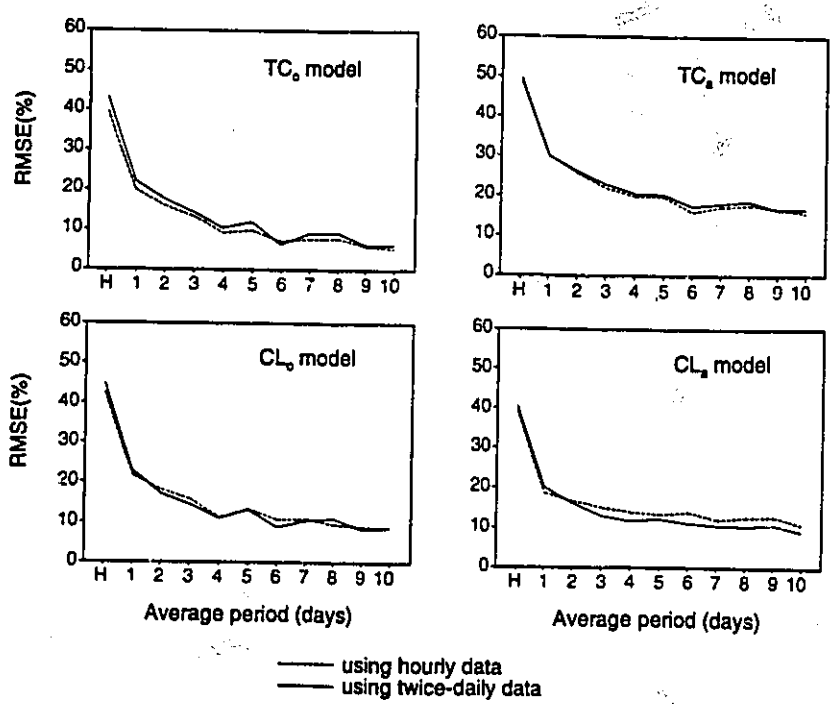

Fig. 5. Decrease of percentage root mean square error (RMSE) with length of averaging period for the four models computed using hourly data and using twice-daily data.

compare well with those of the daily version after 2 or 3 days of data averaging.

5. CONCLUSIONS

This study has shown that solar radiation in the Arctic can be estimated satisfactorily by a total cloud model (TC_o) and cloud layer models (CL_o and CL_a), yielding errors that fall within the range of other radiation models which demand more input information. Acceptable results are obtained using hourly or twice-daily input cloud data, rendering the TC_o, CL_o, and CL_a models appropriate for many arctic sites where data are limited. The model performance improves greatly when the calculated values are summed over 4 days or more. These three models are useful to arctic ecologists and earth scientists interested in mapping solar radiation over large but remote areas.

Overall, it is suggested that cloud opacity or cloud amount data should be obtained at Arctic field camps. This allows the application of the cloud layer model when no measured radiation data are available.

Acknowledgments—This work was funded by a research agreement with the Department of Energy, Mines and Resources, a grant from the Natural Sciences and Engineering Research Council, and a Northern training grant from the Department of Indian and Northern Affairs. The logistical support of the Polar Continental Shelf Project and Dr. S. A. Edlund is gratefully acknowledged. We wish to thank Dr. Bea Alt, Sharon Reedyk, Tim Siferd, Kelly Thompson, and Paul Wolfe for their assistance in the field, and Angus Headley for the loan of instruments. We acknowledge the A.E.S. Canadian Climate Centre through Bill Webb for providing Eureka station data. We wish to thank Dr. John Davies and two anonymous referees for their reviews of the manuscript.

REFERENCES

AES Guidelines for Co-operative Climatic Autostations, Climatic Applications Branch, Canadian Climate Centre, Downsview, Ontario-Environment Canada, Atmospheric Environment Service, 59 pp. (June 30, 1989).

M. A. Atwater and J. T. Ball, A numerical solar radiation model based on standard meteorological observations, *Solar Energy* **21**, 163–170 (1978).

J. D. Bowers and W. G. Bailey, Summer energy balance regimes for alpine tundra, Plateau Mountain, Alberta, Canada, *Arct. and Alp. Res.* **21**, 135–143 (1989).

J. A. Davies and D. C. McKay, Evaluation of selected models for estimating solar radiation on horizontal surfaces, *Solar Energy* **43**(3), 153–168 (1989).

J. A. Davies and D. C. McKay, Estimating solar radiation from incomplete cloud data, *Solar Energy* **41**(1), 15–18 (1988).

J. A. Davies, M. Abdel-Whahab, and D. C. McKay, Estimating solar irradiation on horizontal surfaces, *Inter. J. of Solar Energy* **2**, 405–424 (1984).

J. A. Davies, W. Schertzer, and M. Nunez, Estimating global solar radiation, *Boundary-Layer Meteorol.* **9**, 33–52 (1975).

J. A. Davies, M. Abdel-Wahab, and J. E. Howard, Cloud transmissivities for Canada, *Mon. Weather Rev.* **113**, 338–348 (1985).

J. A. Davies and D. C. McKay, Estimating solar irradiance and components, *Solar Energy* **29**(1), 55–64 (1982).

E. L. Deacon, The derivation of Swinbank's longwave radiation formula, *Q.J.R. Meteorol. Soc.* **96**, 313–319 (1970).

S. A. Edlund and B. T. Alt, Regional congruence of vegetation and summer climate patterns in the Queen Elizabeth Islands, Northwest Territories, Canada, *Arctic* **42**(1), 3–23 (1989).

H. G. Houghton, On the heat balance of the northern hemisphere, *J. of Meteorol.* **11**, 1–9 (1954).

D. L. Kane, R. E. Gieck, G. Wendler, and L. D. Hinzman, Snowmelt at a small Alaskan Arctic watershed. 2. Energy related modelling results, *9th International Northern Research Basins Symposium/Workshop*, Canada, 1992, NHRI Symposium No. 10, (editors) T. D. Prowse, C. S. L. Ommanney, and K. E. Ulmer, 227–247 (1992).

F. Keller, Automated mapping of mountain permafrost using the program PERMAKART within the Geographical Information System ARC/INFO, *Perm. and Periglacial Process.* **3**, 133–138 (1992).

K. Kimura and D. G. Stephenson, Solar radiation on cloudy days, *Research Paper No.* 418, Division of Building Research, National Research Council, Ottawa, 9 pp. (1969).

K. Y. A. Kondratyev, *Radiation in the atmosphere*, Academic Press, New York, 912 pp. (1969).

P. M. Lafleur, A. V. Renzetti, and R. Bello, Seasonal changes in the radiation balance of subarctic forest and tundra, *Arct. and Alp. Res.* **25**(1), 32–36 (1993).

J. Lean, Variations in the sun's radiative output, *Rev. of Geophys.* **29**(4), 505–535 (1991).

B. Y. H. Liu and R. C. Jordan, The interrelationship and characteristic distribution of direct, diffuse and total solar radiation, *Solar Energy* **4**(3), 1–19 (1960).

T. J. Lyons and P. R. Edwards, Estimating global solar irradiance for Western Australia, part 1, *Arch. Meteorol., Geoph., Biockl. Ser. B.* **30**, 357–369 (1982a).

T. J. Lyons and P. R. Edwards, Estimating global solar irradiance for Western Australia, part 2, *Arch. Meteorol., Geoph., Biockl, Ser. B.* **30**, 371–382 (1982b).

J. L. Monteith, An attenuation of solar radiation: A climatological study, *Q. J. R. Meteorol. Soc.* **88**, 508–521 (1962).

D. S. Munro and G. Y. Young, An operational net shortwave radiation model for glacier basins, *Water Resour. Res.* **18**(2), 220–230 (1982).

D. S. Munro, A surface energy exchange model of glacier melt and net mass balance, *Inter. J. of Clim.* **11**, 689–700 (1991).

S. F. Oberbauer and T. E. Dawson, Water relations of Arctic vascular plants, (editors) F. S. Chapin III, R. L. Jefferies, J. F. Reynolds, G. R. Shaver, J. Svoboda, and E. W. Chu, *Arctic ecosystems in a changing climate-an ecophysiological perspective*, Academic Press, San Diego, 259–280 (1992).

T. R. Oke, *Boundary layer climates*, Meuthen, London, 378 pp. (1987).

G. W. Paltridge and C. M. R. Platt, *Radiative processes in meteorology and climatology*, Elsevier, Amsterdam, 318 pp. (1976).

K. J. A. Revfeim, Estimating solar radiation income from "bright" sunshine records, *Q. J. R. Meteorol. Soc.* **107**, 427–435 (1981).

H. R. Rietveld, A new method to estimate the regression coefficients in the formula relating radiation to sunshine, *Agric. Meterol.* **19**, 243–252 (1978).

B. Rizzo and E. Wiken, Assessing the sensitivity of Canada's ecosystems to climatic change, *Climatic Change* **21**, 37–55 (1992).

W. R. Rouse, D. Carlson, and E. J. Weick, Impacts of summer warming on the energy and water balance of wet tundra, *Climatic Change* **22**, 305–326 (1992).

P. W. Suckling and J. E. Hay, A Cloud-layer-sunshine model for estimating direct, diffuse and total solar radiation, *Atmosphere* **15**(4), 194–207 (1977).

P. W. Suckling and J. E. Hay, Modelling direct, diffuse and

total solar radiation for cloudless days. *Atmosphere* **14**(4), 288–308 (1976).

G. Wendler, F. D. Eaton, and T. Ohtake, Multiple reflection effects on irradiance in the presence of Arctic stratus clouds. *J. of Geophys. Res.* **86**(C3), 2049–2057 (1981).

L. D. Williams, R. G. Barry, and J. T. Andrews, Application of computed global radiation for areas of high relief, *J. of App. Meteorol.* **11**, 526–533 (1972).

T. K. Won, The simulation of hourly global radiation from hourly reported meteorological parameters-Canadian Prarie area, *Third Conference, Canadian Solar Energy Society*, Edmonton, Alberta (1977).

M.-K. Woo, K. L. Young, and S. A. Edlund, 1989 observations of soil, vegetation, and microclimate, and effects on slope hydrology, Hot Weather Creek basin, Ellesmere Is., N.W.T., *Current Research, Part D*, Geological Survey of Canada Paper **90-1D**, 85–93 (1990).

K. L. Young and A. G. Lewkowicz, Surface energy balance of a perennial snowbank, Melville Island, Northwest Territories, Canada, *Arct. and Alp. Res.* **22**(3), 290–301 (1990).

CHAPTER FOUR

MODELLING NET RADIATION IN AN ARCTIC ENVIRONMENT USING SUMMER FIELD CAMP DATA

Authors: Kathy L. Young, Ming-ko Woo[1]

Submitted to Solar Energy

July 1995

Geography Department, York University, North York, Ontario, M3J 1P3
[1] Geography Department, McMaster University, Hamilton, Ontario, L8S 4K1

ABSTRACT

A model is presented that uses easily obtained twice-daily field data (cloud, temperature, wind) to calculate net radiation for horizontal and slope sites in an arctic setting. Shortwave radiation is calculated using a cloud-layer model, sensible and latent heat fluxes are determined using temperature and wind data, and the surface heat flux is obtained as the residual in the energy balance equation. Surface temperature which is required for longwave radiation is derived using the force-restore approach.

The modelled results compare favourably with field measurements for a cool and wet (1989) and a warm and dry (1990) summer at Hot Weather Creek (HWC). Significant departures in the results tend to appear during the snowmelt period, suggesting that a better understanding of rapid albedo changes during the snowmelt season are required. A better agreement occurred in 1990 and may partly reflect lower errors in global radiation estimates (15% versus 19% in 1989) and lower windspeeds which dampened turbulent transfers. A variable dust coefficient used in the model and the use of cloud data twice daily may partly explain the discrepancy in the two years, since, measured global radiation values were slightly underestimated in 1989 and overestimated in 1990. This may have attributed to the underestimate of Q^* in 1989 and its overestimate in 1990.

Overall, the root-mean-square error for 1990 was 15-25% when net radiation was averaged over a 5 day period. The model could be applicable to geomorphologists, hydrologists and ecologists interested in mapping the spatial pattern of net radiation for slopes, transects or drainage basins in the north.

1. INTRODUCTION

Global Climate Models (GCMs) suggest temperature increases in the Arctic under a doubling of atmospheric concentration of greenhouse gases (Maxwell, 1992). There is little certainty regarding how alterations in cloud cover, aerosol amounts and changes in ground surface characteristics (Barker and Davis, 1992; Etkin and Agnew, 1992; McGuffie and Henderson-Sellers, 1987) may affect the energy balance under a climate warming scenario. Energy considerations are particularly important in the Arctic where snow and ice melt, and evaporation require considerable latent heat (Kane et al., 1992). Furthermore, changes in cloudiness, snow and ice regime, soil moisture and plant cover may produce negative feedbacks to the radiation balance.

While the GCMs provide scenarios for large areas, local variations in radiation balance are especially relevant to hydrologic, geomorphic and ecological studies. There is a dearth of radiation measurements, over different slopes and under different soil and vegetation conditions. Indeed, radiation measurements are scarce for the arctic region as a whole (Young et al. 1995).

Modelling offers a viable means of estimating net radiation for arctic sites where direct measurements of radiation are scarce. Most field parties supported by the Polar Continental Shelf Project (PCSP) of the Canadian Department of Natural Resources, scattered over large parts of the Arctic during the summers, offer temperature, wind and cloud data on a twice-daily basis. This paper presents a model, that uses such limited input data to compute the surface energy balance for flat and sloping surfaces. The modelled results will be compared with field measurements of net radiation obtained on several sites during the summers of contrasting weather conditions.

2. THEORY

The surface energy balance is

$$Q^* = K^* + L^* = Q_h + Q_e + Q_s \qquad (1)$$

where Q^* is net radiation, K^* is net shortwave radiation, L^* is net longwave radiation and Q_h, and Q_e are sensible and latent heat fluxes. Q_s is the surface energy flux

being equal to the melt energy when a snow cover exists and is equivalent to the ground heat flux (Q_g) otherwise.

The fundamental problem of simulating net radiation is the requirement of T_s which is required in determining outgoing longwave radiation ($L\uparrow$). During the snow period, the estimation of $L\uparrow$ is simplified because $T_s = T_z$ before melt and $T_s = 0°C$ during melt (see section 2.4). However, in summer $L\uparrow$ is not known and T_s needs to be determined before $L\uparrow$ can be calculated. This is possible only through knowing Q_s which is used in the force-restore approach (Deardorff, 1978) (see section 2.4) to solve for T_s. Q_s, itself is obtained as the residual in the surface energy balance equation (eqn. 1) which requires that the turbulent fluxes (Q_h, Q_e) to be calculated during the snowfree period.

In this paper, the turbulent fluxes are also considered during the snow period. This is done so that the model framework can allow for energy losses and gains to the snow surface during the pre- and snowmelt period to be determined, if so desired. These are quantities which may be of interest to hydrologists, climatologists and ecologists working in the north.

2.1 Short-wave radiation

K* can be obtained when the surface albedo, α, and the global radiation, G, are known:

$$K^* = (1 - \alpha)\, G \tag{2}$$

$$G = G_b + G_d \tag{3}$$

where the subscripts b and d distinguish the direct and diffuse components.

The calculation of global radiation (both G_b and G_d) using temperature and cloud data has been presented in Young et al. (1995) and will not be repeated here. Several additional considerations are needed for the present study.

$$\alpha(t) = \alpha(0) - \{[\alpha(0) - \alpha] / [\exp(\beta_1 + \beta_2\, t) + 1]\} \tag{4}$$

(1) The surface albedo, α, is assigned a value of 0.8 for the pre-snowmelt period. During melt, where t is the time since melt began, $\alpha(0)=0.8$ is the snow albedo on the first day of melt, α is the albedo of the ground surface, set at 0.12 (1989-wet) and 0.16 (1990-dry) for the study site, values that fall within the range of a tundra environment (Bowers and Bailey, 1989; Lafleur et al., 1993; Petzold and Rencz, 1975). Values for β_1 and β_2 are 2.46 and -0.26 (Woo and Dubreuil, 1985).

Snow on the first day of melt is rarely clean and an $\alpha(0) = 0.8$ may be too high. Woo (1984) proposed that if the albedo for the first day of melt is $\alpha_e(0)$, it may be equivalent to the albedo for day τ, or $\alpha(\tau)$ in eqn. 4. In other words, the effective albedo on day τ after the initiation of melt is to be shifted by τ-days.

$$\alpha_e(t) = \alpha(t + \tau) \tag{5}$$

The initiation of continuous melt at each experimental site was established from field observations.

(2) Direct solar radiation on a slope (G'_b) is modified by

$$G_b' = G_b \cos i \mu^{-1} \tag{6}$$

in which μ is the cosine of the zenith angle (Young et al., 1995) and i is the angle between the sun's rays and a line normal to the slope, given by Kondratyev (1969) as:

$$\cos i = \cos\theta \sin h_o + \sin\theta \cos h_o \cos(\Psi - \Phi) \tag{7}$$

where θ is slope angle, h_0 is the solar elevation, ψ is solar azimuth, and ϕ is slope azimuth.

Topographic shading is invoked when the cloud fraction (n) is between 0 and 0.7. The aspect of a slope is checked for +/- 90° of its azimuth (Table 1). If the

solar angle is less than the slope angle, shading occurs. Then, n is set to 1.0, the transmissivity function is set to 0.32 (low cloud type) and the cloud coefficient used in longwave radiation calculations (eqn. 10) is set to 0.24 (equivalent to stratus cloud type).

(3) Diffuse radiation on the slope (G'_d) following Barry (1992) is:

$$G'_d = [(G_b/I_0)\cos i\mu^{-1} G_d] + \{G_d\cos^2(\theta/2)(1 - G_b/I_0)\} + [\alpha(G_b + G_d)\sin^2(\theta/2)] \quad (8)$$

where I_0 is the solar constant. Here, the first term is the anisotropic radiation, the second term defines the isotropically distributed radiation and the third term represents diffuse radiation reflected onto the slope by its surrounding ground hemisphere.

(4) For net shortwave radiation on a slope, G'_b and G'_d are substituted into eqn. (3) to obtain G and field determinations of α' specific to each site are used in eqn. (2) (Table 1).

2.2 Longwave radiation

Outgoing longwave radiation, both from a horizontal and a slope surface, is determined by

$$L\uparrow = \epsilon_s \sigma T^4 \quad (9)$$

where σ is the Stefan-Boltzmann constant, ϵ_s is the surface emissivity, considered here to be 0.97 (Kondratyev, 1969), a value which falls within the range for tundra surfaces (Oke, 1978). T_s is the surface temperature (see section 2.4). The incoming longwave is

$$L\downarrow = \epsilon_a \sigma (1+a_c n^2) T_z^4 \quad (10)$$

where ϵ_a is the clear sky emissivity, and is calculated according to Idso and Jackson (1969). T_z is the air temperature at height z. A correction is made for elevation as suggested by Deacon (1970):

$$\epsilon_a = 1-0.261\exp[-7.77\times10^{-4}(273.2-T_z)^2]-z/1000 \quad (11)$$

here, a_c is an empirical coefficient related to cloud type (Monteith, 1973). For two cloud levels with the same cloud cover (n), the a_c value for the lower cloud type will be used because it has more influence on the longwave radiation (Pluss and Mazzoni, 1994).

For slopes less than 30°, incoming longwave radiation can be determined adequately using eq. 12b (Barry, 1992). For steeper slopes, their incoming longwave radiation ($L'\downarrow$) is

$$L'\downarrow = L_i + L_r + L_b \quad (12a)$$

where L_i is the atmospheric emission to the slope,

$$L_i = L\downarrow\cos^2(\theta/2) \quad (12b)$$

with $L\downarrow$ being the incoming longwave onto the horizontal, θ is the slope angle. L_r is the atmospheric emission reflected from the adjacent surfaces to the slope

$$L_r = (1-\epsilon_s)L\downarrow\sin^2(\theta/2) \quad (12c)$$

and L_b is the infra-red flux from the adjacent surface to the slope

$$L_b = \epsilon_s\sigma T_s^4\sin^2(\theta/2) \quad (12d)$$

2.3 Turbulent fluxes

During the melt period, the snow surface is close to 0°C and saturated. A bulk transfer expression is used for sensible heat (Q_h) and latent heat (Q_e) fluxes, assuming melting conditions at the snow surface:

$$Q_h = \rho_a\, C\, D_h\, u_z(T_s-T_z) \quad (13)$$

$$Q_e = \rho_a \lambda \, (\epsilon/P_\rho) \, D_e u_z (e_s - e_z) \tag{14}$$

where, Q_h is the sensible heat flux term, ρ_a and C are the density and the heat capacity of air, u_z is wind speed at height z, T_s and T_z are surface and air temperature respectively. Q_e is the latent heat flux term, λ is the latent heat of vaporization, ε is the dimensionless ratio of the molecular weights of water and air and P_p is the atmospheric pressure, e_s is the saturated vapour pressure of the melting snow surface and e_z is the saturated vapour pressure at height z, calculated from T_z using an equation given by Dilley (1968). D_h and D_e are drag coefficients, considered to be equivalent to the common drag coefficient (D)

$$D_h = D_e = D = k_0^2/[\ln(z-d_0)/z_0)]^2 \tag{15}$$

where k_0 is the von Karman constant, z is the height of the instrument (here taken as 0.5 m) and d_0 is the zero-plane displacement and z_0 is the surface roughness. Field determination of d and z_0 yielded d = 0.0 m, z_0 = 0.005 m for the pre-snowmelt and melt period. In the snowfree season, d = 0.067 m and z_0 = 0.005 m.

The drag coefficient is corrected for atmospheric stability using correction factors presented by Price and Dunne (1976):

$$D_s = D/(1 + \vartheta Ri), \; Ri > 0 \tag{16a}$$

$$D_u = D(1 - \vartheta Ri), \; Ri < 0 \tag{16b}$$

Here, Ri is the Richardson number and ϑ = 10 and D_s and D_u are the coefficients under stable and unstable conditions.

After the snowmelt period, the Penman-Monteith (Monteith 1965, 1973) model is used to calculate the latent heat flux. A change to this model takes advantage of the resistance terms which allows the effects of vegetation growth to be incorporated. "This equation is an improvement because the stomatal resistance term produces an equation that simulates actual evaporation rather than just potential evaporation" (DeCoursey, 1991). Here,

$$Q_e = \frac{S(Q^*-Q_s) + \rho_a C_p(e_z - e_d)/r_a}{S+\gamma(1 + r_s/r_a)} \quad (17)$$

where S is the slope of the saturation vapour pressure-air temperature curve at T_z (Bowers and Bailey, 1989; Dilley, 1968), Q_s is the ground heat flux (see eqn. 1), C_p is the specific heat of the air, e_z is the saturated vapour pressure at T_z , e_d is the saturated vapour pressure at the dewpoint temperature (here assumed to be the minimum of the two daily readings taken at base-camp) (Jury and Tanner, 1975), γ is the psychrometric constant, r_a and r_s are the aerodynamic and the surface resistances. The term r_a is approximated by

$$r_a=(Du_z)^{-1} \text{ under neutral conditions} \quad (18a)$$

$$r_a=(D_s u_z)^{-1} \text{ under stable conditions} \quad (18b)$$

$$\text{and } r_a=(D_u u_z)^{-1} \text{ under unstable conditions} \quad (18c)$$

The surface resistance was not determined in the field, but results from tundra sites with comparable plant types and moisture conditions were applied to this study. Stoner and Miller (1975) offered a relationship between mean leaf resistance (r_s) and global radiation (G) for tundra plants in the wet coastal zone at Barrow, Alaska:

$$r_s=100[2.14+8.67(G/697.32)] \quad (19)$$

This relationship may be compared with those derived by Bowers and Bailey (1989) for an alpine tundra, sparsely vegetated. They found average values of r_s = 100 (moist conditions) and r_s = 650 (dry conditions).

2.4 Surface temperature (T_s)

During the pre-snowmelt period, the surface temperature (T_s) is set to T_z, an approximation used also by Marks and Dozier (1992) in the Sierra Nevada. During melt, T_s is set to 0°C.

After the disappearance of snow, T_s is calculated by the force-restore scheme (Deardorff, 1978; Koster and Suarez, 1992 and Munro, 1991). Deardorff's (1978) scheme is used to model the surface temperature response (dT_s / dt) to the surface energy flux (Q_s or Q_g) which is determined as the residual in the surface energy balance equation:

$$\frac{dT_s}{dt} = 2Q_g/(C_s h_d) - 2\pi(T'_s - T_g)/\Gamma \qquad (20)$$

where, C_s is the heat capacity of the substrate (at 0 - 0.10 m depth) determined using field data (Young et al., 1995, submitted) (Table 2) and calculated using the method described by De Vries (1963). The daily damping depth (h_d) is calculated by,

$$h_d = (K_s \Gamma)^{1/2} \qquad (21)$$

where K_s is the average seasonal thermal diffusivity (Table 2). The value (Γ) is the number of seconds in a day and T'_s and T_g are the temperatures of the surface and subsurface layers, given by

$$T'_s = Q_g/(C_s h_d)\Delta t \qquad (22)$$

$$T_g = Q_g/(C_s h_g)\Delta t \qquad (23)$$

Δt is the time step (3600 s). The annual damping depth (h_g) is also calculated following Deardorff (1978),

$$h_g = (365K_g\Gamma)^{1/2} \quad (24)$$

The surface temperature of the previous time step (T_t) is then updated on an hourly basis so that

$$T(t+1) = T_t + \frac{dT_s}{dt} \quad (25)$$

3. STUDY AREA

Five sites located within 1 km^2 of the base-camp (BC) at Hot Weather Creek (HWC), Fosheim Peninsula, Ellesmere Island (79°58'N, 84°28'W) (Fig. 1) provided data for modelling (Tables 1-3).

A Northwest (NW) facing slope has a gradient of 0.2 (11.5°) and a slope length of 44 m. The upper two-thirds of the slope has under 5% of vegetation while the lower zone is more completely covered by a *Cassiope tetragona* community, grading into a wetland-type vegetation *(Carex aquatilis var. stans, Eriophorum scheuchzeri,* and *Dupontia fisheri*) adjacent to a small tundra pond. The Southeast (SE) facing slope lies directly across from the NW slope and has a gentler gradient of 0.12 (6.8°). Its slope is longer (approx. 73 m). The vegetation cover *Salix arctica* is nearly complete on the lower part of the slope near the pond and for a short distance up the slope (15 m). For the rest of the slope, plant cover is sparse, largely concentrated in small depressions and along soil cracks where moisture collects. The East (E) facing slope consists of three sections: two segments with a gradient of 0.2 (11.3°) separated by a gentler slope of 0.03 (1.9°). The entire slope measures approximately 98 m. The two steeper zones are populated by a *Salix arctica-Dryas integrifolia* community, but the intermediate more gentle slope section is largely devoid of vegetation. The West (W) facing slope is steep (0.38 or 20.1°) and short with a slope length of only 21 m. It is sparsely vegetated by *Salix arctica* and *Dryas*

integrifolia. On the Plateau (P), the vegetation cover (15-35%) is dominated by *Salix arctica*.

4. DATA

Data for these sites came from two summers of contrasting weather conditions: 1989 (cool, wet) July precipitation was 48 mm (P)and 1990 which was warm and dry (July precipitation was only 6 mm (P)). Two sets of data were collected: as input to the model (Tables 1, 2) and data used (a) for assessing the feasibility of employing weather data gathered at BC to represent all sites (both level and slope) and (b) for model validation (Table 3).

The first set of data consisted of location type information (latitude, longitude); site characteristics (slope, aspect and angle, elevation, surface albedo, soil attributes); and twice-daily weather observations of cloud data (cloud type and amount), wind speed and temperature (dry bulb, and minimum temperatures). This collection of weather data generally comprises the minimum amount of data provided twice a day at field camps scattered in the Canadian Arctic and supported by PCSP.

Cloud observations were made following the standard Environment Canada procedures, specifying cloud layer heights, amounts and the types of clouds in each layer (Young et al., 1995). Dry-bulb air temperatures were obtained with mercury thermometers (± 0.5°C), and minimum air temperatures were obtained from maximum-minimum thermometers (± 0.5°C) (AES, 1989). These instruments were housed in an isolated Stevenson screen approximately 1.5 m above the ground surface. Spot wind speed measurements (in knots) were made twice a day approximately 2 m above the ground using Cassella type anemometers (± 10%) (AES, 1989). In the model these wind speed measurements were adjusted to a height of 0.5 m to make them comparable to measured wind speeds and were also converted to units of ms^{-1}. Measurements taken at 0700 h (LST) are considered to be representative of the period 0100-1200 h, and the values obtained at 1900h (LST) were used to represent weather conditions from 1200 to 2400 h.

The second set of data obtained comprised information which was used (1) for validation of applying the twice-daily data to represent meteorological

conditions at the experimental sites on a hourly basis and (2) for assessing model performance. Air temperature and relative humidity on an hourly basis was measured using Campbell Scientific (CS) 201 probes, set at 0.5 m above the surface. Wind speed was measured with CS met-one anemometers also placed 0.5 m above the surface. Net radiation was measured on four slopes and on the horizontal using Middleton or Swissteco radiometers and these data were recorded by Campbell Scientific CR21 dataloggers with values averaged over hourly intervals (Young et al. 1995, submitted) (Table 3).

5. RESULTS

The percentage root mean square error (%RMSE) and percentage mean bias error (%MBE) will be used as an indicator of the performance of modelled net radiation:

$$\%RMSE=100\left[\sum_{j=1}^{k}(P_j-O_j)^2/k\right]^{0.5} \Big/ \sum_{j=1}^{k} O_j/k \qquad (26)$$

and

$$\%MBE=100\left[\sum_{j=1}^{k}(P_j-O_j)/k\right] \Big/ \sum_{j=1}^{k} O_j/k \qquad (27)$$

where P is modelled net radiation and O is either an observed value or a value obtained by some standard computation method, and k is the number of data points being compared. In the following discussion, simulated net radiation refers to modelled values obtained using cloud data, dry-bulb temperature and windspeed input determined twice a day for all sites.

5.1 Selection of surface resistance (r_s)

The equation proposed by Stoner and Miller (1975) and the findings by Bowers and Bailey (1989) were used to determine r_s. In applying the latter approach, r_s = 100 was applied to the wet summer of 1989 and r_s = 650 was used for the dry summer of 1990. To account for wet, rainy conditions, where r_s would approach 0 (Bowers and Bailey, 1989; Lafleur and Rouse, 1990) r_s was set to 0 when

the cloud transmissivity $C_t \leq 0.32$ (see section 5.2) in the latter approach. The net radiation simulated using r_s that was determined by the two methods were compared. The RMSE indicated no significant difference in the calculated net radiation when employing eqn. 19 to derive r_s. The % RMSE was under 6% for both 1989 and 1990. However, when the calculated cumulative evaporation (mm) was compared with measured lysimeter values (mm) (unpublished data), the results determined by using eqn. 19 were unreasonable (<20 mm) in comparison to measured values of about 45 mm at the experimental sites in both 1989 and 1990.

5.2 Selection of aerosol coefficient (κ)

Young et al. (1995) use a constant value of $\kappa = 0.96$ in the calculation of global radiation (G), but Davies et al. (1975) indicate that κ may change in space and in time due to variable atmospheric dust loadings under clear and cloudy conditions. For instance, a value of $\kappa = 0.88$ provided better agreement for a site at Grimsby, Ontario, during cloudless days in 1988. Under cloudy conditions, a value of 0.91 was selected and it produced the best result. On these types of days, winds are usually stronger and atmospheric pollution is less than on cloudless, anticyclonic days. Lyons and Edwards (1982) working in Australia also allowed κ to vary between 0.85 and 1.00.

In view of the occurrence of arctic aerosol (Barrie, 1992), κ may be variable in the arctic atmosphere. It is proposed that much of the aerosol may be removed during rain events. Assuming that precipitation events are accompanied by abundant low clouds, a switch in the value of κ is applied to the model:

$$\kappa=1.00,\ C_t \leq 0.32 \qquad (28)$$

otherwise, $\kappa=0.96$. Overall, a variable κ-value reduces the error of simulated global radiation (%RMSE=19, %MBE= -1 for 1989, %RMSE=15, and %MBE=7 for 1990) compared with the computations where κ is held constant at 0.96 or 1.00.

5.3.1 Wind speed (u)

Net radiation (Q*) for all sites simulated using 2x/d inputs was compared with simulated Q* using hourly measured wind speed. The latter set of simulated values was used as the standard against which the performance of the 2x/d inputs were gauged.

The results were highly variable, with %RMSE ranging from 8 to 21% (Table 4). To examine further the cause of the large errors, the Q* simulated using 2x/d wind data were plotted against those calculated using hourly data. Figure 2 indicates that most points fall on the 1:1 line except those obtained for the calm days (u=0) and for days when speeds were high.

To explore the effect of windspeeds on the error values, the 2x/d wind speed was increased incrementally between 0 and 22 knots (11.3 ms^{-1}). Q* simulated by each of these runs were compared with those calculated using hourly u measured on all the slopes. Figure 3 provides an example from the NW site in 1990, showing that extremely high %RMSEs occurred when u=0 and when u>19 knots, accompanied by very large negative %MBEs.

Considering that these wind conditions are infrequent in the study area, subsequent simulations set u=1 knot (0.51 ms^{-1}) as a minimum and u = 19 knots (9.8 ms^{-1}) as a maximum windspeed. In so doing the %RMSEs and %MBEs were reduced significantly (Table 4).

5.3.2 Air temperature

Simulated Q* using 2x/d field camp data were compared with Q* simulated using measured hourly air temperatures. The %RMSEs were small (<13%) when 2x/d air temperature was substituted for hourly observations. Similarly, measured hourly relative humidity (R_H) was used to simulate Q*, by replacing e_z (eqn. 14) and e_d (eqn. 17) with hourly derived actual vapour pressure (e_a) approximations. Here

$$e_a = (R_H/100)e_z \qquad (29)$$

The %RMSEs indicate small errors (< 9%) when temperatures (2x/day) are used to approximate actual vapour pressure (e_a) in the simulation of net radiation

(eqns. 14 and 17). However, in a comparison of daily latent heat flux calculations, there was a large decrepancy between using hourly measured R_H and using temperature data (2x/d). Large departures arose during episodes of high winds.

5.4 Model validation

(a) The seasonal radiation rhythm

Using 2x/d data obtained at BC extended to the five experimental sites, Q* was simulated. A seven day start-up period was used for each simulation to avoid model instability due to initializations.

The simulated results reproduced the strong seasonal regime of Q* (Fig. 4). In the pre-melt period, values were low, approaching negligible amounts of negative quantitives. This was due to the large snow albedo and below-freezing air temperatures. As albedo declined and as temperatures rose during the snowmelt period, Q* increased. Discrepancy between observed and simulated results during the melt season may partially reflect the occasional movement of the net radiometer over a more complete snowcover, so that it was not monitoring bare ground. Subsequently, the net radiometer may have been monitoring surfaces with varying dust contents.

After the snowmelt, both simulated and observed Q* showed high values around the summer solstice which corresponded with periods with little cloud. Q* fell in July and August, as the solar altitude declined and as greater cloudiness prevailed. Departures between the curves, on a daily basis, may reflect the use of cloud data only twice daily which may not be representative of the hourly changes in cloud amounts. For instance, when simulated and measured global radiation are compared during the snowfree period in 1989 (between Julian days 165-232), the %RMSE increases to 24% and the %MBE drops to -5%, possibly accounting for the underestimation of simulated net radiation during the snowfree period in 1989. Conversely, during the same period in 1990, the %RMSE increased slightly to 17% while the %MBE rose sharply to 11%. This pattern likely accounted for the overestimation of simulated net radiation values (NW, SE, E). The sizeable underestimates in 1989 may also be attributed to the surface albedo used during the snowfree period. For the wet soils, only a limited number of albedo measurements

were made and this could have over-estimated the value (Table 1). DeCoursey (1991) indicated that the albedo of wet soil can range from 0.05-0.24, with an average of 0.11.

(b) Seasonal rhythm of surface energy fluxes

To better understand the net radiation patterns, the energy fluxes were examined throughout entire field seasons of 1989 and 1990 (Fig. 5). During the pre-snowmelt periods, contributions of Q_h and Q_e were negligible given $T_s = T_z$ and consequently, Q_s was dominated by Q^* which was itself small or negative. At times during the melt period, Q_h and Q_e contributed to large Q_s values (see Fig. 5a). Following the snowmelt period which varied among the sites during the two years, Q_s become less dominant and most net radiation was consumed by the turbulent fluxes. In 1989, Q^* was partitioned almost evenly between Q_h and Q_e. During high radiation days (e.g. Julian day 173) Q_h tended to be more important, while on low radiation days (e.g. day 192) Q_e was higher than Q_h. This may be partly a reflection of the model logic, in that r_s was set to 0 when cloud conditions were low ($\leq$0.32). Such a condition would enhance evaporation if wind conditions were moderate as well.

Following the snowmelt season of 1990, Q^* was again largely consumed by Q_h and Q_e. Due to the dry conditions during this season, more energy was used in Q_h and less energy for evaporation (Q_e), except for several days when cloud conditions decreased ($\leq$0.32) and the surface resistance fell to 0. On these occasions, with moderate wind speeds, Q_e dominated (e.g. day 198) and Q_h became small.

(c) Mean Bias Error (%MBE)

In 1989, the %MBEs for the sites were large ranging from -35% (P) to -17% (W). Conversely, the %MBEs were reduced in 1990 and were positive except for the W slope (-2%). Here, the positive values range from about 1% (SE) to about 14% for the E slope (Fig. 6).

(d) Averaging effect of Root Mean Square Error (%RMSE)

The %RMSEs were higher for the simulated daily Q* of 1989 (42-59%) than of 1990 (27 to 39%) (Fig. 7). In 1989, most slopes experienced a 10% improvement in the results when averaged over 5 days, while the W slope experienced the greatest improvement of 18%. This same pattern was duplicated in 1990, where most sites again saw improvements of about 10%, while the W slope showed the best overall performance of 15%. The large error drop for this W slope in both years may be attributed to its low mean bias errors (Fig. 6). There were both under and overestimated values to lower the %MBE and hence average out the error differences over time, resulting in greater %RMSE drops over a 5 day period.

For the other sites in 1989, the high negative %MBEs (see Fig. 6) may have caused the %RMSEs to decline less dramatically. Although the %MBEs were reduced in 1990, the consistent overestimation by the modelled values is again reflected in the gradual declines in %RMSE. The lowest decline in %RMSE occurred for the P site (1989) and likely reflects the small sample size (46 days) versus (85-87 days) for the other sites and the higher %RMSE occurring when 2x/day air temperature is substituted for hourly air temperature (see Table 4).

6. DISCUSSION AND CONCLUSIONS

This paper has demonstrated the feasibility of simulating Q* using limited input data, providing an opportunity to map the radiation over the Arctic where direct measurements are scarce.

The model presented allows an extension of point observations in space to cover different terrains and under various ground surface conditions. Microclimatologists and hydrologists will find it useful in extrapolating snowmelt and evaporation for various slopes and drainage basins. Ecologists can apply the model to compute radiation input for plot or transects; and geomorphologists can estimate the energy available for geomorphic processes to occur over a range of spatial scales.

In the future, this model can be used to investigate the sensitivity of net radiation to changing values of cloud cover, surface conditions, and air temperatures, thus offering a tool to study radiation responses to surface and climatic changes.

ACKNOWLEDGEMENTS

This work was funded by a research agreement with the Department of Energy, Mines and Resources, a grant from the Natural Sciences and Engineering Research Council to M.-k. Woo and a Northern training grant from the Department of Indian and Northern Affairs. The logistical support of the Polar Continental Shelf Project and Dr. S.A. Edlund is gratefully acknowledged. We wish to thank Dr. Bea Alt, Sharon Reedyk, Tim Siferd, Kelly Thompson and Paul Wolfe for their assistance in the field, and Angus Headley for the loan of instruments and for providing unpublished climate data from the automatic weather station at Hot Weather Creek. We wish to thank Kathy Armstrong for typing the manuscript and Carol Randall for drafting the figures.

AES Guidelines for Co-operative Climatic Autostations, Canadian Climate Centre, Downsview, Ontario, Environment Canada, Atmospheric Environment Service, 89-1, 59 pp. (1989).

H.W. Barker, and J.A. Davies, Solar radiative fluxes for broken cloud fields above reflecting surfaces, *J. of Atm. Sci.*, 49, 9, 749-761. (1992).

R.G. Barry , *Mountain weather and climate*, 2nd Edition, Routledge, London, 402 pp. (1992).

J.D. Bowers, and W.G. Bailey, Summer energy balance regimes for alpine tundra, Plateau Mountain , Alberta, Canada. *Arct. and Alp. Res.*, 21, 135-143 (1989).

J.A. Davies, M. Abdel-Wahab and J.E. Howard, Cloud transmissivities for Canada, Mon. Weather Rev., 113, 338-348 (1985).

J.A. Davies, and D.C. McKay, Estimating solar irradiance and components, *Solar Energy*, 29, 1, 55-64 (1982).

E.L. Deacon, The derivation of Swinbank's longwave radiation formula, *Q.J.R. Meteorol. Soc.*, 96, 313-319 (1970).

J.W. Deardorff, Efficient prediction of ground surface temperature and moisture, with inclusion of a layer of vegetation, *J. Geophys. Res.*, 83, 1889-1903 (1978).

D.G. DeCoursey, Environmental features important in nonpoint source models-microclimatology, in (editors) D.S. Bowles and P.E. O'Connell, *Recent advances in the modelling of hydrologic systems*, 205-240, (1991).

D.A. De Vries, *Physics of plant enviornments*, in (editor) W.R. Van Wijk, North Holland Publishing Co., Amsterdam, 382 pp, (1963).

R.E. Dickenson, Land surface processes and climate-surface albedos and energy balance, *Adv. in Geophys.*, 25, 305-352 (1983).

A.C. Dilley, On the computer calculation of vapour pressure and specific humidity gradients, *J. of Appl. Meteorol.*, 7, 717-719 (1968).

D. Etkin, and T.A. Agnew, Arctic climate in the future, in (editors) M.-k. Woo and D.J. Gregor, *Arctic environment: past, present and future,* Proceedings of a Symposium held at McMaster University, Nov. 14-15, 1991, 17-34, (1992).

A. Henderson-Sellers, and A.J. Pitman, Land-surface schemes for future climate models: specification, aggregation, and heterogeneity, *J. of Geophys. Res.*, 97, no. D3, 2687-96 (1992).

H.G. Houghton, On the heat balance of the northern hemisphere, *J. of Meteorol.*, 11, 1-9 (1954).

S.B. Idso, and R.D. Jackson, Thermal radiation from the atmosphere, *J. of Geophys. Res.*, 74, 23, 5397-5403 (1969).

W.A. Jury, and C.B. Tanner, Advection modification of the Priestley and Taylor evapotranspiration formula, *Agron, J.*, 67, 819-812 (1975).

D.L. Kane, L.D. Hinzman, M.-k. Woo and K.R. Everett, Arctic hydrology and climate change, in (editors) F.S. Chapin III, R.L. Jefferies, J.F.Reynolds, G.R. Shaver, J. Svoboda, and E. Chu, *Arctic ecosystems in a changing climate - an ecophysiological perspective,* Academic Press, Toronto, 35-57, (1992).

K.Y.A. Kondratyev, *Radiation in the atmosphere*, Academic Press, New York, 912 pp, (1969).

R.D. Koster, and M.J. Suarez, Modelling the land surface boundary in climate models as a composite of independent vegetation stands, *J. of Geophys. Res,* 97, no. D3, 2690-2715 (1992).

P.M. Lafleur, A.V. Renzetti and R. Bello, Seasonal changes in the radiation balance of subarctic forest and tundra, *Arct. and Alp. Res.*, 25, 32-36 (1993).

P.M. Lafleur, and W.R. Rouse, Appli ·ation of an energy combination model for evaporation from sparse canopies, *Agri. and For. Meteorol.*, 49, 135-153 (1990).

J. Lean, Variations in the sun's radiative output, *Rev. of Geophys.*, 29, 505-535 (1991).

T.J. Lyons, and P.R. Edwards, Estimating global solar irradiance for Western Australia, Part I, *Arch. Met. Geoph. Biokl., Ser. B,* 30, 357-369 (1982).

D. Marks, and J. Dozier, Climate and energy exchange at the snow surface in the Alpine region of the Sierra Nevada-2. snow cover energy balance, *Water Res. Res.* 28, 11, 3043-3054 (1992).

B. Maxwell, Arctic climate (editors), F.S. Chapin III, R.L. Jefferies, J.F. Reynolds, G.R. Shaver, J. Svoboda, E.W. Chu, *Arctic ecosystems in a changing climate- an ecophysiological perspective*, Academic Press, San Diego, 259-280 (1992).

J.L. Monteith, *Principles of Environmental Physics*, Edward Arnold Ltd., London, 241 pp. (1973).

J.L. Monteith, Evaporation and environment, *Symp. Soc., Exp. Bio.*, 19, 205-234 (1965).

D.S. Munro, A surface energy exchange model of glacier melt and net mass balance. *Inter. J. of Clim.* 11, 689-700 (1991).

T.R. Oke, *Boundary-layer climates*, Methuen and Co. Ltd., London, 372 pp (1978).

D.E. Petzold, and A.N. Rencz, The albedo of selected subarctic surfaces, *Arct. and Alp. Res.*, 7, 4, 393-398 (1975).

C. Plüss and R. Mazzoni, The role of turbalent heat fluxes in the energy balance of high alpine snow cover, *Nor. Hydrol.* 25, 25-38 (1994).

A.G. Price, and T. Dunne, Energy balance computations of snowmelt in a sub-arctic area, *Water Res. Res.*, 12, 686-694 (1976).

W.A. Stoner, and P.C. Miller, Water relations of plant species in the wet coastal tundra at Barrow, Alaska, *Arct. and Alp. Res.*, 7, 2, 109-124 (1975).

M.-k. Woo, Simulating the effects of dust on arctic snowmelt, Proceedings of the Fifth Northern Research Basins Symposium, *The role of snow and ice in northern basin hydrology*, Vierumaki, Finland, March 19-23, 97-116 (1984).

M.-k. Woo, and M-A. Dubreuil, Empirical relationship between dust content and arctic snow albedo, *Cold Reg. Sci. and Technol;* 10, 125-132 (1985).

K.L. Young, M.-k. Woo and D.S. Munro, Simple approaches to modelling solar radiation in the Arctic, *Solar Energy*, 54, 33-40 (1995).

K.L. Young, M.-k. Woo, and S.A. Edlund, Influence of local topography, soil and vegetation on microclimate and hydrology at a High Arctic site, submitted to *Arct. and Alp. Res.* (March, 1995).

C	heat capacity of air (1200)	$Jm^{-3}K^{-1}$
C_p	specific heat of air (1010)	$Jkg^{-1}K^{-1}$
C_s	heat capacity of the substrate	$Jm^{-3}K^{-1}$
C_t	cloud transmissivity	dimensionless
D	common drag coefficient	dimensionless
D_e	drag coefficient for latent heat	dimensionless
D_h	drag coefficient for sensible heat	dimensionless
D_s	drag coefficient under stable conditions	dimensionless
D_u	drag coefficient under unstable conditions	dimensionless
G	global radiation	Wm^{-2}
G_b	direct radiation	Wm^{-2}
G_d	diffuse radiation	Wm^{-2}
G'_b	direct radiation on slope	Wm^{-2}
G'_d	diffuse radiation on slope	Wm^{-2}
I_0	solar constant (1370)	Wm^{-2}
K*	net shortwave radiation flux density	Wm^{-2}
K_S	thermal diffusivity (x 10^{-7})	m^2s^{-1}
L↓	atmospheric longwave radiation (level)	Wm^{-2}
L↑	longwave radiation leaving slope, level	Wm^{-2}
L'↓	atmospheric longwave radiation (slope)	Wm^{-2}
L*	longwave radiation flux density	Wm^{-2}
L_b	infra-red flux from the adjacent surface received by the slope	Wm^{-2}
L_i	atmospheric emission of longwave radiation to the slope	Wm^{-2}

L_r	atmospheric emission from the adjacent surface reflected onto the slope	Wm^{-2}
LST	local standard time	h
MBE	mean bias error	
P	computed value	MJm^{-2}
P_p	atmospheric pressure (101330)	P_a
Q*	net radiation flux density	Wm^{-2}
Q_e	latent heat flux density	Wm^{-2}
Q_g	ground heat flux density	Wm^{-2}
Q_h	sensible heat flux density	Wm^{-2}
Q_s	surface energy flux density	Wm^{-2}
R_H	relative humidity (%)	dimensionless
Ri	Richardson number	dimensionless
RMSE	root mean square error	
S	slope of the saturated vapour pressure-air temperature curve	$P_a°C^{-1}$
T'_S	temperature of the surface layer	K
T_C	thermal conductivity	$Wm^{-1}\ k^{-1}$
T_d	dew-point temperature (here assumed to be the minimum temperature)	K
T_g	temperature of the subsurface layer	K
T_s	surface temperature	K
T_t	surface temperature of the previous time step	K
T_z	air temperature	K
0	observed value	MJm^{-2}

a_c	cloud coefficient	dimensionless
d_0	zero-plane displacement (0.0 snow; 0.067 snowfree)	m
e_a	actual vapour pressure	P_a
e_d	saturated vapour pressure at T_d (assumed to be the minimum air temperature)	P_a
e_s	saturated vapour pressure of the melting snow surface (611)	P_a
e_z	saturated vapour pressure at T_z	P_a
h_0	solar elevation	radians
h_d	daily damping depth	m
h_g	annual damping depth	m
i	the angle between the sun's rays and a line normal to the slope	radians
k_0	von Karman constant (0.40)	dimensionless
m.asl	metres above sea level	m
n	total cloud amount (tenths of the sky)	dimensionless
r_a	aerodynamic resistance	sm^{-1}
r_s	surface resistance due to stomatal control	sm^{-1}
t	time since melt began	day
u_z	wind speed at height z	ms^{-1}
z	height	m
z_0	surface roughness (0.005)	m
α	surface albedo (background albedo)	dimensionless
α'	albedo of the ground surface (level, slope)	dimensionless
$\alpha(0)$	albedo on the first day of melt	dimensionless

α_e	effective snowmelt albedo	dimensionless
β_1	coefficient in snow surface albedo (2.46)	dimensionless
β_2	coefficient in snow surface albedo (-0.26)	dimensionless
Γ	number of seconds in a day (86400)	s
γ	psychrometric constant (66)	$P_a°C^{-1}$
ε	ratio of the molecular weights of water and air (0.622)	dimensionless
ε_a	clear sky emissivity	dimensionless
ε_S	surface emissivity (0.97)	dimensionless
θ	slope angle	radians
κ	aerosol coefficient	dimensionless
λ	latent heat of vapourization ($x10^6$)	Jkg^{-1}
μ	cosine of the solar zenith angle	radians
π	Pi	dimensionless
ρ_a	air density	kgm^{-3}
σ	Stefan-Boltzmann constant (5.67×10^{-8})	$Wm^{-2}\ K^{-1}$
τ	time shift in the calculation of snow albedo	day
ϕ	slope azimuth	radians
Ψ	solar azimuth	radians
ϑ	constant with a value of 10	dimensionless
Δt	time step	s

Table 1. **Initial conditions and input data for simulation of net radiation at Hot Weather Creek, N.W.T. (1989-1990)**

Initial conditions:

Site	**P**	**NW**	**SE**	**E**	**W**
Latitude	79°58'N	✓*	✓	✓	✓
Longitude	84°28'W	✓	✓	✓	✓
Slope angle (°)	0	11.5	6.8	4.2 (11.3)[a]	21.0
Slope aspect (°) (90)	0	315 (135)[b]	135(-45)	90 (-90)	270
Elevation (m.asl)	118	95	96	99	85
Pre-snowmelt albedo	0.8/[c]-	0.7/0.7	0.8/0.8	0.7/0.8	0.7/0.8
Snowfree albedo 0.11/0.16	0.125/-	0.13/0.19	0.135/0.16	0.10/0.14	
Time shift (τ)	3/-	2/1	5/2	2/1	2/1

Input Data (2x/d) for all experimental sites

Clouds (Amount/Type)
Dry-bulb air temperature (°C)
Minimum air temperature (°C)
Windspeed (Knots)

*✓ same as Plateau (P)

[a] shadow occurred for E slope when sun elevation fell below 11.3° (see study area)
[b] aspect according to Kondratyev (1969)
[c] 1989/1990 values in each year

Table 2. Soil attributes from experimental sites, Hot Weather Creek, N.W.T. (1989-1990)

Site	Year	Thermal * Conductivity (T_c) ($Wm^{-1} K^{-1}$)	Heat* Capacity (C_s) ($x10^6 Jkg^{-1}$)	Thermal** Diffusivity (K_s) ($x10^{-7} m^2s^{-1}$)	Daily Damping Depth (h_d) (m)	Annual Damping Depth (h_y) (m)
NW	1989	0.6 (0.1)	1.7 (0.1)	3.9	0.2	3.5
SE	1989	0.5 (0.1)	1.8 (0.2)	2.7	0.2	2.9
E	1989	0.6 (0.1)	1.8 (0.1)	3.4	0.2	3.3
W	1989	0.7 (0.1)	1.8 (0.2)	3.9	0.2	3.5
P	1989	0.9 (0.1)	2.2 (0.2)	4.0	0.2	3.6
NW	1990	0.5 (0.1)	1.4 (0.2	3.9	0.2	3.5
SE	1990	0.4 (0.2)	1.6 (0.4)	2.7	0.2	2.9
E	1990	0.5 (0.2)	1.5 (0.3)	3.3	0.2	3.2
W	1990	0.5 (0.0)	1.3 (0.1)	3.7	0.2	3.4

* average seasonal value for 0.0 - 0.10 m depth
** $K_s = (T_c / C_s)$
( ) standard deviation
note: soil conditions reflect net radiometer position at expermental site

Table 3. Hourly measured data used for verifying use of 2x/day input data and model validation

Verifying use of 2x/day input data:

Site	1989					1990			
	P	NW	SE	E	W	NW	SE	E	W
Windspeed (ms^{-1})	X		X			X		X	X
Air temperature (°C)	X	X	X	X	X	X		X	X
Relative humidity (%)	X	X	X	X	X	X		X	X

Validation of model:

Site	1989					1990			
	P	NW	SE	E	W	NW	SE	E	W
Net Radiation	X	X	X	X	X	X	X	X	

X Employed

Table 4. Testing feasibility of using input data at base-camp versus hourly measured input data from sites to simulate Q^*, Q_e (observed: hourly measured inputs, simulated: 2x/day inputs)

Year	Site	Wind (%RMSE) Q^*	Dry-bulb (°C)* Wind limit (%RMSE) Q^*	Min. temp. (°C)** Wind limit (%RMSE) Q^*	Min. temp. (°C)** Wind limit (%RMSE) Q_e	Min. temp. (°C)** Wind Limit (%RMSE) Q_e
1989	NW	—	7.0 (76)	8.4 (76)	60.7 (76)	33.4 (65)[a]
	SE	8.2 (30)	6.6 (76)	3.6 (76)	68.0 (76)	41.4 (59)
	E	—	3.1 (72)	3.3 (73)	55.5 (73)	36.7 (63)
	W	—	6.0 (70)	5.3 (68)	62.7 (68)	41.0 (41)
	P	20.4 (82)	12.4 (82)	4.4 (82)	72.0 (82)	44.5 (63)
1990	NW	21.1 (65)	5.8 (58)	1.5 (56)	96.91 (56)	43.0 (52)
	SE	—	—	—	—	—
	E	8.7 (68)	4.1 (72)	3.7 (72)	97.8 (72)	47.1 (64)
	W	8.3 (50)	1.8 (64)	3.0 (63)	104.4 (63)	47.3 (53)

— no continuous measurements
( ) sample size
* Air temp. 2x/d compared with hourly air temp. with limits to wind. If wind = 0 knots, wind = 1 knot and if wind > 19 knots, wind = 19 knots
** Compared with hourly measured relative humidity and wind limit
a took out RMSE > 10 MJm^{-2} which were due to high wind speeds (generally in excess of 10 knots)

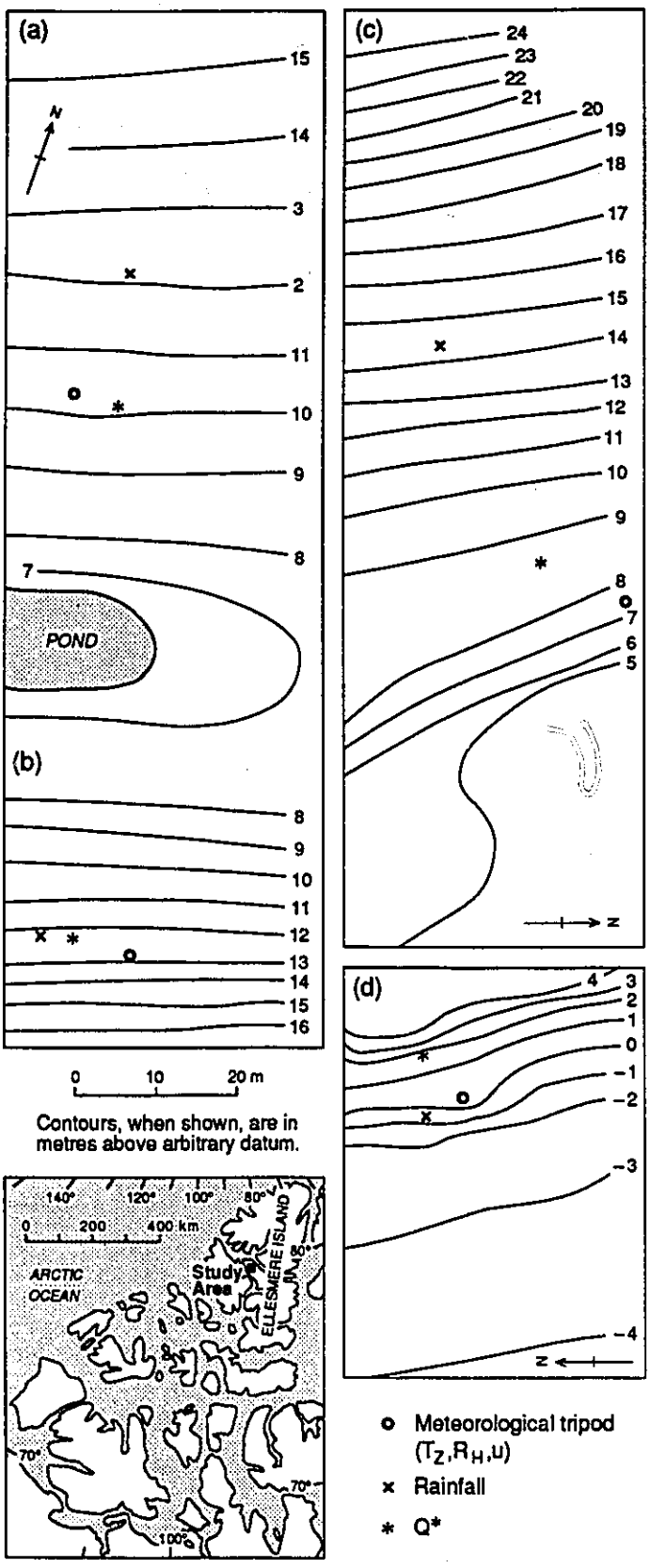
(a)
15
14
3
2
11
10
9
8
7
POND
(b)
8
9
10
11
12
13
14
15
16
0 10 20 m
(c)
24
23
22
21
20
19
18
17
16
15
14
13
12
11
10
9
8
7
6
5
z
(d)
4
3
2
1
0
−1
−2
−3
−4
z
Contours, when shown, are in metres above arbitrary datum.
140°
120°
100°
80°
0 200 400 km
ARCTIC OCEAN
Study Area
ELLESMERE ISLAND
80°
70°
70°
100°
Meteorological tripod (T_Z,R_H,u)
Rainfall
Q*

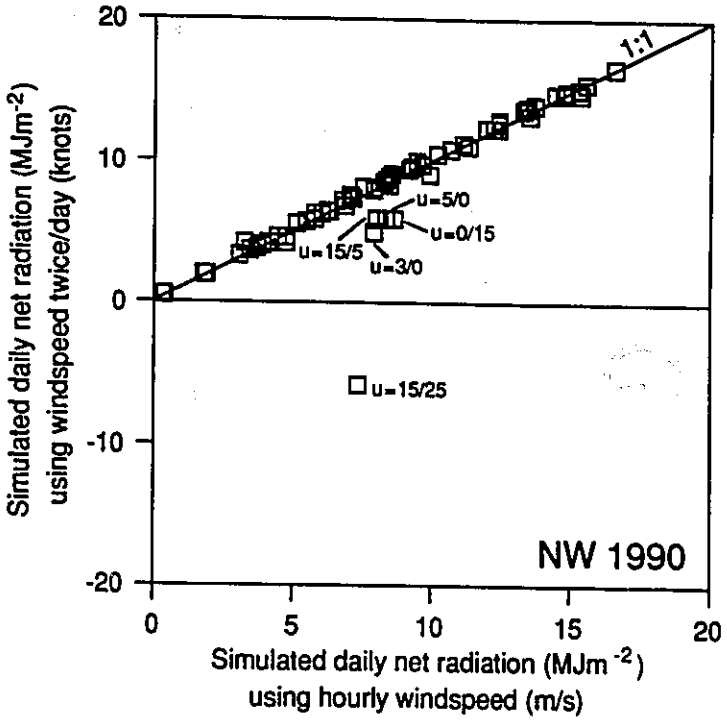
20
10
0
-10
-20
0
5
10
15
20
1:1
u=5/0
u=0/15
u=15/5
u=3/0
u=15/25
NW 1990
Simulated daily net radiation (MJm-2) using windspeed twice/day (knots)
Simulated daily net radiation (MJm -2) using hourly windspeed (m/s)

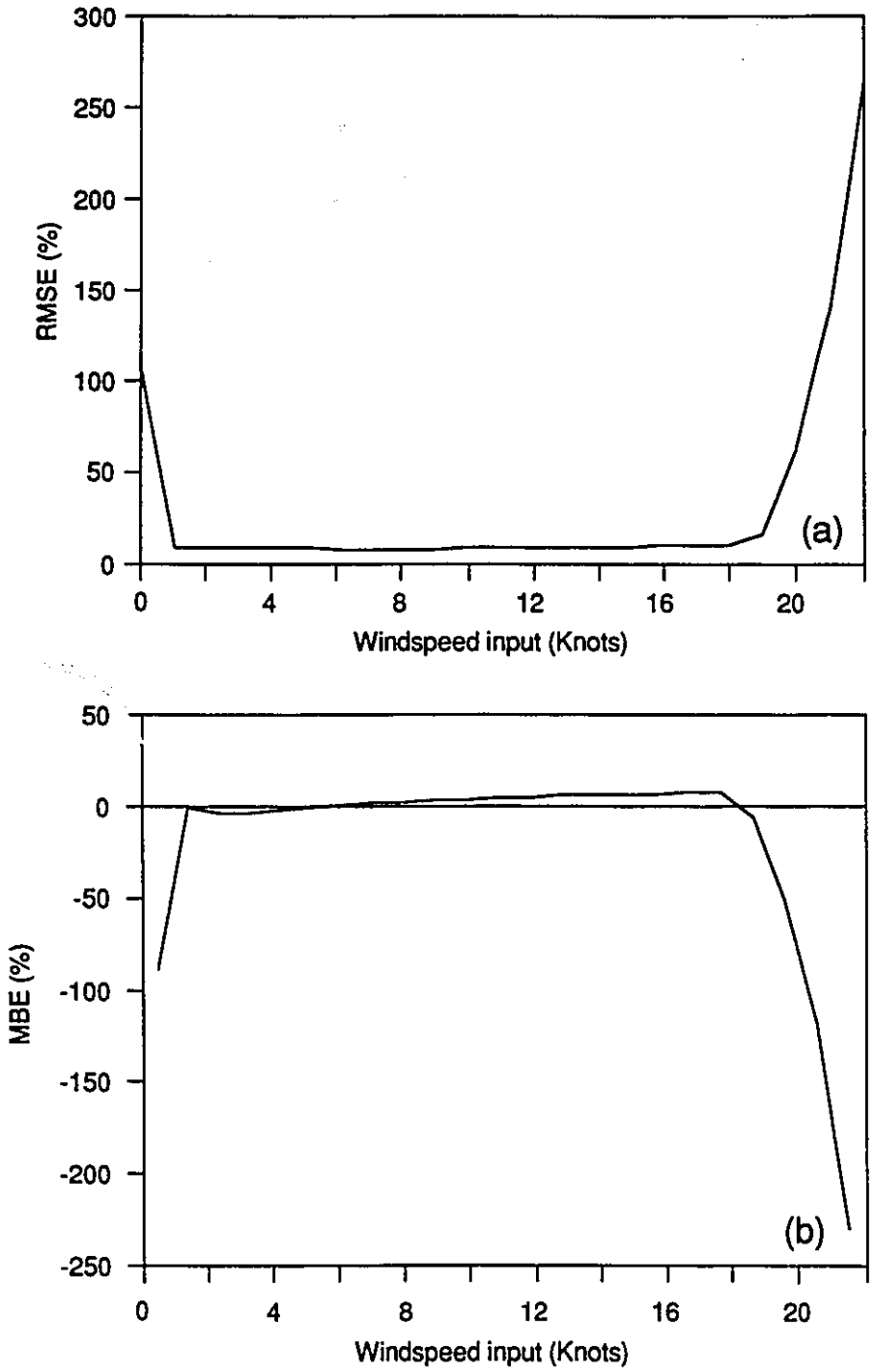
300
250
200
150
100
50
0
RMSE (%)
(a)
0
4
8
12
16
20
Windspeed input (Knots)
50
0
-50
-100
-150
-200
-250
MBE (%)
(b)
0
4
8
12
16
20
Windspeed input (Knots)

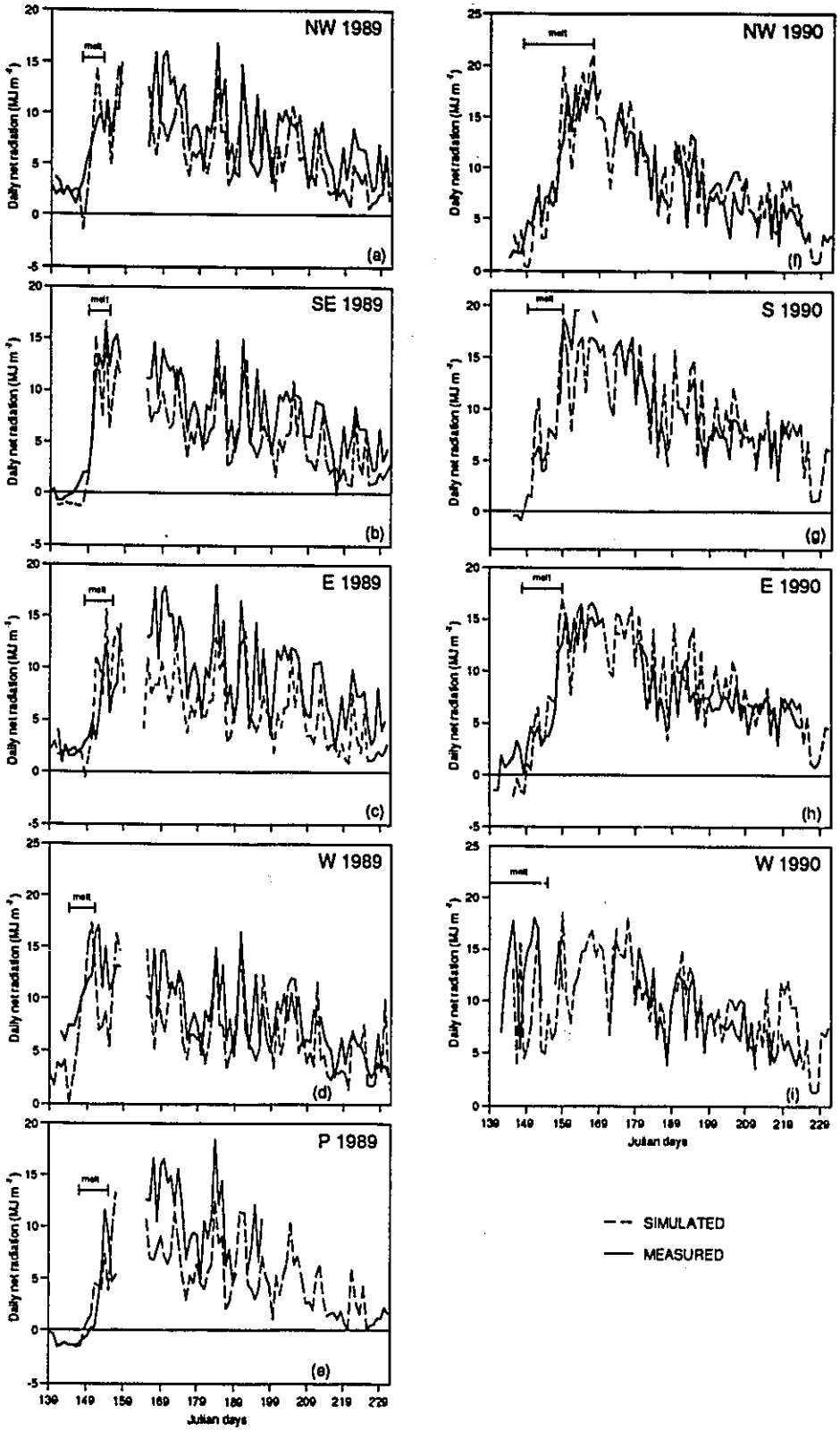
NW 1989
SE 1989
E 1989
W 1989
P 1989
NW 1990
S 1990
E 1990
W 1990
melt
Daily net radiation (MJ m⁻²)
Julian days
SIMULATED
MEASURED

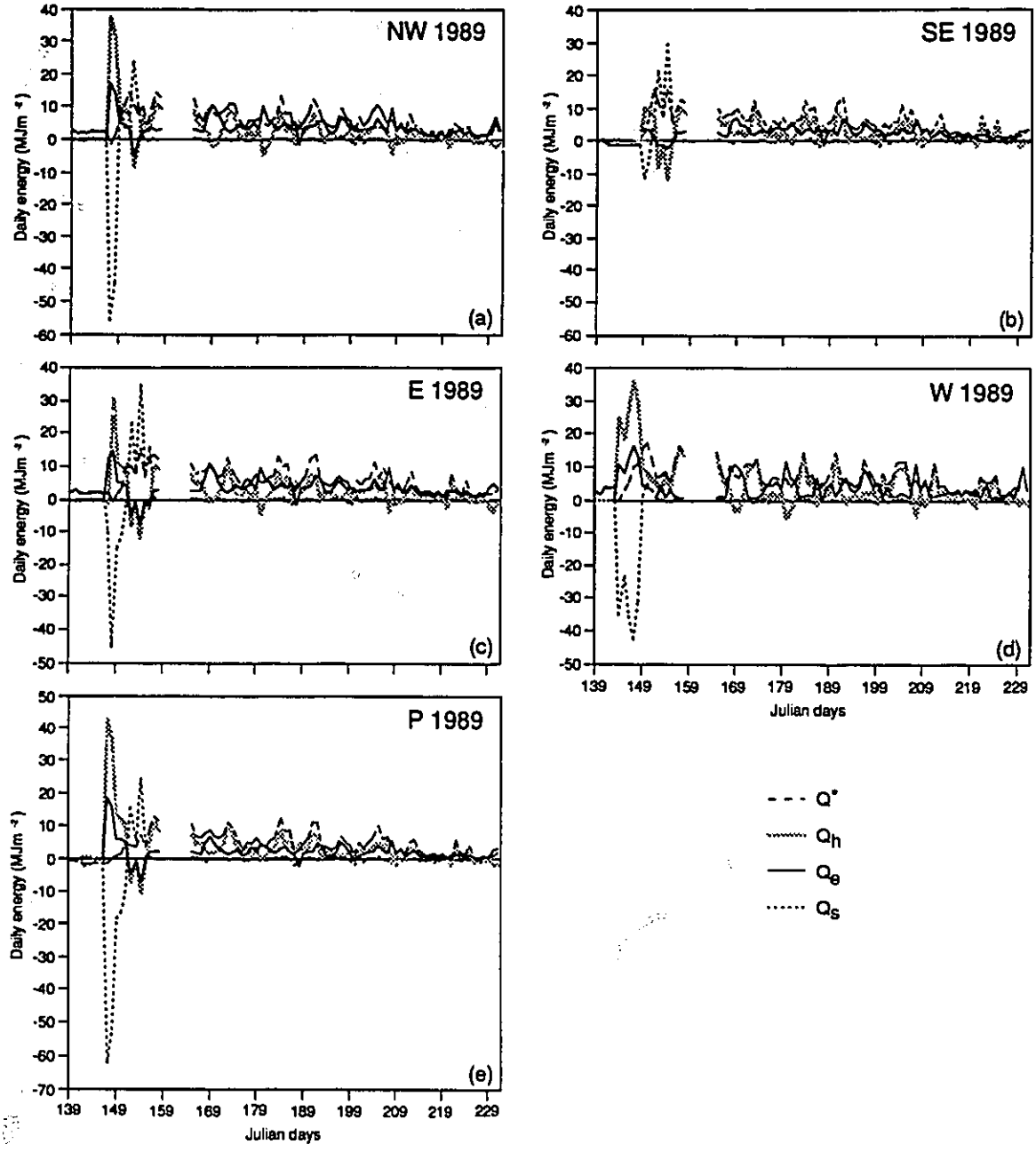
NW 1989
(a)
SE 1989
(b)
E 1989
(c)
W 1989
(d)
P 1989
(e)
Daily energy (MJm⁻²)
Julian days
Q*
Qh
Qe
Qs

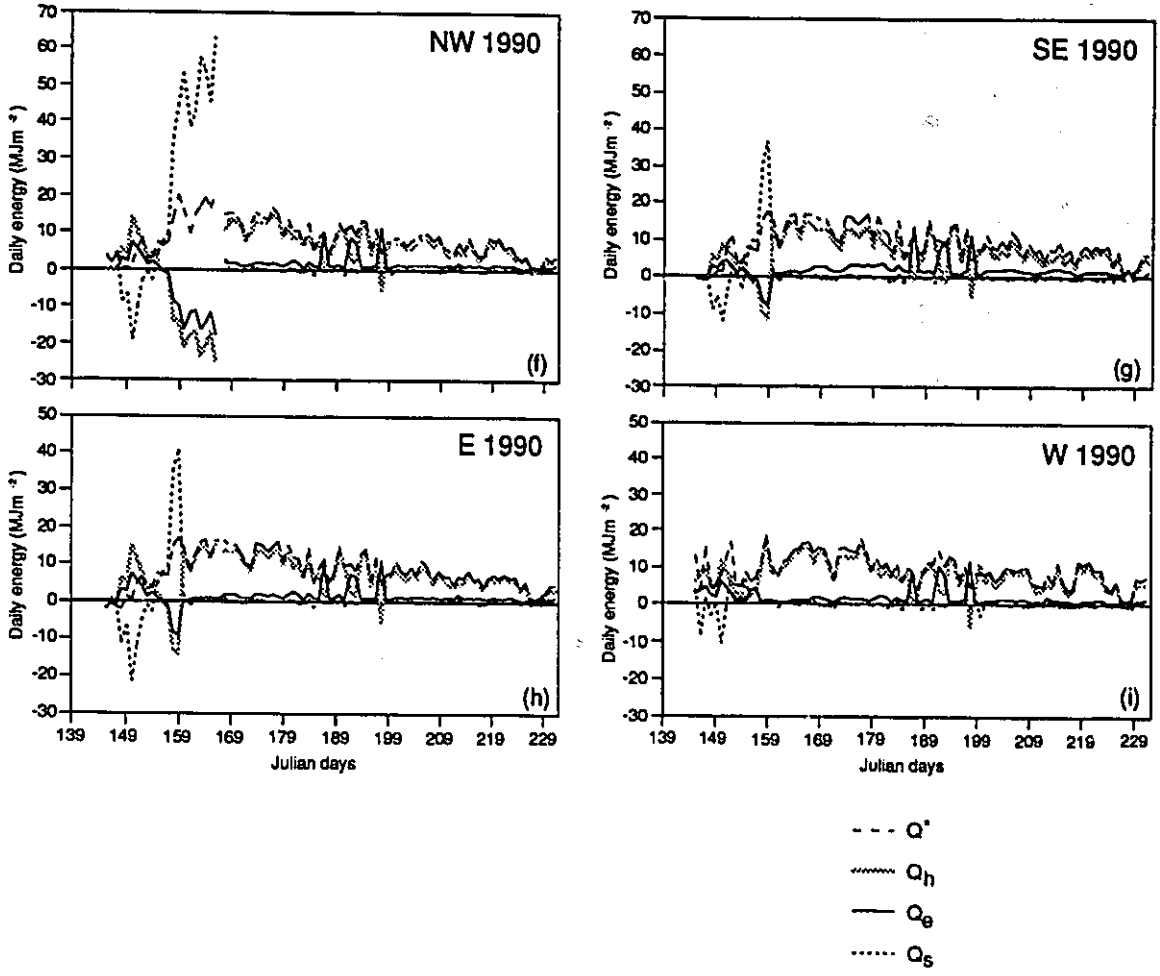
NW 1990
(f)
SE 1990
(g)
E 1990
(h)
W 1990
(i)
Daily energy (MJm⁻²)
Julian days
Q*
Qh
Qe
Qs

Fig. 6

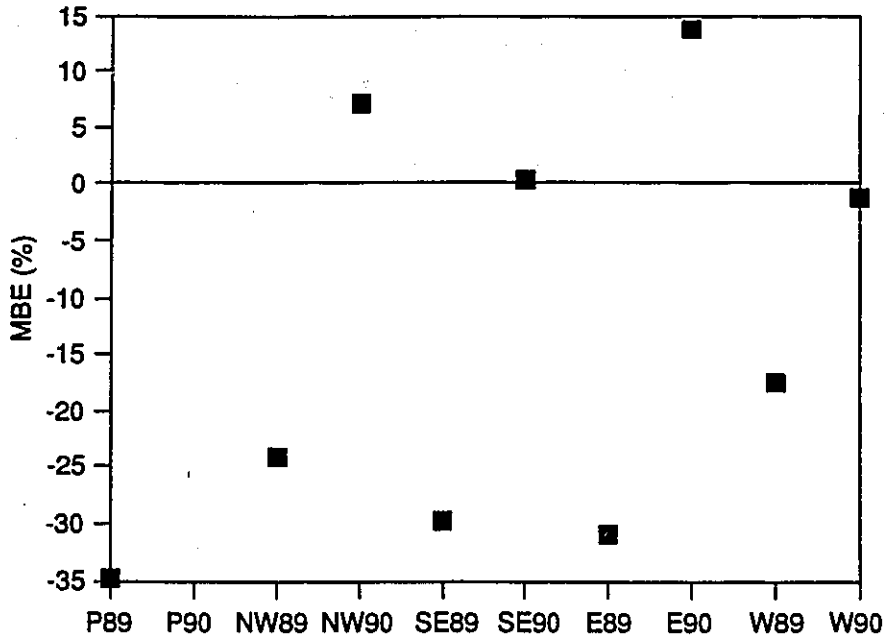
15
10
5
0
-5
-10
-15
-20
-25
-30
-35
MBE (%)
P89
P90
NW89
NW90
SE89
SE90
E89
E90
W89
W90

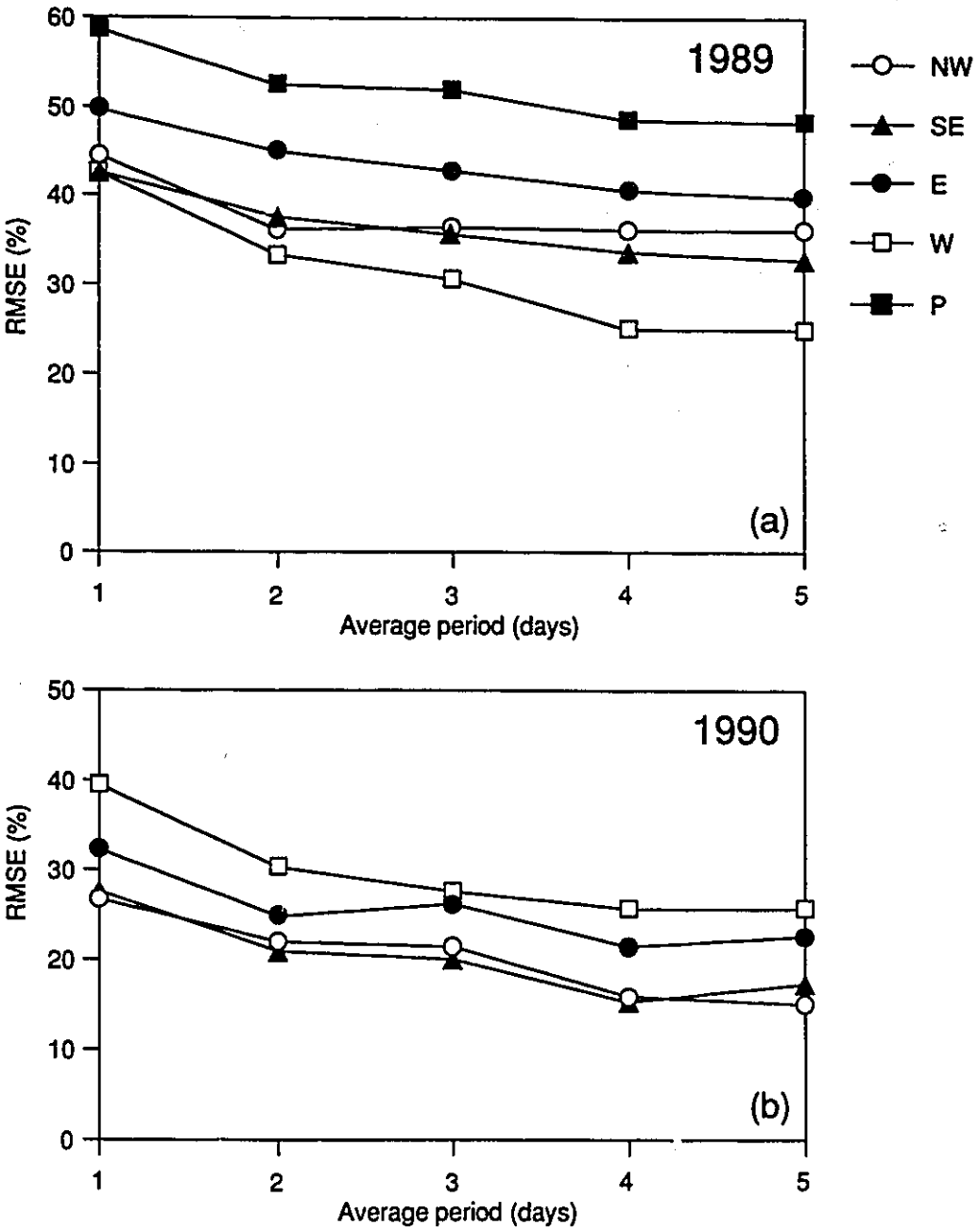
1989
NW
SE
E
W
P
RMSE (%)
Average period (days)
(a)
1990
RMSE (%)
Average period (days)
(b)

CHAPTER FIVE

Hydrologic responses of a small high arctic basin to global change impacts

Kathy L. Young and M-k. Woo[1]

Young, K.L. and M-k. Woo. Hydrologic responses of a small high arctic basin to global change impacts; submitted to Geological Survey of Canada Bulletin, July 1995.

Abstract

This study describes the application of a surface energy balance model which uses limited data input (twice daily cloud, temperature, wind) to model melt and evaporation for a small high arctic basin. Validation of this approach is demonstrated within a water balance framework, where total storage is small relative to total precipitation input during two contrasting summer seasons (1989 - cool, wet and 1990 - warm, dry). In 1989 total storage is $<20\%$ of total precipitation input and in 1990 it is $<12\%$. Using the model, selected global change impacts ($\pm$ 10% of present levels) were investigated, and the results indicate that small atmospheric alterations in temperature, aerosols and clouds can have more effect on basin hydrological processes (melt, evaporation and storage) than slight changes in surface albedo, resistance, and low rainfalls. This study will be of interest to northern scientists wishing to better understand both the present day linkages between atmospheric-terrestrial and hydrological processes, and future global impacts.

Department of Geography, York University, 4700 Keele Street, North York, Ontario, M3J 1P3

[1] Department of Geography , McMaster University, Hamilton, Ontario, L8S 4K1

INTRODUCTION

Northern scientists have all expressed a need to better understand the linkages between atmospheric-terrestrial and hydrologic processes so future global changes to arctic environments can be anticipated. For hydrologists, changes in energy which is the driving force behind melt and evaporation could ultimately influence northern hydrologic regimes, by altering runoff and storage patterns (Kane et al., 1992). Ecologists' main concern is that global change could alter the present vegetation patterns by modifying soil moisture and nutrient levels. This may cause some plant communities to be eliminated or to be replaced by more resilient species (Edlund, 1992) leading eventually to changes in the grazing patterns of northern fauna. Northern geomorphologists are interested in understanding how climatic variability and change may trigger slope instabilities, enhance ground thaw (Lewkowicz, 1992) and alter sediment loadings in northern streams (Lewkowicz and Wolfe, 1994; Woo and McCann, 1994). However, progress in this direction will be hampered until the present-day complex linkages between energy, water and northern terrain (e.g. geology, soil, vegetation, permafrost) are better understood (Lewkowicz, 1992).

To date, much emphasis or speculation has been placed on how arctic environments will change under future temperature and precipitation levels, since these are the two outputs from the General Circulation Models (GCMs) which tend to have the highest certainty (Maxwell, 1992). GCMs indicate that the Canadian Arctic islands could experience warmer summers of about 5°C and higher precipitation levels of about 120% (Maxwell, 1992). Using these types of scenarios, scientists such as Hinzman and Kane (1992) and Kane et al. (1992) have been able to show how warmer summer temperatures will lead to higher evaporation levels and less discharge from a small low-arctic, Alaskan basin underlain by continuous permafrost.

Less is known about how changes in other atmospheric or terrestrial attributes will affect northern drainage systems. For instance, uncertainty exists

regarding how changes in cloud type or amount will modify radiation levels which tends to dominate melt and evaporation rates (e.g. Church and Woo, 1990; Hinzman and Kane, 1991, 1992).

Changes in aerosol levels and their effect on solar radiation and implications for hydrologic processes are also not well established. Little quantitative information exists detailing how changes in vegetation with possible changes in surface albedo (α_s) and surface resistance (r_s) will impact on soil moisture and evaporation rates. These types of information being especially critical for ecologists and planners involved in drafting future environmental policies for northern regions.

Coupled with this level of uncertainty is the question of scale. For instance, GCMs generate temperature and precipitation output at large scales (5°Lat. by 7°Long.). "The models often agree well, with present climate and with one another, for seasonal or annual averages over large areas, but substantial disagreements appear as the scale is reduced below continental" (Maxwell, 1992). Hence, Maxwell (1992) cautions that we should not be overconfident of current GCM predictions for any region, including the Arctic. Given this current problem of scale, several researchers (e.g. Church and Woo, 1990; Running et al., 1987) urge that before the impact of global changes can be addressed at the regional scale, we must take into account the spatial and temporal heterogeneity of the local site and then move upwards (e.g. point-slope-basin-region). Much more realistic results will come from first aggregating meteorological, hydrological and botanical information defined at a small scale and then moving upwards from that point.

A final problem which has plagued scientists trying to understand existing inter-linking processes and future changes is the high cost of arctic research, especially logistics and equipment. For instance, owing to the diverse northern topography which can range from flat, rolling-to mountainous terrain, monitoring temperature or solar radiation at one point may not be representative of the surrounding region. Also, for many sites in the Arctic, twice daily weather data

(temperature, cloud, wind, precipitation) often forms the only available data. Computer modelling, however, offers the possibility of extrapolating information gathered at a point to larger scales (e.g. slope, basin) allowing for spatial variability and also allows one to investigate possible climate change impacts.

Thus, this study outlines the application of a surface energy balance model (Young and Woo 1995, submitted) which uses easily obtained field data to model melt and evaporation for a small high arctic basin. These outputs are then placed in a water balance framework, so that the water balance components can be considered for two contrasting summers, 1989 (wet, cool) and 1990 (warm dry) thus, allowing the utility of this approach to be assessed. This study will also investigate the possible implications on the basin water balance to changes in selected atmospheric and terrestrial impacts.

This study will be of importance to northern scientists interested in an improved understanding of the present linkages and feedbacks in northern ecosystems and their future sensitivity to global changes. The outputs from this study could serve as inputs into other ecological or hydrological models.

STUDY AREA

The Heather Creek basin (HCB) (6.1 km^2), located on the Fosheim Peninsula, Ellesmere Island (79°58'N, 84°28'W) was the focus of this study (Fig. 1) and provided data for modelling and validation. It can be described as rolling terrain and is comprised of different terrain units (slopes of varying aspect, angles, bottomlands and valleys) (see Data section and Table 1). It is a sub-basin of a much larger basin, Hot Weather Creek (HWC) which has an area of about 155 km^2 . The Heather Creek (HC) tributary is the sixth largest in the basin and at low flow, it occupies a single channel 1 to 2 m wide cut into a wet-vegetated valley bottom. It has a beaded morphology and at peak flow, HC overtops the channel and expands into a vegetated floodplain (Lewkowicz and Wolfe, 1994). The HWC watershed is underlain by poorly consolidated sandstone and to a lesser extent siltstone, conglomerate, shale, and coal of the upper Cretaceous-lower

Tertiary Eureka Sound formation (Thorsteinsson, 1969). It is likely that the basin has not been glaciated since late Wisconsian time (Lewkowicz and Wolfe, 1994). HWC lies within the early Holocene marine limit so that areas below 140-145 m have a discontinuous cover of weathered marine, estuarine and deltaic deposits, composed of medium to fine-grained sand, silt and minor clayey silt, sandstone granules, coal fragments,detrital plant materials or molluscs. Permafrost is continuous with active-layer depths ranging from 0.4 to 1.0 m depending on surface materials and summer temperatures (Young et al., 1995, submitted).

The HWC basin is a region that is generally warmer in summer than other sites in the Queen Elizabeth Islands due to the surrounding mountain ranges of Ellesmere and Axel Heiberg which tend to dispel slow-moving cyclones from the Arctic Ocean and Baffin Bay (Edlund and Alt, 1989). Summer temperatures at HWC tend to be slightly higher than the meteorological station at Eureka 25 km to the west (Lewkowicz and Wolfe, 1994), and rainfall levels can be higher in certain years than that measured at Eureka (Young et al., 1995, submitted).

Soil, climate and hydrological information gathered in 1989, 1990 from four varying experimental slopes and plateau: Northwest (NW); Southeast (SE); East (E); Plateau (P) located within HCB and one site; a West - facing slope (W) located about 1000 m downstream from the outlet of HC provided information used for modelling (see Data section). These sites have been extensively described by Young et al. (1995, submitted) and Young and Woo (1995, submitted). The base-camp (BC) (approx. 84 m. a.s.l.) was located about 500 m south of the HCB lower boundary and is within about 1 km^2 of the intensively studied experimental sites. Twice daily meteorological information (temperature, wind, cloud and precipitation) was gathered here as part of a programme initiated by Polar Continental Shelf Project (P.C.S.P.) to obtain meteorological information from summer field camps scattered throughout the Canadian Arctic Archipelago.

Vegetation cover in the study basin is variable and strongly linked to moisture supply (Lewkowicz and Wolfe, 1994; Young et al., 1995, submitted). Complete plant cover generally occurs in thaw ponds, fens and valley bottoms,

consisting of grasses, sedges, cotton grass and mosses. Plateaus tend to have higher vegetative covers (35-50%) dominated by *Salix arctica* and *Dryas integrifolia* communities, while slopes can have quite variable covers ranging from less than 10% in sandy sites prone to disturbance (Young et al., 1995, submitted) to higher levels (> 10%) below late-lying snowbeds, in cracks and depressions where water collects and on the lower parts of slopes where moisture levels tend to be higher. Overall, the dominant plant cover in HCB tends to be a *Salix arctia-Dryas integrifolia* complex (Woo et al., 1990; Young et al., 1995, submitted).

THEORY AND METHODS

Water balance components

It is the intent of this study to examine the feasibility of employing a surface energy balance model which uses easily obtained weather data (twice daily) to provide input (melt, evaporation) for a simple basin water balance model. We wanted to investigate 1) the present-day hydrological status of HCB under two different summer seasons (1989-cool, wet; 1990-warm, dry) in order to justify the feasibility of the surface energy model and 2) to arrive at a baseline so that we could analyze the hydrological sensitivity of the basin to selected atmospheric and terrestrial impacts.

The water budget of any basin (m) can be simply written as

$$M+R-E-Q=\pm\Delta S \qquad (1)$$

where M is snow and ice melt; R is rainfall; E is evaporation loss from the basin; Q is basin runoff including both surface and subsurface flow and ΔS is the change in moisture storage in the basin (increases being positive) including surface, soil, groundwater and biological moisture storage in all phases (Wright, 1981). Over an increasingly long period of time, ΔS should approach zero, but over short periods (i.e. a day), it may assume a significant value.

Each component of the water balance can be considered by either measuring it directly, simulating it or allowing it to be determined as a residual in eqn. 1. In the following section the determination of each component of the basin water balance will be described.

Snow and ice melt (M)

Prior to determination of melt (snow, ice) for HCB, a snow survey in 1990 following the methods described by Woo and Marsh (1978) was conducted. The basin was broken down into different terrain units (see Fig. 1) and a series of transects across these units were carried out and both snow depth and density measurements were made. Table 2 outlines the initial snow water equivalent (areally weighted) for each terrain unit. East-facing slopes (NE, E, SE) have the highest snow contributions owing to their large areas in the basin. In 1989, snow surveys were only conducted on the 5 experimental sites, and no snowmelt runoff measurements were made in the basin. Hence, only the thaw period for 1989 will be considered here.

The surface energy balance model outlined by Young and Woo (1995, submitted) is used to determine the amount of daily energy (Q_m) available for melt within the basin. Here,

$$Q_m = Q^* + Q_h + Q_e \qquad (2)$$

where Q^* is net radiation, Q_h and Q_e are sensible and latent heat fluxes respectively. During the melt period: the surface temperature is set to 0°C, temperature lapse rates are taken into account, only positive melt is accounted for and its duration (e.g. June 1-6) for varying terrain units (Fig. 1, Table 1) is determined from field data obtained in 1990 from the experimental sites (see Young et al., 1995, submitted; Young and Woo, 1995, submitted).

Melt energy is converted into water equivalent terms (m) by the following

Here, L_f is the latent heat of fusion, and ρ_w is the density of water. At each terrain unit, the amount of melt did not exceed the original areally weighted snow input.

$$M = Q_m / (L_f \rho_w) \quad (3)$$

Rainfall (R)

Rainfall was measured at BC twice daily, and was measured at the experimental sites on a daily basis. Unfortunately, these sites were not scattered throughout the basin but were clustered close to the southern boundary of the basin (see Fig. 1), precluding use of the isohyetal or the Theisson polygon approach in areally weighting precipitation input. However, these sites did encompass the types of terrain units found in HCB. To adjust precipitation measured at BC to the other terrain unites, a ratio approach similar to that used by Woo and Drake (1988) was applied. A ratio is determined between BC and the experimental slopes (NW, SE, E, W, P, BL) using July precipitation totals in both 1989 and 1990 (Table 3). Monthly rather than daily totals were compared to avoid spurious ratios which may have occurred through random errors (e.g. tippage). Overall, the ratios determined for the two years (1989, 1990) were similar suggesting the feasibility of this approach. Deviations for the west slope probably reflect local and variable wind conditions which can influence raingauge catch efficiency. Daily precipitation input to the HCB is areally weighted.

Evaporation (E)

The Penman-Monteith combination model is used to simulate evaporation for HCB and it is detailed in Young and Woo (1995, submitted). It offers the opportunity to consider not only meteorological conditions (radiation, temperature, vapour pressure) but also variable surface conditions through the surface albedo (α_s) and surface resistance (r_s) on basin evaporation.

Here it is outlined briefly,

$$Q_e = \frac{S(Q^* - Q_g) + \rho_a C_p (e_z - e_d) / r_a}{s + \gamma(1 + r_s / r_a)} \quad (4)$$

where, S is the slope of the saturation vapour pressure-air temperature curve at T_z (Bowers and Bailey, 1989; Dilley, 1968), Q_g is the ground heat flux, ρ_a is air density, C_p is the specific heat of the air, e_z is the saturated vapour pressure at T_z, e_d is the saturated vapour pressure at the dewpoint temperature (here assumed to be the minimum of the two daily readings at BC) (Jury and Tanner, 1975), γ is the psychometric constant, r_a and r_s are the aerodynamic and the surface resistances. Q_g is determined as the residual in the surface energy balance model during the post-snowmelt period and is used in the force-restore scheme (Deardorff, 1978) to derive surface temperature (T_s) for the thaw season (see Young and Woo, 1995, submitted).

The surface resistance is set to r_s = 100 (moist conditions, 1989) and r_s = 650 (dry conditions, 1990). The surface resistance is allowed to fall to zero, when the cloud transmissivity value used in attenuating incoming solar radiation (see Young and Woo, 1995, submitted) falls below a critical level indicative of cloudy conditions. The assumption that wet weather occurs under these situations is also made.

Discharge (Q)

Stream discharge from HCB comprising both surface and subsurface flow was measured directly in 1989 (thaw period from June 29 to approx. Aug. 20) and in 1990 (melt+thaw period from June 8 to approx. Aug. 20). Stevens Type-F water level recorders with weekly charts were mounted on stilling wells at the exit of the basin to obtain continuous stage records. Prior to August 10, 1989 a 30-L container served as the stilling well at HC. It was not until this date, that a 40 gal. barrel replaced it. Consequently, in 1989, there were periods (e.g., episodes of prolonged rain), when continuous stage measurements could not be obtained.

Absence from camp July 11 - 12, 1989 also resulted in incomplete stage and discharge data during a rain event.

A Price current meter was used at HC, and during low flows, the whole discharge was collected for several seconds in a 30-L container and the volume measured. Stage-discharge curves for HC were developed in 1989 and 1990. In 1990, few low stage-discharge points were obtained, so for stage levels <450 mm, the following polynomial equation (r^2 = 0.96) from Lewkowicz and Wolfe (1994) is used,

$$y=-0.13680 + 1.7324E-3x - 7.3255E-6x^2 + 1.0371E-8x^3 \quad (5)$$

where y is discharge (m^3s^{-1}) and x is stage (mm above arbitrary datum).

Storage (ΔS)

Storage which can be soil moisture storage, groundwater storage, water held in depression storage or tied up in ground ice was not measured in it entirety and subsequently it is determined as the residual in eqn. 1.

Sensitivity analysis

Sensitivity analysis offers a viable and effective method to investigate possible global change impacts on high arctic basins and it can take two approaches. The variables in question (e.g. T_z, R) can be altered by a known level (e.g. 5°C or 120% respectively) (Maxwell, 1992) and then be used to simulate changes in snowmelt or evaporation. When the level of change is less certain for a variable, then equal intervals of change from the present condition can be utilized (e.g. ±5%, ±10%, ±20%) (Hinzman and Kane, 1992; Munro, 1991). This approach is straightforward and offers an insight into very sensitive and robust variables or parameters.

Two things which must be considered in utilizing sensitivity analysis is that 1) rarely do entities (e.g. T_z, α_s) change independently, but are in fact inter-related to other variables or parameters and 2) reasonable levels of change are

necessary and should reflect field results and if possible present levels of knowledge.

In this study, a conservative sensitivity analysis (roughly ±10% change of present conditions) is conducted using selected 1990 atmospheric and terrestrial components. This allows the possible effects of global change to be assessed for the HCB.

Atmospheric

a) Aerosol

Aerosols are defined as suspensions of liquid or solid particles in the air, excluding cloud droplets and precipitation (Peixoto and Oort, 1992). They can alter solar energy by absorbing or scattering the radiation both in cloud-free and cloudy conditions (Peixoto and Oort, 1992). Presently, in the Arctic high levels of aerosols in the early spring (March, April) are responsible for a phenomena known as "arctic haze" (Barrie, 1992). In this study, the dust factor (aerosol) is changed by ±10% of its present (1990) level to a maximum of 1.0. When cloud conditions decline below a critical level, the dust factor still rises to 1.0 (see Young and Woo, 1995, submitted) (Table 4). Fallout of dust particles onto the ground surface are not considered at this stage.

b) Clouds

Clouds reflect incoming solar radiation back to space and reduce the energy available at the earth surface. Conversely, longwave radiation emitted from the earth into the atmosphere is trapped by clouds, thereby reducing longwave energy loss to space. Through these competing processes, clouds can modify the earth's general circulation and climate (Sohn and Robertson, 1993).

In the Arctic, stratus-type clouds predominate due to the high stability of the land masses here. They are described as being low-lying, extensive and average cloud cover in the summer is between 4-5 tenths (Feigelson, 1983). The expansion of more open sea water with climate warming, could lead to higher

evaporation rates and increased cloudiness along arctic coastlines (LeDrew, 1993; Slaymaker and French, 1993).

In this study, the cloud amount of the lowest cloud layer bearing a stratus-type cloud has been altered by ±1/10th. Total cloud cover for all layers is maintained at 1.0. No adjustment is made to the cloud coefficient in the calculation of longwave radiation (see Young and Woo, 1995, submitted). In the final analysis (see Results), only the evaporation changes will be examined (due to missing 1990 cloud data for the snow period at this time).

c) Temperature

Summer temperatures as high as 5°C have been predicted for the High Arctic because of climate change (Maxwell, 1992). Here, we increase temperatures by ±10% from their present 1990 levels (see Table 4).

Terrestrial

a) Site albedo (post-snowmelt)

Presently, the limiting factor to plant growth is not necessarily temperature, but rather water and nutrients (Slaymaker and French, 1993). Climatic warming will thus influence arctic vegetation indirectly by modifying soil moisture levels and nutrient availability. Some plants may disappear, or be replaced and the ratio between bare and plant covered ground could change. These types of terrestrial modifications will likely lead to varying surface albedos, which in turn will influence radiation levels and evaporation rates. Therefore, the site surface albedos have been altered by ±10% (see Table 4). In this simulation, the background albedo is maintained at the 1990 value (see Young and Woo, 1995, submitted).

b) Surface resistance (r_s)

If vegetation patterns are altered then surface resistance (r_s) will probably change as well, affecting evaporation amounts. Here, the 1990 r_s value is

increased by ±10%, but is still allowed to fall to 0 when cloud conditions fall below a certain level, indicative of cloudy and wet conditions (see Young and Woo, 1995, submitted).

c) Summer rainfall

Summer rainfall in the High Arctic may increase by 120% (Maxwell, 1992). Here, summer rainfall for 1990 is varied by ±10% and the resultant effect on the water balance is examined.

DATA

Data for determining the water balance for HCB and its sensitivity to selected global change variables comes from two summers of contrasting weather conditions: 1989 (cool, wet) and 1990 which was warm and dry (Young et al., 1995, submitted). Two sets of data were collected: as input to the surface energy balance and water balance models (Tables 1, 5) and for validation (e.g. stream discharge (Fig. 2) if one considers that ΔS approaches 0 over the season (see eqn. 1)).

The first set of data consisted of location type information (latitude, longitude); site characteristics (slope aspect and angle, elevation, surface albedo, soil attributes); and twice daily weather observations of cloud data (cloud type and amount), wind speed and temperature (dry bulb, and minimum temperatures) and precipitation amounts. This collection of weather generally comprises the minimum amount of data provided twice a day at field camps scattered in the Canadian Arctic and supported by PCSP (Young and Woo, 1995, submitted).

Cloud observations were made following the standard Environment Canada procedures, specifying cloud layer heights, amounts and the types of clouds in each layer (Young et al., 1995). Dry-bulb air temperatures were obtained with mercury thermometers (± 0.5°C), and minimum air temperatures were obtained from maximum-minimum thermometers (±0.5°) (AES, 1989). These instruments were housed in an isolated Stevenson screen approximately 1.5 m above the

ground surface. Spot wind speed measurements (in knots) were made twice a day approximately 2 m above the ground using Cassella type anemometers (± 10%) (AES, 1989). In the model these wind speed measurements were adjusted to a height of 0.5 m to make them comparable to measured wind speeds (see Young and Woo, 1995, submitted) and were also converted to units of ms^{-1} . Measurements taken at 0700 h (LST) are considered to be representative of the period 0100-1200 h, and the values obtained at 1900 h (LST) were used to represent weather conditions from 1200 to 2400 h. Precipitation is measured by Atmospheric Environment Service manual raingauges (± 0.25 mm), by home-made manual raingauges (±1 mm) and a recording tipping bucket raingauge adjacent to Picnic Lake (±0.25 mm). Trace precipitation values represent 0.03 mm (Barrie Goodinson, personal communication, 1993).

Changes to input data not outlined before in Young and Woo (1995, submitted) are:

1) post-snowmelt site albedos are average values from the lower, middle and upper parts of the experimental slopes, and from three locations on the experimental plateau. The average of several albedo values obtained in 1990 adjacent to Picnic Lake (se Fig. 1) is thought to reflect valley (V) terrain types and an average of several sub-arctic bog α values (Petzold and Rencz, 1975) is used for bottomland (BL) sites because they share similar vegetation characteristics.

2) both heat capacity (C_s) and thermal conductivity (T_c) values are seasonal averages determined using soil moisture and soil data obtained from the lower, middle and upper parts of experimental slopes and from 3 locations on the experimental plateau. Soil moisture and soil data from Glenn, (1994, unpublished) provided information which allowed T_c and C_s to be calculated for the BL and an assumption that this information could pertain to V sites is also made.

3) the complex valley network is simply divided into six equal areas, of similar slope angles but varying in aspect and elevation. Shading from nearby slopes is also considered.

Heather Creek (HC) stream discharge data can be described by Figure 2. The short, yet intensive snowmelt dominated discharge in 1990 (June 8 - June 26) suggests that Heather Creek experiences a nival regime, similar to Hot Weather Creek (HWC) (Lewkowicz and Wolfe, 1994) and other high arctic streams (Woo, 1986). Summer rainfall in 1990 is low and the total runoff coefficient (Q/P) is 0.55, a value which is lower than other high arctic basins (Table 6) but is similar to a low-arctic basin in Alaska (see Table 6). The runoff coefficient for HC in 1990 is greater than that estimated for 1991 and may be related to very low snow levels and deep ground thaw in 1991 (see Table 6 and Young et al., 1990, submitted).

Snowmelt runoff was not measured in 1989, but the runoff from frequent rainfall inputs of varying magnitudes in 1989 were measured (see Fig. 2b). Due to the frequent rainfalls, (Young et al., 1995, submitted) HC responded relatively rapidly to rainfall input. For instance a 10 mm rainfall which started on Aug. 15 about 0300 h and lasted 24 hours resulted in peak flow about 0600 h on Aug. 16. The total runoff coefficient for this storm is 0.65, a level again similar to a low-arctic, continuous permafrost basin (Table 6).

RESULTS

Heather Creek Basin (HCB) water balance (1989-1990)

The reliability of the simulation of melt, evaporation and adjustment of precipitation input is assessed by the assumption that the seasonal storage would be small (less than 20%) of the total precipitation into the water balance equation (see eqn. 1). This assumes that most water input into the basin would be lost as either evaporation or discharge over the course of the summer. The summer field seasons of 1989 and 1990 were used for model calibration and verification.

Figure 3 outlines the daily water balance of HCB for 1989 (thaw period) and 1990 (snowmelt + thaw period). Daily variation in the storage component in 1989 indicates that rarely is it possible for inputs into the basin to be sequentially matched by losses on a daily basis. This problem is highlighted by Aug. 5, when

a sizeable precipitation input (approx. 18 mm basin averaged) occurs but peak flow does not occur until two days later. This causes noticeable storage adjustments (Fig. 3a) to occur during this time.

In 1990, snowmelt peaked June 8 after about seven days of continuous melt and peak flow occurred on June 12 (four days later) causing large swings in the storage term during this time (Fig. 3b). Flow decreased rapidly following the end of snowmelt, and only small changes in storage occurred with small rainfall inputs for the rest of the season.

Cumulative totals of water balance components for the two summer seasons (1989, 1990) are plotted in Figure 4 and tabulated in Table 7. They indicate that rainfall is a significant input into the system in the 1989 summer season and that more of it is lost via discharge than through evaporation. The total storage term is larger in 1989 than 1990 likely arising from 1) the underestimate of stream discharge in 1989 and 2) low evaporation rates arising from underestimates of Q^* (Young and Woo, 1995, submitted). Overall the 1989 storage term is calculated to be 18 mm or approximately 19% of the total precipitation input.

Model performance is much improved in 1990. Snowmelt is the most important input into the system, while summer rainfall is small relative to outputs of stream discharge and evaporation. Overall, total storage is 5 mm or 4% of the total calculated input, and indicates that most water from the HCB is lost via discharge and evaporation. If the initial snow storage is considered, then the final storage term is about 11% of total precipitation input. Melt is under-estimated for the W and SW slopes by the model. The better agreement is 1990 may partially reflect that evaporation is likely overestimated since Q^* is overestimated in 1990 (Young and Woo, 1995, submitted). However, this higher estimate is likely dampened by an underestimate in stream Q caused from a few days of missing discharge (see Fig. 2a).

These two years serve to provide an indication that 1) the surface energy balance model using limited field data can provide reasonable estimates of melt

and evaporation for small high arctic basins; 2) that precipitation measured at one location can be adjusted to different terrain units within a small basin and 3) that these results provide a benchmark from which it is possible to evaluate the sensitivity of the HCB to selected atmospheric and terrestrial impacts.

Global change impacts

Table 8 outlines the results of selected atmospheric and terrestrial impacts on the HCB water balance components (e.g. melt, evaporation, storage). Discharge for 1990 is not altered and seasonal totals are only examined.

Atmospheric

a) Aerosol

Evaporation increases slightly when the effect of aerosols is removed (e.g. the aerosol factor (K) is raised by 10% to a maximum value of 1, which indicates clear conditions). Greater amounts of incoming solar radiation allow more water to be evaporated. The greatest changes to melt, evaporation and storage occur when K is decreased by 10% (a level which is perhaps comparable to a large city (e.g. Toronto, Davis et al., 1975). This aerosol level is able to dampen overall melt and evaporation for the basin by impeding incoming radiation to the surface (Table 8).

b) Clouds

Increases in low cloud amounts by 1/10 over present 1990 levels will elevate evaporation rates to levels comparable to higher temperature amounts (Table 8). This is partially a reflection of model logic where $r_s = 0$ when cloud conditions deteriorate and cloud transmissivity is reduced (Young and Woo, 1995, submitted). This low surface resistance indicates a wet surface which poses no terrestrial (vegetation, soil) restriction to evaporation, thus allowing for higher losses over present 1990 levels.

Small decreases in cloud amounts by 1/10 do not alter present evaporation levels. This indicates that 1) r_s values were little changed in the model by small

decreases in low- lying cloud amounts and 2) slightly higher amounts of incoming radiation do not necessarily suggest higher evaporation rates if surface resistance still remains high.

This analysis serves to indicate the linkages which exist between atmosphere and terrestrial components and the complexities involved in understanding the impacts of global change.

c) Temperature

Alterations in temperature even by 10% appear to have sizeable impacts on basin evaporation. Higher temperatures elevate evaporation by about 20 mm over present conditions, a range also found by Kane et al. (1992) while lower temperatures decrease evaporation by about 10 mm for the season. In this study, this leads to marked changes in storage if one considers no adjustments in stream discharge (Table 8).

Terrestrial

Changes in terrain features do not appear to have as great an effect as atmospheric conditions on water balance constituents.

a) Site albedo

Changes in site albedo of about $\pm 10\%$ did not impart significant changes in the water balance constituents. This could be partly due to the fact that the background albedo which plays a role in atmospheric solar radiation is not altered (see Young et al., 1995).

b) Surface resistance

Changes in surface resistance (r_s) of about $\pm 10\%$ also did not cause significant changes in the water balance components. Evaporation rates were slightly higher by about 1 mm when the surface resistance is reduced by $\pm 10\%$ and evaporation is reduced slightly by about 3 mm when r_s is increased by 10% (Table 8).

c) Summer rainfall

Rainfall amounts were low in the summer of 1990 (12 mm) and as such, storage terms varied by about 1 mm when precipitation is increased and varied by about 2 mm when precipitation is decreased by 10%. Greater differences may exist for seasons when summer rainfall is high (e.g. 1989) or if one considers the levels of change dictated by the GCMs (Maxwell, 1989).

This limited sensitivity study reveals that atmospheric constituents (e.g. aerosol levels, clouds) deserve further attention regarding their present and future influence on hydrological processes in northern environments. Terrestrial simulations suggest that slight changes in site albedo, surface resistance, and low summer precipitation amounts may not have dramatic effects on non-glacerized basins. Sensitivity analysis should continue at varying levels of change to identify any dramatic change in melt and/or evaporation.

DISCUSSION AND CONCLUSIONS

1) This study successfully utilizes a surface energy balance model which uses easily acquired field data (temperature, cloud, wind) to model melt and evaporation for a small high arctic basin (HCB) composed of varying terrain units (level/sloping).

2) This model takes into account spatial variability using field data established at experimental sites (e.g. site albedo, heat capacity, thermal conductivity) which are then applied to similar terrain facets. Precipitation obtained at a point (BC) is also adjusted to the different terrain units and areally weighted.

3) Reasonable results from both the 1989 (thaw season) and 1990 (melt + thaw season) suggest that the surface energy balance model could be applicable to other sites in the High Arctic where limited field data also exist.

4) The ability of the model to move from a point-to slope-to a small basin, provides flexibility to scientists interested in working at different scales and adheres to the suggestions by Church and Woo (1990) and Running et al. (1987) that the spatial variability on the local scale needs to be considered, if reliable

predications of future global change impacts are to be realized for northern environments.

5) Sensitivity analysis of selected atmospheric and terrestrial impacts indicate that slight changes in atmospheric constituents have perhaps a greater effect than small modifications in the terrestrial environment. This study suggests that different levels of sensitivity should be investigated, and several more years of record should be evaluated to provide a comprehensive baseline which would detail the present variability in the water balance system.

Acknowledgements

This work was funded by a research agreement with the Department of Energy, Mines and Resources, by a grant from the Natural Sciences and Engineering Research Council to M.-k. Woo, and by a northern training grant from the Department of Indian and Northern Affairs. The logistical support of the Polar Continental Shelf Project and Dr. S.A. Edlund is gratefully acknowledged. We wish to thank Dr. Bea Alt, Sharon Reedyk, Tim Siferd, Kelly Thompson, Paul Wolfe, for their assistance in the field, and Angus Headley for the loan of instruments. We would like to thank B. McCann for his review of the manuscript.

References

AES
1989: AES Guidelines for Co-operative Climatic Autostations, Climatic Applications Branch, Canadian Climate Centre, Downsview, Ontario. Environment Canada, Atmospheric Environment Services, 59 (June 20, 1989).

Anderson, J.C.
1974: Permafrost-hydrology studies at Boot Creek and Peter Lake Watershed, N.W.T., in Permafrost Hydrology, Canadian National Committee, Ottawa, p. 39-44.

Anonymous
1967: Hydrology of the Lewis Glacier, north-central Baffin Island, N.W.T., and discussion of reliability of the measurements, Geographical Bulletin, v. 9, p. 232-261.

Barrie
1992: Natural and anthropogenic influences on the chemical composition of the arctic troposphere, in (editors) M.-k. Woo and D.J. Gregor, Arctic Environment: Past, Present and Future, Proceedings of a Symposium held at McMaster university, Nov. 14-15, 1991, p. 71-78.

Bowers, J.D. and Bailey, W.G.
1989: Summer energy balance regimes for alpine tundra, Plateau Mountain, Alberta, Canada; Arctic and Alpine Research, v. 21, no. 2, p. 135-143.

Brown, J., Dingman, S.L., and Lewellen, R.I.
1968: Hydrology of a drainage basin on the Alaska Coastal Plain, U.S. Army Cold Regions Research and Engineering Laboratory, Hanover, New Hampshire, Research Report no. 240.

Church, M. and Woo, M-k.
1990: Geography of surface runoff: some lessons for research, in (editors) Anderson, M.G. and T.P. Burt, Process Studies in Hillslope Hydrology, p. 299-325.

Davies, J.A., Schertzer, W., and Nunez, M.
1975: Estimating global solar radiation, Boundary-Layer Meteorology, v. 9, p. 33-52.

Deardorff, J.W.
1978: Efficient prediction of ground surface temperature and moisture, with inclusion of a layer of vegetation, Journal of Geophysics Research, v. 84, p. 1889-1903.

Dickenson, R.E.
1983: Land surface processes and climate-surface albedos and energy balance. Advances in Geophysics, v. 25, p. 305-352.

Dilley, A.C.
1968: On the computer calculation of vapour pressure and specific humidity gradients, Journal of Applied Meteorology, v. 7, p. 717-719.

Edlund, S.A.
1992: Climate change and its effects on Canadian Arctic plant communities, in (editors) M.-k. Woo and D.J. Gregor, Arctic Environment: Past, Present and Future. Proceedings of a Symposium held at McMaster University, November 14-15, 1991, p. 121-138.

Edlund, S.A. and Alt, B.T.
1989: Regional congruence of vegetation and summer climate patterns in Queen Elizabeth Islands, Northwest Territories, Canada. Arctic, v. 42, no. 1, p. 3-23.

Hinzman, L.D. and Kane, D.L.
1992: Potential response of an arctic watershed during a period of global warming, Journal of Geophysical Research, v. 97, no. D3, p. 2811-2820.

Hinzman, L.D. and Kane, D.L.
1991: Snow hydrology of a headwater arctic basin. 2. Conceptual analysis and computer modelling, Water Resources Research, v. 27, no. 6, p. 1111-1211.

Glenn, S.
1994: Hydrology of a High Arctic wetland, M.Sc. thesis, McMaster University, Hamilton, Ontario, (unpublished), p. 1-97.

Kane, D.L., Hinzman, L.D., Woo, M-k., and Everett, K.R.
1992: Arctic hydrology and climate change, in (editors) F.S. Chapin III, R.L. Jefferies, J.F. Reynolds, G.R. Shaver, J. Svoboda, and E. Chu, Arctic ecosystems in a changing climate - an ecophysiological perspective, Academic Press, Toronto, p. 35-57.

LeDrew, E.F.
1993: Climate variability, change, and sensitivity, in (editors) French, H.M., and O. Slaymaker, Canada's Cold Environments, McGill-Queen's University Press, Montreal & Kingston, p. 248-271.

Lewkowicz, A.G.
1992: Climatic change and permafrost landscape, in (editors) M.k. Woo and D.J. Gregor, Arctic Environment: Past, Present and Future. Proceedings of a Symposium held at McMaster University, November 14-15, 1991, p. 91-104.

Lewkowicz, A.G. and Wolfe, P.
1994: Sediment transport in Hot Weather Creek, Ellesmere Island, N.W.T., Canada, 1990-91, Arctic and Alpine Research, v. 26, no. 3, p. 213-226.

Maxwell, B.
1992: Arctic climate, in (editors), F.S. Chapin III, R.L. Jefferies, J.F. Reynolds, G.R. Shaver, j. Svoboda, E.W. Chu, Arctic ecosystems in a changing climate - an ecophysiological perspective. Academic Press, San Diego, p. 259-280.

Marsh, P. and Woo, M-k.
1979: Annual water balance of small arctic basins, in Canadian Hydrology Symposium: 79, National Research Council of Canada, Ottawa, p. 536-546.

Munro, D.S.
1991: A surface energy exchange model of glacier melt and net mass balance, International Journal of Climatology, v. 11, p. 689-700.

Ostrem, G., Bridge, C.W. and Rannie W.F.
1967: Glaciohydrology discharge, and sediment transport in the Decade Glacier area, Baffin Is., N.W.T., Geografiska Annaler, v. 49a, p. 268-282.

Peixoto, J.P. and Oort, A.H.
1992: Atmospheric Physics. American Institute of Physics, New York, 520 p.

Petzold, D.E. and Rencz, A.N.
1975: The albedo of selected subarctic surfaces, Arctic and Alpine Research, v. 7, no. 4, p. 393-398.

Running, S.W., Nemani, R.R., and Hungerford, R.G.
1987: Extrapolation of synoptic meteorological data in mountainous terrain and its use for simulating forest evapotranspiration and photosynthesis, Canadian Journal of Forest Research, v. 17, p. 472-483.

Slaymaker, O. and French, H.M.
1993: Cold environments and global change, in (editors) French, H.M., and O. Slaymaker, Canada's Cold Environments, McGill-Queen's University Press, Montreal & Kingston, p. 248-271.

Sohn, B-J. and Robertson, F.R.
1993: Intercomparison of observed cloud radiative forcing: a zonal and global perspective. Bulletin of the American Meteorological Society, v. 74, no. 6, 997-1004.

Thorsteinsson, R.
1969: Geology, Greely Fiord West, District of Franklin. Geological Survey of Canada Map 1311A.

Walker, E.R., Lewis, E.L. and Lake, R.A.
1973: Runoff from a small high arctic basin (abstract), EOS: Translations of American Geophysical Union, v. 54, no. 1090.

Woo, M-k.
1986: Permafrost hydrology in North America. Atmospheric-Ocean, v. 24, p. 201-234.

Woo, M-k.
1983: Hydrology of a drainage basin in the Canadian High Arctic, Annals Association of the American Geographer, v. 73, p. 577-596.

Woo, M-k. and McCann, B.
1994: Climatic variability, climatic change, runoff, and suspended sediment regimes in Northern Canada, Physical Geography, v. 15, p. 201-226.

Woo, M-k., Young, K.L. and Edlund, S.A.
1990: 1989 observations of soil, vegetation, and microclimate, and effects on slope hydrology. Hot Weather Creek basin, Ellesmere Island, N.W.T., in Current Research, Part D, Geological Survey of Canada Paper, 90-1D, p. 85-93.

Woo, M-k. and Drake, J.J.
1988: A study to model the effects of uranium mine tailings in a permafrost environment. Environmental Studies No. 53, Northern Affairs, Canada, Ottawa, Ontario, 41 p.

Woo, M-k. and Marsh, P.
1978: Analysis of error in the determination of snow storage for small High Arctic basins; Journal of Applied Meteorology, 17, p. 1537-1541.

Wright, R.K.
1981: The water balance of a lichen tundra underlain by permafrost; McGill Subarctic Research Paper No. 33, Climatological Research Series No. 11, Centre for Northern Studies and Research, McGill University, p. 1-110.

Young, K.L. and Woo, M-k.
1995: Modelling net radiation in an arctic environment using summer field camp data, submitted to Solar Energy, July 1995.

Young, K.L., Woo, M-k., and Edlund, S.A.
1995: Influence of local topography, soil and vegetation on microclimate and hydrology at a High Arctic site, submitted to Arctic and Alpine, March, 1995.

Young, K.L., Woo, M-k. and Munro, D.S.
1995: Simple approaches to modelling solar radiation in the Arctic, Solar Energy, v. 54, p. 33-40.

List of Symbols

		UNITS
C_p	specific heat of air (1010)	$Jkg^{-1}\ K^{-1}$
C_s	heat capacity of the substrate	$Jm^{-3}\ K^{-1}$
E	evaporation	m
L_f	latent heat of fusion (0.33)	$MJkg^{-1}$
LST	local standard time	
M	melt	m
Q	discharge	m
Q^*	daily net radiation	MJm^{-2}
Q_e	daily latent heat flux	MJm^{-2}
Q_g	daily ground heat flux	MJm^{-2}
Q_h	daily sensible heat flux	MJm^{-2}
Q_m	daily melt energy	MJm^{-2}
R	rainfall	m
S	slope of the saturated vapour pressure - air temperature curve	$Pa°C^{-1}$
ΔS	storage	m
T_c	thermal conductivity	$Wm^{-1}\ K^{-1}$
T_s	surface temperature	K
T_z	air temperature	K
T_d	minimum air temperature	k
e_z	saturated vapour pressure at T_z	P_a
e_d	saturated vapour pressure at T_d (assumed to be the minimum air temperature)	P_a
h_d	daily damping depth	m
h_g	annual damping depth	m
r_a	aerodynamic resistance	sm^{-1}
r_s	surface resistance	sm^{-1}
α_s	albedo of the ground surface (level, slope)	dimensionless
κ	aerosol term	dimensionless
ρ_a	density of air	kgm^{-3}
ρ_w	density of water (1000)	kgm^{-3}

Table 1: Initial conditions and input data for simulation of melt and evaporation at Heather Creek, N.W.T. (1989-1990)

Initial Conditions:

Site	Latitude	Longitude	Slope angle (°)	Slope aspect (°)	Elevation (m a.s.l.)	Pre-snowmelt albedo 1990	Snowfree albedo 1989/1990	Area (m^2)
NE	79°58'N	84°28'W	1.1	45	130	✓	0.10/0.15	229203.
NE	✓	✓	11.3	✓	105	✓	✓	10418.
NE	✓	✓	✓	✓	100	✓	✓	38201.
NE*	✓	✓	1.0	✓	115	✓	✓	916814.
E	✓	✓	3.4	90	180	✓	✓	1023497.
E	✓	✓	2.3	✓	155	✓	✓	76401.
E*	✓	✓	1.6	✓	165	✓	✓	652883.
E	✓	✓	1.9	✓	125	✓	✓	69456.
E	✓	✓	7.6	✓	110	✓	✓	13891.
E	✓	✓	4.2/11.3[a]	✓	99	✓	✓	20837.
E	✓	✓	2.3	✓	110	✓	✓	17416.
SE	✓	✓	2.3	135	170	0.8	0.13/0.16	551477.
SE	✓	✓	1.1	✓	135	✓	✓	159748.
SE	✓	✓	11.3	✓	95	✓	✓	31255.
SE	✓	✓	6.8	✓	96	✓	✓	39937.

Table 1: continued

Site	Latitude	Longitude	Slope angle (°)	Slope aspect (°)	Elevation (m a.s.l.)	Pre-snowmelt albedo 1990	Snowfree albedo 1989/1990	Area (m^2)
SE*	✓	✓	2.9	✓	140	✓	✓	48619.
S	✓	✓	3.8	180	140	✓	✓	55564.
S	✓	✓	3.8	✓	105	✓	✓	27782.
SW	✓	✓	5.7	225	110	0.8	0.10/0.16	69456.
SW	✓	✓	9.9	✓	110	✓	✓	138911.
SW	✓	✓	11.3	✓	105	✓	✓	6946.
SW	✓	✓	5.7	✓	108	✓	✓	34728.
W	✓	✓	2.3	270	175	✓	✓	69456.
W	✓	✓	11.3	✓	145	✓	✓	83347.
W	✓	✓	1.9	✓	125	✓	✓	83347.
W	✓	✓	5.7	✓	130	✓	✓	20837.
NW	✓	✓	11.5	315	95	0.7	0.11/0.18	20837.
NW	✓	✓	11.3	✓	✓	✓	✓	48619.
P	✓	✓	0	0	100	0.8	0.13/0.16	312550.
P	✓	✓	✓	✓	115	✓	✓	368115.
P	✓	✓	✓	✓	118	✓	✓	236149.
BL	✓	✓	1.3/7	135	125	0.8	0.12[b]	34728.

Table 1: continued

Site	Latitude	Longitude	Slope angle (°)	Slope aspect (°)	Elevation (m a.s.l.)	Pre-snowmelt albedo 1990	Snowfree albedo 1989/1990	Area (m^2)
BL	✓	✓	1.4/7	45	85	✓	✓	20837.
BL	✓	✓	1.3/7	90	85	✓	✓	20837.
V	✓	✓	1.8/4	315	180	0.7	0.15	58667.
V	✓	✓	1.8/7	135	180	0.8	✓	✓
V	✓	✓	✓	90	110	✓	✓	✓
V	✓	✓	1.8/4	270	110	✓	✓	✓
V	✓	✓	✓	315	95	0.7	✓	✓
V	✓	✓	1.8/7	135	95	0.8	✓	✓

[a] shading occurs when sun elevation falls below larger slope angle
[b] value from Petzold and Rencz (1975)
* bowl type terrain

Input Data (Twice Daily) for all experimental sites

Clouds (Amount/Type)
Dry-bulb air temperature (°C)
Minimum air temperature (°C)
Windspeed (knots)

Table 2: Snow water equivalent (1990) for experimental sites

Site	Total area (m^2)	Areal weighted Snow water equivalent (mm)	Site contribution to basin (%)
NE	1194636.	22	19.6
E	2028381.	41	36.5
SE	831036.	12	10.9
S	83347.	1	1.1
SW	250040.	4	3.5
W	298659.	5	4.1
NW	69456.	2	2.1
P	916814.	16	14.1
BL	76401.	1	0.9
V	352001.	8	7.2
HCB	**6100771.**	**112**	**100.00**

Table 3: Adjustment ratios for rainfall measured at basecamp (BC) to sites in the Heather Creek basin (HCB) during a wet (1989) and dry (1990) summer.

Site	Wet Season (1989) Ratio	Dry Season (1990 Ratio
BC	1.0	1.0
NE	1.3	1.7
E	1.3	1.7
SE	1.5	2.3
S	1.5	2.3
SW	0.8	2.4
W	0.8	2.4
NW	2.4	2.6
P	1.1	1.4
BL	1.1	1.1
V	1.1	1.1

Ratios are based on July Totals (1989/1990) of BC in relation to experimental sites described in Young et al., 1995, submitted.

Ratio for BL and V derived from 1989 rainfall data from the BL between NW and SE experimental slopes (see Young et al., 1995, submitted).

Table 4: Simulation treatments for Heather Creek Basin (HCB) using 1990 field data.

Atmospheric	Treatment	
Aerosol (K)[a]	+10%	-10%
Temperature	+10%	-10%
Cloud amount (Tenths)[b]	+1/10	-1/10

Terrestrial	Treatment	
Slope albedo (α_s)	+10%	-10%
Surface resistance (r_s)	+10%	-10%
Precipitation (rainfall)	+10%	-10%

[a] aerosol max. to 1.0
[b] max. change to n = 1.0

Table 5: Soil attributes at experimental sites, Heather Creek, N.W.T. (1989-1990)

Site	Year	Thermal* Conductivity (T_c) ($Wm^{-1} K^{-1}$)	Heat* Capacity (C_s) ($x10^6$ (Jkg^{-1})	Thermal** Diffusivity (K_s) ($x10^{-7}$ m^2s^{-1})	Daily Damping Depth (h_d) (m)	Annual Damping Depth (h_s) (m)
NE	1989	0.6	1.9	3.2	0.2	3.2
E	1989	0.6	1.9	3.2	0.2	3.2
SE	1989	0.4	1.7	2.6	0.2	2.9
S	1989	0.4	1.7	2.6	0.2	2.9
SW	1989	0.8	1.9	3.9	0.2	3.5
W	1989	0.8	1.9	3.9	0.2	3.5
NW	1989	0.7	1.8	4.0	0.2	3.5
P	1989	0.7	2.0	3.7	0.2	3.4
BL	1989	0.3[a]	3.0[a]	0.9	0.1	1.6
V	1989	0.3	3.0	0.9	0.1	1.6
NE	1990	0.5	1.6	3.3	0.2	3.2
E	1990	0.5	1.6	3.3	0.2	3.2
SE	1990	0.4	1.5	2.7	0.2	2.9
S	1990	0.4	1.5	2.7	0.2	2.9
SW	1990	0.5	1.4	3.7	0.2	3.2
W	1990	0.5	1.4	3.7	0.2	3.2
NW	1990	0.6	1.6	3.9	0.2	3.5

Table 5: continued

Site	Year	Thermal* Conductivity (T_c) ($Wm^{-1} K^{-1}$)	Heat* Capacity (C_s) ($x10^6$ (Jkg^{-1})	Thermal** Diffusivity (K_s) ($x10^{-7}$ m^2s^{-1})	Daily Damping Depth (h_d) (m)	Annual Damping Depth (h_g) (m)
P	1990	0.6	1.6	3.5	0.2	3.3
BL	1990	0.3[a]	3.0	0.9	0.1	1.6
V	1990	0.3	3.0	0.9	0.1	1.6

[a] based on 1993 field observations (Glenn, 1994, unpublished)

* average seasonal value for 0.0 - 0.10m depth

** $K_s = (T_c / C_s)$ note: soil conditions are average values for experimental sites (E, SE, W, NW, P, BL).

Table 6: Selected water balance data from Arctic watersheds of North America

Location	Area (km^2)	Study period	Precipitation			Runoff			Evapotranspiration (mm)	Change in soil storage (mm)	Snowmelt runoff index	Rainfall runoff index	Total runoff index	Reference
			Snow (mm)	Rain (mm)	Total (mm)	Snow (mm)	Rain (mm)	Total (mm)						
HIGH ARCTIC														
McMaster River	33	1976	163	28	191			161	31	-1			0.84	Woo (1983)[a]
basin,	33	1977	97	23	120			155	31	-37			1.29	
Cornwallis	33	1978	212	61	273			213	38	23			0.78	
Island, NWT	33	1979	136	42	178			143	30	5			0.80	
	33	1980	128	37	165			130	51	-16			0.79	
	33	1981	148	67	215			148	47	21			0.69	
	33	1982	162	27	189									
Hot Weather Creek, Ellesmere Is., N.W.T.	155	1990						38						Lewkowicz and Wolfe (1994)
		1991						13						
F2 Watershed, Baffin Is.	2.5	1967			616			462	154				0.75	Church (1974)[a]
BaffinIsland,	125	1965			375			430					1.15	Ostrem et al.
N.W.T.	12.8	1965			375			252					0.67	(1967)[a]
	7.2	1965			461			450	10				0.98	
Heather Creek,	6.1	1989		95			45	10	32				0.47	This study
Ellesmere Is.,		1990	112	12	124			68	42				0.55	
N.W.T.		1991	35[b]	90[c]	125								0.08	Lewkowicz and Wolfe (1994)
Lewis River, Baffin Is., NWT	208	1963-66			550			500	50				.90	Anonymous (1967)[a]

Table 6: continued

Location	Area (km^2)	Study period	Precipitation			Runoff			Evapotranspiration (mm)	Change in soil storage (mm)	Snowmelt runoff index	Rainfall runoff index	Total runoff index	Reference
			Snow (mm)	Rain (mm)	Total (mm)	Snow (mm)	Rain (mm)	Total (mm)						
LOW ARCTIC														
Imnavait	2.2	1985	102			66					.65			Hinzman[a]
watershed,	2.2	1986	109	163	272	57	62	119	153		.52	.38	.44	(1990)
Alaska	2.2	1987	108	272	380	71	179	250	130		.66	.66	.66	
	2.2	1988	78	252	330	39	72	110	219		.50	.29	.33	
	2.2	1989	155	257	412	94	78	172	240		.61	.30	.42	
Boot Crk., NWT	31	1973	140	145	285	119		210			.85		.74	Anderson[a] (1974)
Barrow	1.6	1963		42			20					.46		Brown et al. (1968)[a]
watershed,		1964		8			0.08					.01		
Point Barrow,		1965		14			0.55					.04		
Alaska		1966		42			2.2					.05		

a found in Kane, et al. 1992
b calculated using 1991 snow survey
c calculated from BC data and ratio adjustments (see Table 3).

Table 7: Seasonal water balance for Heather Creek Basin (HCB) (1989-1990)

Year	TOTAL INPUTS		TOTAL OUTPUTS		STORAGE
	Melt (mm)	Precipitation (mm)	Evaporation (mm)	Discharge	Storage (mm)
1989 (June 29 - Aug. 20)	—	95	32	45	18
1990 (May 25 - Aug. 20)	102[a] / 112[b]	12	42	68	5/14[c]

[a] melt calculated according to model
[b] snow water equivalent of HCB determined by snow survey early May
[c] overall storage if one considers initial basin snow survey snow storage input

Table 8: Sensitivity of Heather Creek (1990) water balance components to selected climatic and environmental changes

ATMOSPHERIC

Water Balance Components (mm)	Aerosol			Temperature			Cloud amount		
	+10%	0	-10%	10%	0	-10%	+1/10	0	-1/10
M	104	102	92	102	102	105	102	102	102
P	12	12	12	12	12	12	12	12	12
E	44	42	33	65	42	31	69	42	42
Q	68	68	68	68	68	68	68	68	68
S	3/11[a]	5/14	3/23	-19/-9	5/14	18/24	-23/-13	5/14	5/14

TERRESTRIAL

Water Balance Components (mm)	Slope albedo (α_s)			Surface resistance (r_s)			Precipitation (rainfall)		
	+10%	0	-10%	10%	0	-10%	+10%	0	-10%
M	103	102	103	103	102	103	102	102	102
P	12	12	12	12	12	12	14	12	11
E	39	42	42	39	42	43	42	42	42
Q	68	68	68	68	68	68	68	68	68
S	8/17	5/14	5/14	8/17	5/14	3/12	6/15	5/14	3/13

[a] If initial snow storage is considered.

List of Figures

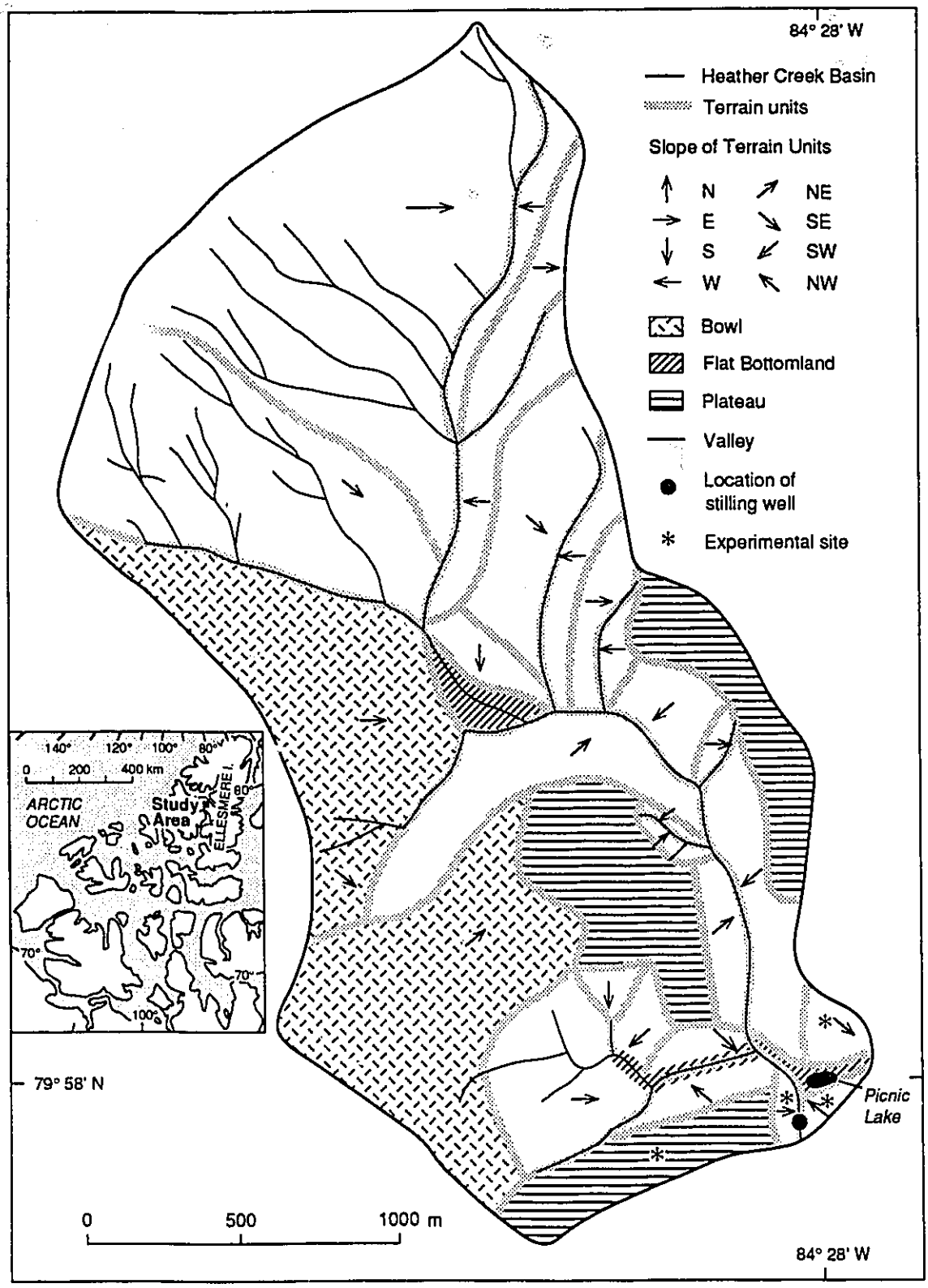
84° 28' W
Heather Creek Basin
Terrain units
Slope of Terrain Units
N
NE
E
SE
S
SW
W
NW
Bowl
Flat Bottomland
Plateau
Valley
Location of stilling well
Experimental site
140°
120°
100°
80°
0
200
400 km
ARCTIC OCEAN
Study Area
ELLESMERE I.
80°
70°
70°
100°
79° 58' N
Picnic Lake
0
500
1000 m
84° 28' W

Fig. 2

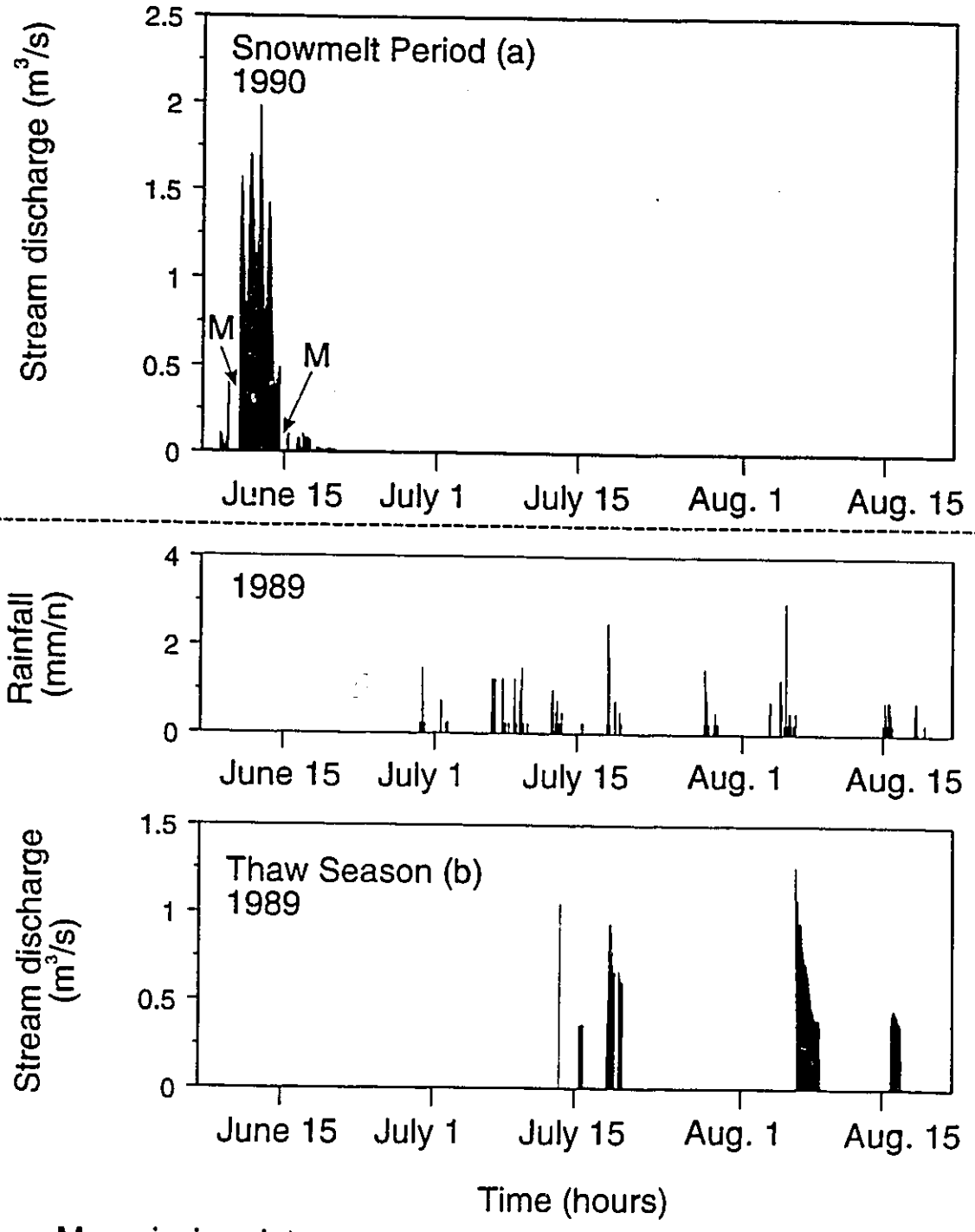

M = missing data

Fig. 3

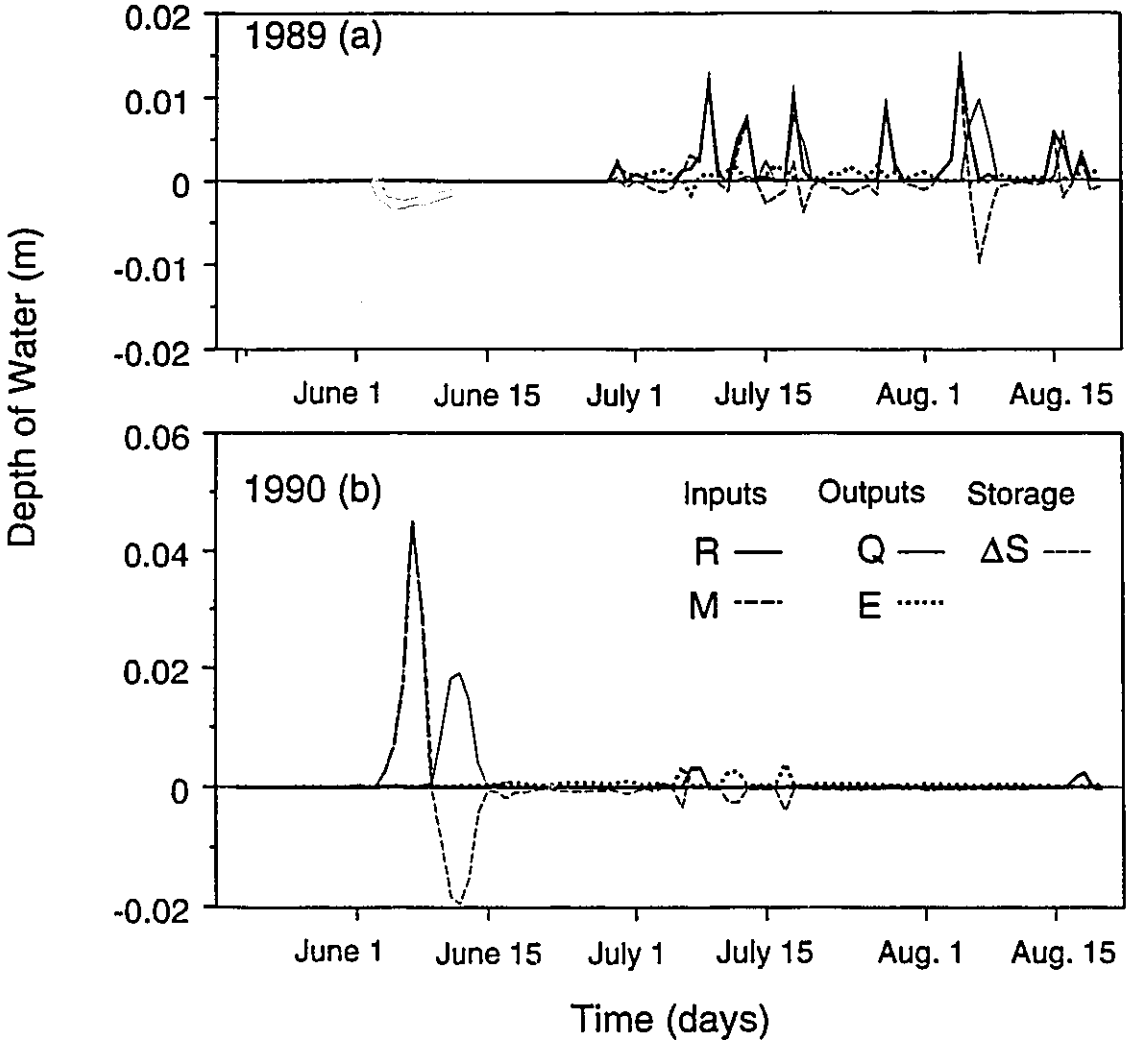
1989 (a)
1990 (b)
Inputs
Outputs
Storage
R
Q
ΔS
M
E
0.02
0.01
0
-0.01
-0.02
0.06
0.04
0.02
0
-0.02
June 1
June 15
July 1
July 15
Aug. 1
Aug. 15
Depth of Water (m)
Time (days)

Fig.4

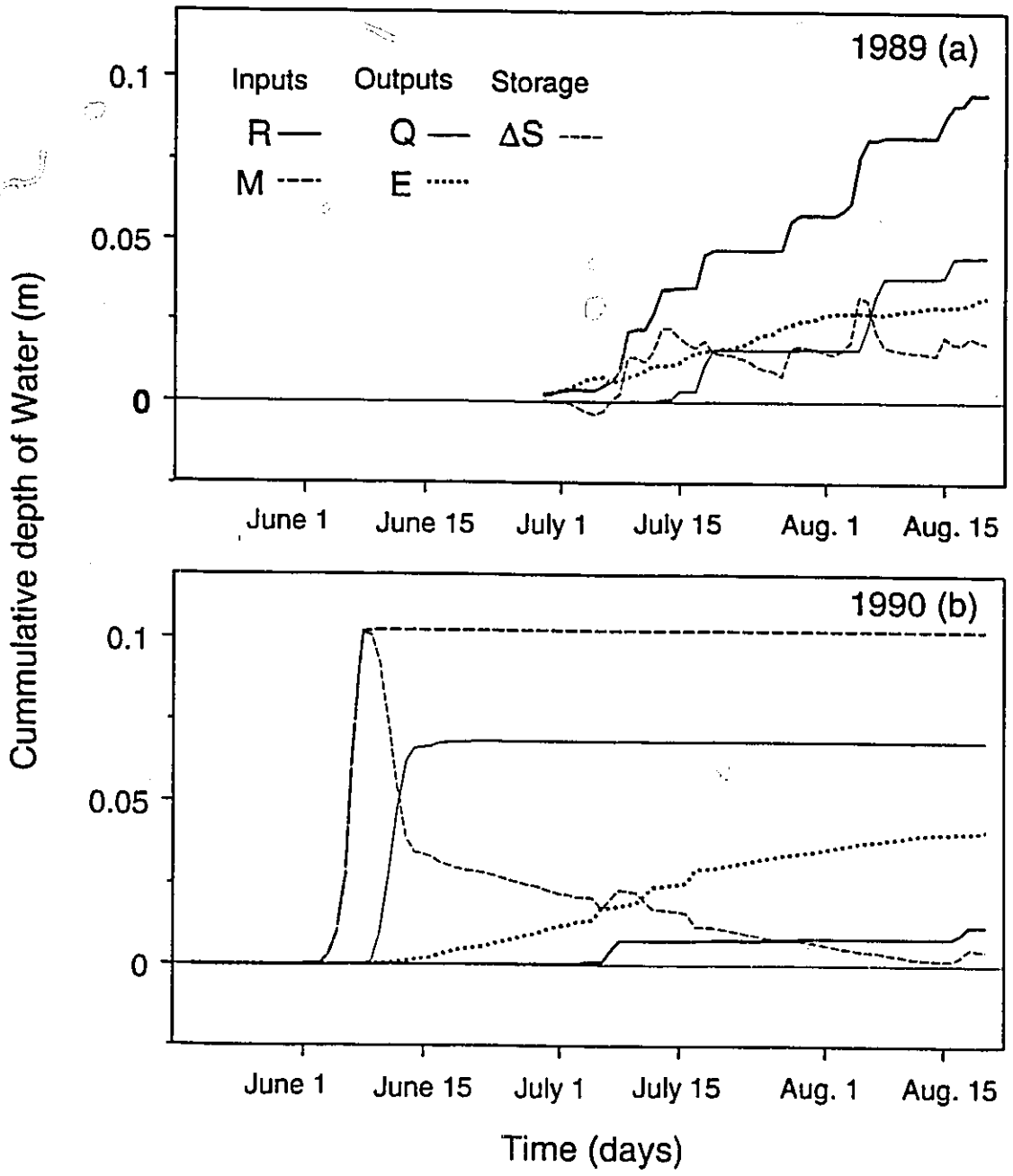
1989 (a)
Inputs
Outputs
Storage
R
Q
ΔS
M
E
0.1
0.05
0
June 1
June 15
July 1
July 15
Aug. 1
Aug. 15
1990 (b)
0.1
0.05
0
June 1
June 15
July 1
July 15
Aug. 1
Aug. 15
Cummulative depth of Water (m)
Time (days)

CHAPTER 6

CONCLUSIONS

Future global changes require that interactions between atmospheric, hydrologic and land surface processes be more carefully considered for arctic environments. This study examined the local variation of environmental variables (topography, microclimate, soils and hydrology) and their linkages and feedbacks at both level and sloping sites within the Hot Weather Creek basin, located on the Fosheim Peninsula, Ellesmere Islands, NWT. A surface energy balance model framework incorporating a cloud-layer solar radiation model allowed these environmental relationships to be considered when snowmelt and evaporation were simulated for the Heather Creek basin, a sub-basin of Hot Weather Creek. This model which uses easily obtained filed data as input (twice-daily cloud, temperature, wind, precipitation) was calibrated and tested suing field measurements obtained from the Hot Weather Creek experimental site during two contrasting summer seasons (1989-cool/wet; 1990-warm/dry). Hydrologic responses to selected atmospheric and terrestrial impacts in Heather Creek, a small continuous permafrost basin were investigated using this surface energy balance model. Several results can be drawn from this study:

1) Baseline information obtained in 1989 and 1990 at Hot Weather Creek indicate that the temporal and spatial responses of environmental variables to the local conditions can be identified as direct, recurrent or long-termed. For example, under direct responses, microclimate, itself affected by topography and the regional climate often sets the conditions for other variables to respond. Variations of radiation on slopes, particularly during years with few cloudy

periods, have effects on the initiation, duration, and intensity of snowmelt, as well as evaporation. Snow distribution, frost table configuration and groundwater flow exhibit recurrent spatial patterns, even though the magnitudes vary from year to year. The spatial distribution of vegetation and soil represents long-term adaption to the microclimate, hydrology, and geomorphological activities of the local site.

2) Field measurements at Hot Weather Creek caution that the spatial and temporal variation of local environments must be considered before point measurements of frost depth, snow amount, vegetation cover, soil moisture, etc. are upscaled for use in climate change detection.

3) This study has demonstrated that it is possible to model solar radiation satisfactorily using a cloud-layer model using twice-daily input of cloud data. The study shows that model performance improves greatly when calculated values are summed over four days or more, indicating that this model is useful to arctic ecologists and earth scientists interested in mapping solar radiation over large but remote areas.

4) This study has demonstrated the feasibility of simulating net radiation using limited input data, providing an opportunity to map the net radiation over the Arctic where direct measurements are scarce.

5) The surface energy balance model allows an extension of point observations in space to cover different terrains and under various surface conditions. Microclimatologist and hydrologists will find it useful in extrapolating snowmelt and evaporation for various slopes and drainage basins. Ecologists can apply the

model to compute radiation input for plot or transects; and geomorphologists can estimate the energy available for geomorphic processes to occur over a range of spatial scales.

6) A simple surface water balance for Heather Creek (1989 and 1990) demonstrates that a surface energy balance model using easily acquired field data (twice-daily temperature, cloud, wind, precipitation) can model melt and evaporation successfully for a small high arctic basin composed of varying terrains and surface conditions.

7) Sensitivity analysis of selected atmospheric and terrestrial impacts indicate that slight changes in atmospheric constituents (e.g. temperature, low-level cloud amounts and aerosols) have perhaps a greater effect on basin hydrologic responses (snowmelt, evaporation, and storage) than small modifications in the terrestrial environments (e.g. surface albedo, and resistance).

Future work is required to assess present-day variability of the Heather Creek hydrologic system through long-term monitoring. A more comprehensive sensitivity analysis which considers a larger number of variables (both atmospheric, and terrestrial), greater levels of change and combinations of variables (e.g. changes in precipitation and temperature simultaneously) (e.g. Hinzman and Kane, 1992) would broaden and provide a greater appreciation of the possible hydrologic responses that continuous permafrost environments will experience. The good performance of the surface energy balance model at the small basin scale (6.1 km^2) suggests that it could be used to simulate snowmelt and evaporation at a larger scale (e.g. Hot Weather Creek, 155 km^2). Snow and

stream discharge data from 1989–1993 is available for the Hot Weather Creek basin. The model's performance should also be tested at other sites in the Canadian Arctic. Future research is needed to couple this model with ecological-type models so as to assess present and future global impacts on plant productivity and structure in northern environments. In the near future, this model should be coupled with permafrost hydrological models (e.g. Woo and Drake, 1988) so as to extend their applicability from a point to larger surfaces (slopes-basin-region).

REFERENCES

Bazzaz, F.A.

1990: The response of natural ecosystems to the rising global CO_2 levels, Annual Review of Ecological Systems, v. 21, p. 167-96.

Blanchet, J-P.

1989: Toward estimation of climatic effects due to arctic aerosols, Atmospheric Environment, v. 23, no. 11, p. 2609-25.

Bergström, S.

1976: Development and application of a conceptual runoff model for Scandinavian Catchments. Swedish Meteorological and Hydrological Institute, Norrkoping, Sweden, Report No. RH07.

Church, M. and M-K. Woo

1990: Geography of surface runoff: some lessons for research, in (editors) Anderson, M.G. and T.P. Burt, Process Studies in Hillslope Hydrology, p. 299-325.

Dooge, J.C.I.

1992: Hydrologic models and climate change, Journal of Geophysical Research, v. 97, no. D3, p. 2667-86.

Harte, J. and J. William

1988: Arctic aerosol and arctic climate: results from an energy budget model, Climatic Change, v. 13, p. 161-89.

Hinzman, L.D. and D.L. Kane

1991: Snow hydrology of a headwater arctic basin 2. Conceptual analysis and computer modelling. Water Resources Research, v. 27, no. 6, p. 1111—1211.

Hinzman, L.D. and D.L. Kane

1992: Potential response of an arctic watershed during a period of global warming; Journal of Geophysical Research, v. 97, no. D3, p. 2811-20.

Hostetler, S.W.

1994: Hydrologic and atmospheric models: The (continuing) problem of discordant scales, Climatic Change, v. 27, p. 345-350.

Kane, D.L.; L.D. Hinzman; M-K. Woo and K.R. Everett

1992: Arctic hydrology and climate change, in (editors) Chapin III, F.S.; R.L. Jefferies, J.F. Reynolds, G.R. Shaver, J. Svoboda and E.W. Chu, Arctic ecosystems in a changing climate—an ecophysiological perspective, Academic Press, Toronto, p. 34-57.

Kane, D.L.; L.D. Hinzman and J.P. Zarling

1991: Thermal response of the active layer in a permafrost environment to climatic warming. Cold Regions Science Technology, v. 19, no. 2, p. 111-22.

LeDrew, E.F.

1993: Climate variability, change and sensitivity; in (editors) French, H.M. and O. Slaymaker, Canada's Cold Environments, McGill-Queen's University Press, Montreal and Kingston, p. 248-71.

Lewkowicz, A.G.

1992: Climatic change and permafrost landscape, in (editors) Woo, M-K. and D.J. Gregor, Arctic Environment: Past, Present and Future, Proceedings of a Symposium held at McMaster University, November 14–15, 1991, p. 91–104.

Maxwell, B.

1992: Arctic climate, in (editors), Chapin III, F.S.; R.L. Jefferies; J.F. Reynolds; G.R. Shaver; J. Svoboda and E.W. Chu, Arctic ecosystems in a changing climate—an ecophysiological perspective, Academic Press, San Diego, p. 259–80.

Rizzo, B and E. Wiken

1992: Assessing the sensitivity of Canada's ecosystems to climatic change, Climatic Change, v. 21, p. 37–55.

Robinson, P.J. and P.L. Finkelstein

1991: The development of impact-oriented climate scenarios. Bulletin American Meteorological Society, v. 72, no. 4, p. 481–90.

Running, S.W.; R.R. Nemani and R.G. Hungerford

1987: Extrapolation of synoptic meteorological data in mountainous terrain and its use for simulating forest evapotranspiration and photosynthesis, Canadian Journal of Forest Research, v. 17, p. 472–83.

Wetherald, R.T. and S. Manabe

1986: An investigation of cloud cover change in response to thermal forcing, Climatic Change, v. 8, p. 5–23.

Woo, M-K and J.J. Drake

1988: A study to model the effects of uranium mine tailings on a permafrost environment. Environmental Studies No. 53, Northern Affairs Program, Indian and Northern Affairs, Canada, Ottawa, Ontario, 41p.

Xia, Z-J.

1993: Modelling permafrost hydrology using limited data, PhD thesis, McMaster University, Hamilton, Ontario (unpublished), p. 1-228.